ASSESSMENT OF A CHEMOGENOMIC APPROACH TO CHARACTERIZING THE METABOLIC AND FUNCTIONAL ROLE OF A CONSERVED SQUALENE-BINDING PHOSPHATIDYLINOSITOL TRANSFER PROTEIN

A Dissertation

by

ELLIOTT MARTINEZ

Submitted to the Office of Graduate and Professional Studies of
Texas A&M University
in partial fulfillment of the requirements for the degree of

DOCTOR OF PHILOSOPHY

Chair of Committee, Michael Polymenis
Committee Members, Vytas A. Bankaitis
Hays Rye
Richard Gomer
Head of Department, Joshua Wand

May 2021

Major Subject: Biochemistry

ABSTRACT

Phosphoinositides (PIPs) are phosphorylated derivatives of a membrane lipid called phosphatidylinositol that act as signaling molecules. These signaling molecules regulate hundreds of biological events ranging from growth, proliferation, migration, autophagy, exo- and endocytosis. Consequently, when these signaling pathways become dysfunctional, they lead to a wide array of devastating diseases such as diabetes, Alzheimer's disease, cancer, and developmental disorders. However, there are only a handful of distinct PIP species in eukaryotes; only five in yeast and seven in mammals. Therefore, an unresolved question in the field of PIP signaling is: how can such a limited number of PIP species properly regulate such a wide array of complex and essential biological functions?

In this context, Sec14-like phosphatidylinositol transfer proteins (PITPs) channel phosphatidylinositol 4-OH kinase activities to specific yet diverse biological outcomes. PITPs are predicted to sense and translate specific lipid metabolic information into phosphoinositide signaling events that initiate distinct biological functions through a biophysical mechanism called heterotypic ligand exchange. The characterization of individual members of the yeast Sec14 PITP family will reveal more about the individual biological functions they regulate; especially in terms of the lipid composition the functions require.

The overarching aim of this research was to elucidate the functional and biophysical characteristics of the yeast Sec14-like PITP, Sfh2. This aim was attained by determining the biological function of Sfh2, identifying its secondary ligand, and characterizing its ligand-binding dynamics. The analysis of chemogenomic data revealed that Sfh2 is involved in vesicle formation/transport and, potentially, in the endosome/trans-Golgi network (TGN) system in

response to perturbed lipid metabolism under nutrient deprived conditions. The identification of its secondary ligand as squalene implies that squalene is acting as metabolic information to be translated into a phosphoinositide signal and a specific cellular function; according to the Sec14-based model of PITP function. Finally, the data demonstrates that Sfh2 ligand-binding abilities can be uncoupled. However, better ligand-binding mutants need to be designed before the canonical heterotypic ligand exchange model can be validated in vivo. This final aim will establish that squalene metabolism is indeed coupled to PIP synthesis and vesicle transport by Sfh2.

DEDICATION

To my wife Diana and my daughter Sophia

ACKNOWLEDGEMENTS

Firstly, I would like to thank my parents for raising me instilling in me a desire to serve others through the use of my mind, always encouraging me to not be afraid of challenges, for their constant prayers on my behalf.

I would also like to thank my wife Diana, who is always there to listen and encourage me when I need someone the most. Through the good times and the bad. For marrying me during a time where I would be completely invested in my work. For her wisdom and her advice. For giving me a daughter and learning how to be parents together. For so many things.

I would also like to thank my advisor Vytas, who always provided wisdom and guidance when I needed it the most. For teaching me how to think and speak like a scientist. For his persistence and for believing in me through success and failure.

I thank my committee members Dr. Richard Gomer, Dr. Michael Polymenis, and Dr. Hays Rye for all the wisdom and guidance they gave me throughout the years. For guiding me through this time in graduate school to completion. For believing in me as well.

I too thank all the members of the Bankaitis Lab throughout the years, for being my friends and fellow scientists. For their kindness and support. For making this lab a family.

Ultimately, I thank God for his presence and guiding hand throughout my life. For calling me out of darkness and into the light when I needed Him the most. For the gifts of wisdom and prudence and the graces of peace and perseverance through suffering. For His forgiveness and mercy.

CONTRIBUTORS AND FUNDING SOURCES

Contributors

This work was supported by a dissertation committee consisting of Dr. Vytas Bankaitis, Dr. Michael Polymenis, and Dr. Hays Rye of the Department of Biochemistry & Biophysics and Dr. Richard Gomer of the Department of Biology.

Figures 2-6, 2-7, 2-8, and 5-1 were created using BioRender.com. Erg1 antibody was a generous gift from Dr. Pedro Carvalho, University of Oxford, Oxford, United Kingdom. Dr. Ashutosh Tripathi in the Bankaitis lab generated the Sfh2 homology model, conducted all molecular modeling experiments found in Chapter three, and wrote a majority of that manuscript. The Laboratory for Molecular Simulation and High-Performance Research Computing at Texas A&M University provided software, support, and computer time. Dr. Prasanna Iyer performed the plasmid shuffle experiment in Figure 4-4C.

All other work conducted for the thesis (or) dissertation was completed by the student independently.

Funding Sources

This work was supported by grants to Vytas Bankaitis from the National Institutes of Health: RO1 (GM44530) and R35 (GM131804).

NOMENCLATURE

CPY	Carboxypeptidase Y
HIPHOP	Haploinsufficiency/Homozygous profiling
PIP	Phosphoinositide
PITP	Phosphatidylinositol transfer proteins
PtdIns	Phosphatidylinositol
PtdIns4P	Phosphatidylinositol-4-phosphate
Sfh2	Sec14-homolog 2
TGN	trans-Golgi network

TABLE OF CONTENTS

Page

LIST OF FIGURES

Page

LIST OF TABLES

Page

CHAPTER I – INTRODUCTION AND BACKGROUND[*]

Introduction

Cellular membranes possess countless essential functions in the eukaryotic cell. Membranes are utilized for functions ranging from protection from the extracellular environment, the sensing and transport of essential nutrients and ions, cellular mobility, division and proliferation, mating, to the engulfment of macromolecules. However, membrane-associated functions require internal and external signals to initiate these events. Phosphoinositides (PIPs) are phosphorylated derivatives of a membrane-embedded lipid called phosphatidylinositol that serve as internal signaling molecules that mediate these events. Consequently, derangements in PIP signaling are implicated in a wide array of devastating diseases such as Alzheimer's disease, cancer, and diabetes (McCrea and De Camilli, 2009). However, there are only a handful of distinct PIP species in eukaryotes; a total of five in yeast and seven in humans. Therefore, an unresolved question in the field of PIP signaling is: how can such a limited number of PIP species properly regulate such a wide array of complex and essential biological functions?

Further, for membranes to perform their essential functions, another variable must be considered: lipid composition. Biological membranes are composed of a wide variety of lipids that include sterols, glycerophospholipids, and sphingolipids. Each of these types of lipid hold

[*] Indicated figures reprinted with permission from Tripathi, Ashutosh, et al. "Functional diversification of the chemical landscapes of yeast Sec14-like phosphatidylinositol transfer protein lipid-binding cavities." *Journal of Biological Chemistry* 294.50 (2019): 19081-19098 and Bankaitis, Vytas A., Carl J. Mousley, and Gabriel Schaaf. "The Sec14 superfamily and mechanisms for crosstalk between lipid metabolism and lipid signaling." *Trends in biochemical sciences* 35.3 (2010): 150-160.

distinct and essential functions. They allow membranes to be flexible or rigid, thick or thin, curved or flat. Lipid composition can even be organized to form localized functional domains called lipid rafts (Lingwood and Simons, 2010).

Therefore, if membrane functions depend on both phosphoinositide production and proper lipid composition, we need to ask a few questions: do these lipid metabolic pathways communicate? How do PtdIns kinases know that the membrane lipid composition is competent to perform a specific function? How does the kinase know when and where to generate a pool of PIPs with signaling potential? It is precisely at this interface that the family of eukaryotic proteins called Phosphatidylinositol Transfer Proteins (PITPs) execute their function of integrating the lipid metabolome with PIP synthesis and a specific membrane function (Figure 1-1; Bankaitis et. al. 2010).

Sec14-based model of PITP function

This Sec14-based model of PITP function can be described as follows. PtdIns kinases alone do not have the ability to generate enough PIP to initiate a signaling event and biological function (Figure 1-2A; Routt et. al., 2005; Tripathi et. al., 2019). This is due to certain eraser proteins that dampen their signaling potential (i.e. PIP phosphatases or PIP binding proteins; Figure 1-2A; Nemoto et. al., 2000; Li et. al., 2002). However, when a PtdIns kinase coordinates with a PITP, it is then able to produce enough PIP to induce a signaling event and biological function (Figure 1-2A; Routt et. al., 2005).

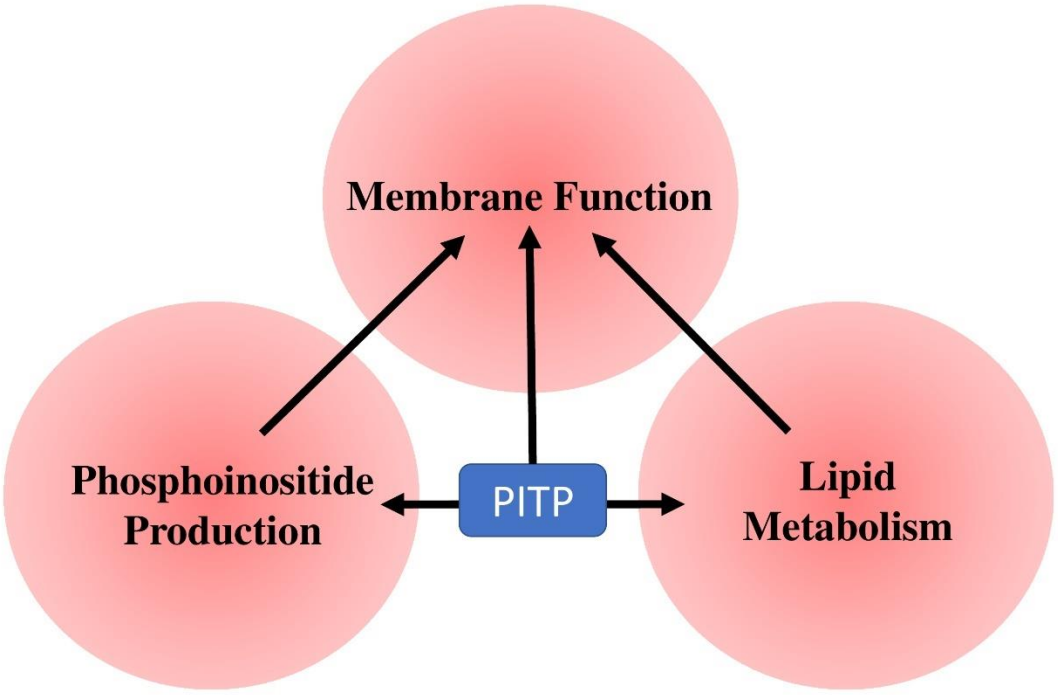

Figure 1-1. PITPs integrate phosphoinositide production and lipid metabolism to promote a membrane function

Both phosphoinositide production and proper lipid composition are required for the optimal function of a cellular membrane. The role of a PITP is to integrate these two metabolic pathways to promote a specific membrane function.

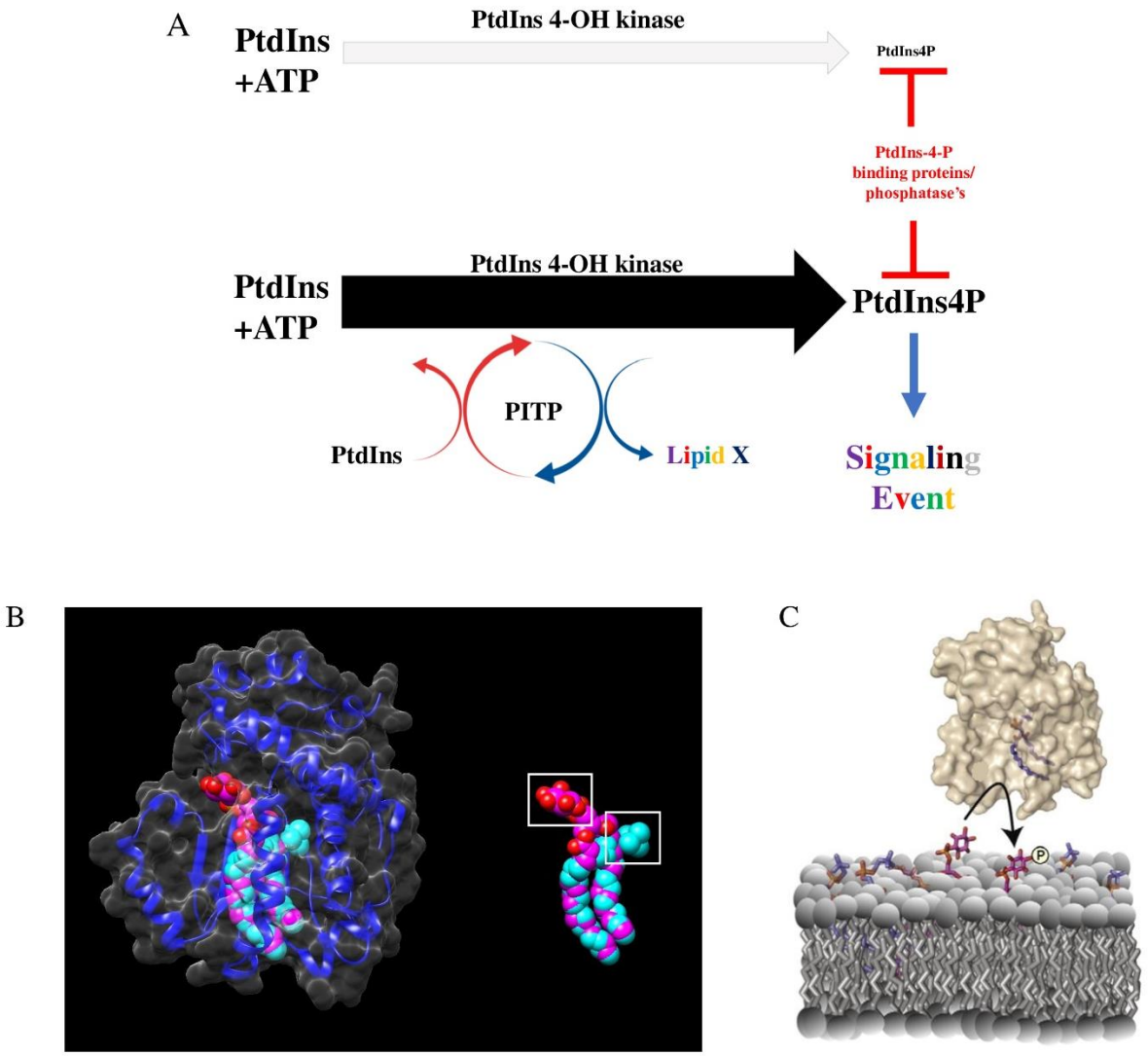

Figure 1-2. Sec14-based model of PITP function

(A) Coordination of a PtdIns kinase with a PITP overcomes the dampening of PtdIns4P signaling potential by antagonistic proteins (highlighted in red). Identity of ligand X that is sensed by a PITP is linked to a PIP signaling event and a specific biological function. (B) (left) PtdIns (magenta) and PtdCho (cyan) superimposed into the ligand-binding pocket of Sec14. Ligands exhibit two headgroup-specific binding sites. Acyl chain binding regions overlap. This architecture promotes heterotypic ligand exchange reactions. (right) Phospholipid configurations are shown in the absence of protein. Headgroups are boxed. Phospholipids were extracted from PDB ID: 3B7Z - which describes crystals composed of a mixture of Sfh1-PtdIns and Sfh1-PtdCho unit cells - and superimposed into the Sec14 crystal structure (PDB ID: 1AUA) (C) PtdCho bound by Sec14 obstructs the entry of PtdIns into the hydrophobic pocket. The temporary membrane-extracted state of PtdIns allows it to be a superior substrate for a PtdIns 4-OH kinase (not shown). Adapted from Bankaitis et. al., 2010.

Heterotypic Ligand Exchange

The ability of Sec14 to perform its function lies in its ability to bind two distinct ligands and through heterotypic ligand exchange (HLE) reactions (Figure 1-2A.; Bankaitis et. al., 2010). HLE allows a Sec14 to simultaneously sense the lipid composition of the membrane and instruct phosphatidylinositol (PtdIns) kinases when and where to generate a distinct PIP pool. This instruction occurs by the physical presentation of PtdIns to its kinase by Sec14 in an interfacial manner (Schaaf et. al., 2008). To understand this concept, the anatomy of Sec14 must be considered. Sec14 contains a hydrophobic pocket which can occupy two distinct ligands: PtdIns and PtdCho. What is unusual about this architecture is that these ligands occupy a significant portion of the same space in the hydrophobic pocket (Figure 1-2B). Notably, in the region that binds the hydrocarbon tails of these lipids. However, the phospholipid headgroups bind two distinct regions of the protein. When bound to Sec14 hydrophobic cavity, the PtdIns headgroup is oriented towards the surface of the protein and the aqueous environment. However, the PtdCho headgroup is buried deep within the Sec14 molecule (Figure 1-2B). This architecture is precisely what drives heterotypic ligand exchange and PtdIns presentation to its kinase.

There are three contributing factors to the HLE model (Figure 1-2C). (1) As a PITP associates with the membrane, hydrophobic residues on its surface disrupt the thermodynamic stability of the membrane surface. (2) Because the binding cavity has a hydrophobicity equivalent to the membrane bilayer, lipids can partition into the binding cavity without the expenditure of any thermodynamic energy. (3) The final contributing factor supporting this model is the kinetics by which individual lipid molecules enter and exit the cavity. In vitro PtdIns transfer rates are 20-fold faster than PtdCho transfer rates (Bankaitis et. al., 2010). Therefore, multiple PtdIns binding attempts can accompany a single round of PtdCho clearance

from the Sec14 hydrophobic pocket. This leads to the possibility that PtdIns, neither membrane- nor protein-bound, is exposed to the aqueous environment for a prolonged period where it is more accessible to its kinase (Figure 1-2C). Computationally intensive molecular dynamics analysis will be required to validate this model.

Lipid metabolism coordinates with phosphoinositide synthesis

The final aspect of the Sec14-based model of PITP function is the ability to coordinate phosphoinositide synthesis with lipid metabolism. The significance of PtdCho as the secondary ligand of Sec14 is that it serves as a signal for the functional competence of the membrane. PtdIns4P and diacylglycerol (DAG) are two lipids required for the formation and transport of vesicles from the trans-Golgi network (TGN; Figure 1-3; Bankaitis et. al., 2010). Because PtdCho biosynthesis consumes DAG, the accumulation of PtdCho serves as a signal for the depletion of this pro-secretory lipid (Figure 1-3; Bankaitis et. al., 2010). Sec14 responds to this metabolic state by performing HLE reactions between PtdCho and PtdIns to supplement the membrane with a secondary pro-secretory lipid, PtdIns4P (Figure 1-3). In this way, Sec14 acts primarily as a PtdCho sensor that instructs the PtdIns-4-OH kinase when and where to execute its biochemical reaction.

The yeast Sec14-like PITP family

In the way that the study of Sec14 bridged an intellectual divide between PIP-driven cell signaling and the biochemical conditions necessary for vesicle transport, the study of its yeast homologs will clarify whether and how various aspects of the lipid metabolome are coordinated

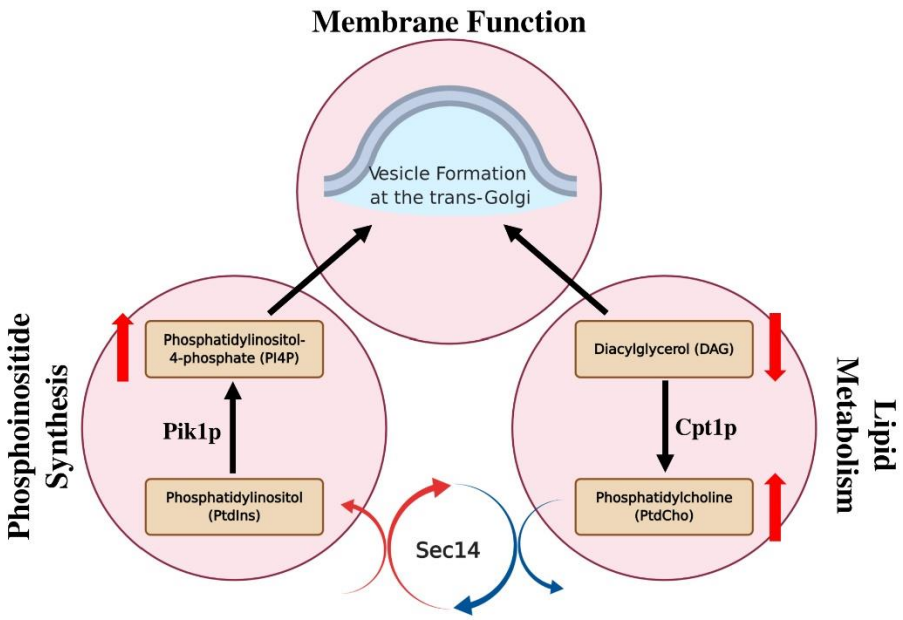

Figure 1-3. Sec14 integrates phospholipid metabolism and PIP production to regulate vesicle transport

PtdIns4P and DAG are both pro-secretory phospholipids. Vesicle transport from the TGN is perturbed by DAG consumption during the biosynthesis of PtdCho. Sec14 ameliorates this situation by stimulating PtdIns4P production by the Pik1p PtdIns 4-OH kinase through HLE reactions. (Cpt1 – choline phosphotransferase).

with PIP signaling and specific biological functions. This is approached by characterizing the functional properties of the five Sec14 homolog proteins (Sfh1-5) expressed in *S. cerevisiae* and confirming whether the canonical model of PITP function is upheld. Further, because we know the function of Sec14 depends on HLE, we must ask two questions: Do the other Sfh proteins function by heterotypic ligand exchange as well? And if so, what are their secondary ligands?

Structural determinants of PITP function

In one of our latest publications, we characterized the properties of the yeast Sec14-like PITPs that contribute to their ability to channel PIP pools to different biological outcomes (Tripathi et. al., 2019). To describe these properties, we must first understand the structural similarities and differences between the five Sec14 homologs.

Comparison of the crystal structures of Sec14, Sfh1, and Sfh3, and the 3D homology models of Sfh2, Sfh4, and Sfh5 demonstrated that all the yeast Sec14-like PITPs share the canonical Sec14-fold (Figure 1-4A; Tripathi et. al., 2019). However, comparison of their electrostatic potential surfaces revealed that the protein-surface properties varied widely (Figure 1-4B). These observations indicate that they differ in binding partners or the types of membrane they associate with. This also implies that the yeast PITP family regulates different membrane-associated functions.

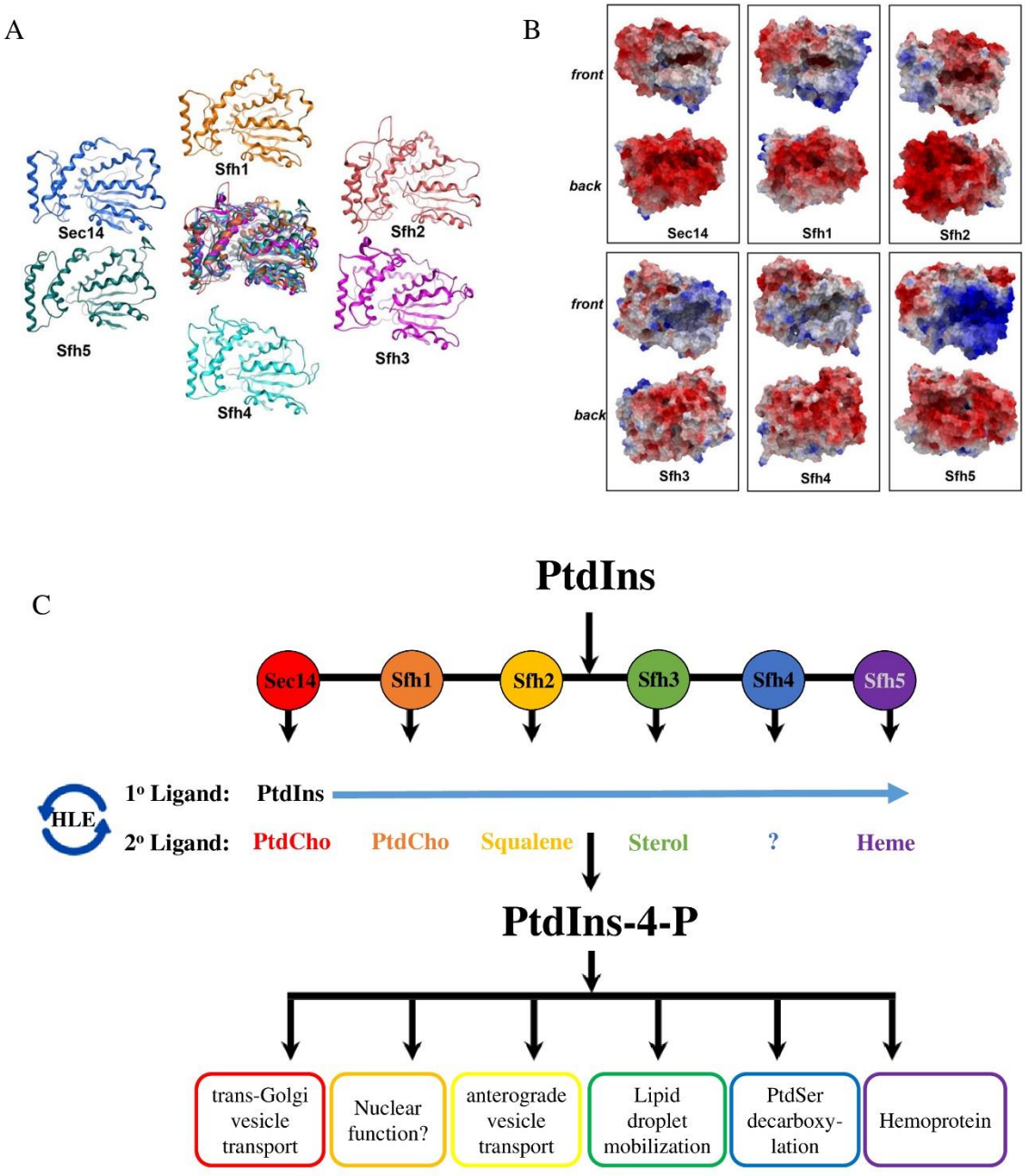

Figure 1-4. Structural and functional analysis of Sec14-homologs

(A) *S. cerevisiae* Sec14-homologs conserve the canonical Sec14 fold. Sec14 and Sfh PITPs are indicated. At the center is the overlay of all yeast α-carbon backbones superimposed onto Sec14. Adapted from Tripathi et. al., 2019. (B) electrostatic potential surfaces of open conformers Sec14 and indicated Sfh PITPs are shown. Surfaces with electropositive potential are rendered blue, and the electronegative surfaces are highlighted in red. Adapted from Tripathi et. al., 2019. (C) Illustration of the concept that the biological outcome of PtdIns4P signaling is determined by the identity of a PITP and is coordinated with an aspect of lipid metabolism represented by the identity of the PITP secondary ligand.

Further, all Sec14-like PITPs in yeast contain what is known as the PtdIns-binding barcode. This primary sequence "barcode" consists of highly conserved residues that are critical for PtdIns headgroup coordination (Nile et. al. 2014). These barcode residues translate to the capacity of all yeast Sec14-like PITPs to bind and transfer PtdIns between membranes *in vitro*. Where Sec14-like PITPs differ is in the "barcode" residues that coordinate the PtdCho molecule in Sec14 and its orthologs among divergent species. Only Sec14 and Sfh1 conserve these barcode residues and, as one would expect, only Sec14 and Sfh1 are able to bind and transfer PC *in vitro*. Sfh2, Sfh3, Sfh4, and Sfh5 diverge in amino acid identity at the corresponding PtdCho-binding barcode residues. Therefore, if the canonical model is upheld, a major prediction is that these PITPs must bind distinct secondary ligands (Figure 1-4C).

Yeast PITP binding cavities and secondary ligands

Not only do yeast Sec14-like PITPs diverge in their protein-surface properties and primary sequences at the PtdCho barcode, but they also diverge in their ligand-binding pocket topographies. The crystal structures or homology models of the yeast PITPs were mapped by the VICE/HINT (vectorial identification of cavity extents/hydropathic interactions) algorithm that characterized the properties of the ligand-binding pocket such as volume, surface area, hydropathic character, and entrance cross-sectional surface area (Tripathi et. al., 2019). These maps report the physical and chemical properties of the ideal ligand that would bind the ligand-binding pocket. As one would predict, the binding pockets of Sec14 and Sfh1 have very similar microenvironments. However, mapping the other four yeast PITPs revealed distinct physical and chemical environments of their ligand-binding cavities (See chapter 3 for the full discussion). Indeed, as will be discussed below, the identity of the secondary ligands of Sfh2, Sfh3, and Sfh5 have been identified as a sterol, squalene, and heme b, respectively (Figure 1-4C; Tripathi et. al.,

2019; Khan et. al., 2020). In the following sections, the biological functions associated with the yeast Sec14-like PITPs will be discussed.

Yeast Sec14-like PITPs

Sec14

Sec14 is the essential and founding member of the yeast PITP superfamily which is required for membrane trafficking through the TGN-endosomal system and which coordinates multiple metabolic pathways with this trafficking function (Cleves et. al., 1991). This conclusion was demonstrated by the isolation and characterization of 'bypass Sec14p' mutations. Cells lacking Sec14 function are normally inviable. However, loss of function mutations in a set of genes that code for phospholipid metabolism/sequestration leads to a restoration of viability in Sec14-deficient cells. Three enzymes in the PtdCho biosynthetic pathway (Cki1, Pct1, Cpt1), one PtdIns-4-phosphate (PtdIns4P) phosphatase (Sac1), and one PtdIns4P-binding protein of the oxysterol-binding protein family (Kes1) effect the "bypass-Sec14" phenotype in Sec14-deficient cells. These observations demonstrate that Sec14's essential function can be replaced by modulating specific aspects of lipid metabolism in the context of membrane trafficking. Because of these observations and a few more decades of research, the characterization of Sec14-like PITPs as simply transporting and supplying PtdIns when and where it is needed proved to be an inadequate hypothesis and paved a new way of thinking about lipid transfer proteins.

Sfh1

Sfh1 is a nuclear localized Sec14-like protein that shares the highest primary sequence similarity to Sec14 (64% identity) and conserves its PtdIns- and PtdCho-binding barcode and overall structural fold (Schnabl et. al., 2003). However, Sfh1 is a nonfunctional PITP both *in vitro* and *in vivo* (Li et. al., 2000). Neither cytosol prepared from yeast overexpressing Sfh1 nor

recombinant Sfh1 protein purified from *E. coli* was able to transfer PtdIns or PtdCho between membranes *in vitro* (Li et. al., 2000). Unlike the yeast Sec14-like homologs Sfh2 and Sfh4, the overproduction of Sfh1 cannot rescue either the growth or the secretory defects associated with Sec14 dysfunction (Li et. al., 2000; Schnabl et. al., 2003). This indicates that Sfh1 cannot stimulate PtdIns4P production *in vivo*. The unusual characteristics of Sfh1 provoked the question of what structural motifs are inhibiting its ability to act as a PITP. To this end, missense mutations were incorporated into the *SFH1* gene to resurrect Sec14-like activities in Sfh1 (Sfh1*; Schaaf et. al., 2011). These mutations reconfigure atomic interactions between amino acid side chains and internal water in an unusual hydrophilic microenvironment within the hydrophobic Sfh1 ligand-binding cavity. The net effect is enhanced rates of phospholipid-cycling into and out of the Sfh1* hydrophobic pocket (Schaaf et al., 2011). Further, analysis of crystal structures of Sfh1 bound to various phospholipids facilitated the design of Sec14 PtdIns- and PtdCho-binding mutants. This latter work elucidated the canonical heterotypic ligand exchange model of Sec14-like PITP function (Schaaf et. al., 2008). Although the biological function of Sfh1 remains enigmatic, its structural analysis has helped us understand much about the mechanism of Sec14-like PITP function.

Sfh2

Sfh2 is an enigmatic yeast PITP that has been associated with biological functions ranging from trans-Golgi transport, lipid and fatty acid metabolism, yeast cell wall formation, and a cytoplasmic thiol peroxidase (Li et. al., 2000, Wong et. al. 2005, Desfougères et. al., 2008; Cha et. al. 2003). However, with the identification of its unique secondary ligand and by considering the Sec14-based functional model, the specific *in vivo* role of Sfh2 is starting to gain more solid footing (Tripathi et. al., 2019). Mapping a Sfh2 homology model with the

VICE/HINT algorithm revealed a unique "toroid-shaped" ligand-binding pocket. Comparing the pocket topographies of this Sfh2 model and the crystal structure of Sec14L2, a mammalian squalene-binding PITP, demonstrated a striking similarity (Tripathi et. al., 2019). Accordingly, Sfh2 was found to show robust squalene transfer (~3:1 signal to noise ratio) in an *in vitro* [^{3}H]-labeled squalene transfer assay measuring ligand transfer from liposomes to bovine heart mitochondria (Tripathi et. al., 2019). This ability was unique to Sfh2 as no other yeast PITP demonstrated significant squalene transfer. Further, this squalene transfer ability of Sfh2 is relevant *in vivo* as Sfh2 deletion strains are hypersensitive to terbinafine, an allylamine inhibitor of squalene epoxidase that causes squalene to accumulate in yeast cells (Tripathi et. al., 2019; Garaiová et. al., 2014). This data suggests is that Sfh2 is implicated in the sterol metabolic pathway and specifically through sensing the squalene metabolite. This case-study supports the PITP functional model because the identity of squalene as the secondary ligand of Sfh2 indicates that a specific metabolic pathway (sterol biosynthesis) is being integrated with PIP signaling by a PITP. Sfh2 will be the subject of discussion throughout this dissertation.

Sfh3

Sfh3 is a yeast PITP that is involved in the inhibition of lipid mobilization from lipid droplets (LD; Ren et. al., 2014). LDs are phospholipid-enveloped energy-storage depots of neutral lipids such as sterol esters (SE) and triacylglycerides (TAG) in eukaryotic cells. LD are utilized in times of starvation and nutrient deprivation through lipid mobilization and the action of lipid hydrolases (Ren et. al., 2014). Sfh3-GFP colocalizes with the Erg6-RFP LD marker but is also detected in the cytosol, plasma membrane (PM) and/or peripheral endoplasmic reticulum (ER) which indicates that this PITP engages in dynamic associations with LDs (Ren et. al., 2014). It was discovered that in haploid yeast, overexpression of Sfh3 (Sfh3OE) clearly increased the LD

load relative to wild-type (WT) cells by imaging data. This data was supported by the observation that Sfh3OE led to an increase in ~2 and ~1.5-fold increases in total SE and TAG mass in yeast cells, respectively (Ren et. al., 2014). However, compared to WT and *sfh3Δ* yeast, the lipid composition ratios of purified lipid droplets coming from Sfh3OE cells remained the same, indicating that the LDs were not generated as a result of lipid metabolism derangement. Further, it was shown that Sfh3OE did not increase the rate of [^{3}H]-oleate incorporation into TAG and SE but rather decreased the rate of lipolysis. Taken together, this data establishes that Sfh3 inhibits neutral lipid mobilization from LDs. Importantly, overexpression of a PtdIns-binding mutant, sfh3^{T264W}, was unable to recapitulate the WT Sfh3OE phenotypes and the ablation of a PtdIns4P phosphatase, Sac1, was able to phenocopy Sfh3OE (Ren et. al., 2014). This data indicates that Sfh3 function is mediated by its ability to bind PtdIns and potentiate PtdIns4P production.

Sfh3 is also required for resistance to azole antimycotics in pathogenic fungi. In the absence of Sfh3, yeast cells are hypersensitive to azoles which target Erg11, the lanosterol 14-alpha-demethylase (Holič et. al., 2014). In the presence of azole antifungals, sterol metabolic intermediates such as lanosterol and squalene accumulate in *sfh3Δ* cells (Holič et. al., 2014). Overexpression of Sfh3 causes resistance to fluconazole, another azole antifungal that targets Erg11 (Holič et. al., 2014). This evidence supports the idea that Sfh3 function is mediating a response to perturbations in sterol biosynthesis. Further, the ablation of its PtdIns-binding activity in the Sfh3p$^{E235A,\ K267A}$ mutant phenocopies the hypersensitivity to miconazole in *sfh3Δ* yeast (Holič et. al., 2014). Indeed, it has been discovered that the secondary ligand of Sfh3 is a sterol through structural modeling and docking, and *in vitro* transfer assays (Tripathi et. al., 2019). In the case of this fascinating yeast PITP, again we present evidence that supports a coordination between lipid metabolism and PIP signaling that is dependent upon a dual ligand-binding ability.

Sfh4

Sfh4 is an example of a Sec14-like protein which supports the model that states that PITPs coordinate PIP-driven biological events by modulating the lipid metabolome as opposed to acting as mere lipid transporters. Sfh4 is an essential component in one of the two pathways in yeast that generate phosphatidylethanolamine (PtdEtn) through the decarboxylation of Phospatidylserine (PtdSer; Wang et. al., 2020). This pathway involves the endosome-localized PtdSer decarboxylase, Psd2, that assembles with other components at ER-endosome membrane contact sites (MCS). Sfh4 function was assumed to transport lipids between the apposed biological membranes. However, although this pathway is regulated by PtdIns4P, Sfh4 is not implicated in its production because Sfh4 function in the pathway does not depend on its PtdIns-binding ability (Wang et. al., 2020). Rather, Sfh4 function in this pathway is entirely dependent upon a physical interaction with Psd2. For this reason, Sfh4 is considered a noncanonical PITP but one which still conserves the general role of a PITP supported by the Sec14 model. The secondary ligand of Sfh4 has yet to be identified but its discovery may clarify its precise biophysical mechanism.

Sfh5

Sfh5 is an unusual Sec14-like PITP that has recently been characterized as a hemoprotein (Khan et. al., 2020). Sfh5 is atypical in that although it adopts the Sec14 structural fold and preserves the PtdIns-binding "barcode", it demonstrates marginal *in vitro* PtdIns transfer activity and lacks the ability to potentiate PtdIns4P *in vivo* (Khan et. al., 2020). Sfh5 has been crystallized bound to a heme b prosthetic group which is coordinated by co-axial tyrosine/histidine interactions on the distal side of its iron (Khan et. al., 2020). Electron paramagnetic resonance (EPR) and Mössbauer spectroscopy analysis of Sfh5 demonstrates that

the heme iron is a high-spin Fe^{3+}. Further, dithiothreitol treatment and reduction to Fe^{2+} demonstrated that this iron is redox-active (Khan et. al., 2020). Like all other Sec14-like PITPs with identified secondary ligands, the heme sits in the region of its binding cavity which overlaps the presumed PtdIns-binding region. In fact, by introducing mutations that lead to the loss of heme binding in Sfh5, it's *in vitro* PtdIns exchange ability and *in vivo* PtdIns kinase stimulation is resuscitated (Khan et. al., 2020). However, it was demonstrated that this heme is not exchangeable with other heme b binding proteins and does not seem to be able to transfer its ligand between membranes (Khan et. al., 2020). Finally, chemogenomic analysis of the *sfh5* homozygous *Δ/Δ* diploid strain suggests a hypothesis that Sfh5 functions in some aspect of redox control, and/or regulation of heme homeostasis, under stress conditions induced by exposure to organic oxidants. These hypotheses are currently being investigated. This data demonstrates that even in an atypical PITP like Sfh5, the Sec14 fold is utilized for translating the binding of distinct ligands to a distinct cellular activity and not to act as mere lipid transporters.

Summary

Translating specific metabolic information to the action of lipid-modifying enzymes and a major biological function is a fascinating yet underappreciated regulatory mechanism in the eukaryotic cell. This concept defines PITPs primarily as lipid sensors that instruct PIP kinases when and where to execute their function rather than merely transferring lipid from one biological membrane to another. Although this paradigm is historically founded on the structural and functional analysis of Sec14 and Sfh1, the recent discoveries regarding the other yeast Sec14-homologs lend more support to this model. Most notably, the observation that there is a wide diversity in secondary ligand identity among the yeast PITPs indicates that each Sec14 homolog channels unique metabolic information to distinct biological outcomes via PIP

signaling. This observation also demonstrates that the Sec14 structural fold is a versatile scaffold for the sophisticated coordination of a wide variety of ligands. With respect to this regulatory theme, of major interest is determining whether this functional mechanism is conserved across diverse eukaryotic species. The investigation of this question will help resolve the complexity of PIP-driven cell signaling and provides alternative strategies for the therapeutic intervention of PIP-associated malignancies.

Although the discoveries highlighted above progressed our understanding of Sec14-like proteins, several obstacles remain to fully characterize the yeast PITP family. In the case of Sfh1, it remains unknown why the wild type form does not behave like Sec14 in vivo even though it shares the highest structural homology to Sec14 among all the yeast PITPs. In the case of Sfh2 and Sfh5, although their unique secondary ligands are identified, their precise biological functions remain elusive. In the case of Sfh4, it is unclear why PtdIns binding is not necessary in the context of PtdSer decarboxylation and its secondary ligand remains unknown. Clarifying these enigmas provides several opportunities to reveal unique insights into the complex and dynamic interface between lipid metabolism and PIP signaling in the eukaryotic cell.

CHAPTER II – CHEMOGENOMIC PROFILING OF SFH2 DESCRIBES A CANONICAL SEC14-LIKE PHOSPHATIDYLINOSITOL TRANSFER PROTEIN THAT REGULATES STEROL METABOLISM AND VESICLE TRANSPORT

Summary

Sec14-like phosphatidylinositol transfer proteins (PITPs) channel phosphatidylinositol 4-OH kinase activities to specific yet diverse biological outcomes. The function of Sec14-homolog 2 (Sfh2) has yet to be precisely characterized although we have identified its secondary ligand as squalene, an intermediate of sterol biosynthesis in the eukaryotic cell. PITP secondary ligands serve as metabolic information that is channeled through a PITP into a phosphoinositide (PIP) signaling event and a precise biological function. In this work, chemogenomic data was analyzed to elucidate the precise biological function that results from Sfh2's ability to bind (sense) squalene. Analysis of chemogenomic data revealed that, much like Sec14, Sfh2 shares functional similarity with biological processes such as vesicle transport and lipid metabolism. These hypotheses were validated in vivo. However, chemogenomic data also highlighted other biological processes that have not been investigated in relation to the yeast Sec14-like PITPs. These functions include membrane protein homeostasis, nutrient sensing pathways, and regulation of the cell cycle. This work presents a case-study of the value of chemogenomic profiling and offers a systematic approach to navigating chemogenomic data to provide functional information about a gene of interest.

Introduction

Members of the Sec14-like family of phosphatidylinositol transfer proteins (PITPs) are predicted to translate specific lipid metabolic information into phosphoinositide signaling events that initiate distinct biological functions (Bankaitis et. al. 2010). Sec14-homolog 2 (Sfh2) is a

squalene-binding PITP with an enigmatic function in the yeast cell. Thus, a chemogenomic database generated by the Giaever and Nislow labs (Lee et al., 2014) was employed to generate and test hypotheses regarding the *in vivo* role of Sfh2. This chemogenomic database utilizes haploinsufficiency/homozygous profiling (HIPHOP) to present functional interactions between genes, chemicals, and biological processes in an unbiased manner (Lee et al., 2014). The chemogenomic data was generated by screening the diploid heterozygous and homozygous yeast deletion library (~5900 strains) against ~3250 small molecule inhibitors of wild-type (WT) yeast growth. This yeast chemogenomic platform quantifies the requirement for each gene for resistance to a compound in vivo (Lee et al., 2014).

Chemogenomic analysis of the homozygous *sfh2Δ/Δ* strain revealed associations with various biological processes including membrane trafficking, lipid and sterol metabolism, and cellular signaling pathways. Some of these associations were validated, however, several produced inconclusive results. The chemogenomic profile of a specific compound, terbinafine - whose mode of action is relevant to Sfh2's in vivo function - was also analyzed to propose hypotheses about its specific biological effects in relation to Sfh2 function. This analysis produced both positive and negative data that refined our means of mining and interpreting chemogenomic data.

Materials and Methods

Metabolic Labeling and Immunoprecipitation

Yeast were grown in minimal media lacking methionine and cysteine to midlogarithmic phase (OD600nm = 0.5) and radiolabeled with [35S]-amino acids (Translabel; PerkinElmer; 11 mCi/ml). Chase was initiated by introduction of unlabeled methionine and cysteine (2 mM each, final concentration) for the specified time. Chase was terminated by addition of trichloroacetic acid (5% w/v final concentration). Immunoprecipitation of CPY with rabbit antiserum and resolution by SDS-PAGE and autoradiography were performed as previously described (Cleves et al., 1991; Schaaf et al., 2008).

Cycloheximide shut-off experiments

Cycloheximide shut-off experiments were performed in exponentially growing cells, as described (Carvalho et al., 2010).

Results

Chemogenomic data demonstrates that Sfh2 is implicated in vesicle transport

The HIPHOP chemogenomic database demonstrates that *sfh2Δ/Δ* homozygous and *sec21Δ*/SEC21 (Sec21- the gamma subunit of the COPI coatomer coat required for retrograde Golgi-to-ER vesicle transport) heterozygous diploid yeast share hypersensitivity to two structurally similar compounds, k007-0610 and 4069-0007 and that these compounds appear to specifically perturb Sec21p function (Figure 2-1). Additionally, the chemogenomic profiles of *sfh2Δ/Δ* and *sec21Δ*/SEC21 diploid yeast share highly significant similarity in response to the chemical screen which suggests an overlap between these two gene functions (correlation score: 0.211, estimated significance of profile similarity p-value: 3.7 E-35).

To determine whether Sfh2 plays a role in vesicle transport, temperature sensitivity assays were performed in strains harboring temperature sensitive alleles of components involved in COPI, COPII, and trans-Golgi network (TGN) vesicle trafficking (i.e. Cop1 and Sec21, Sec12, and Sec14, respectively) in the presence or absence of Sfh2. Further, the transit of vacuolar carboxypeptidase Y (CPY) from the ER to the vacuole was monitored in these same strains.

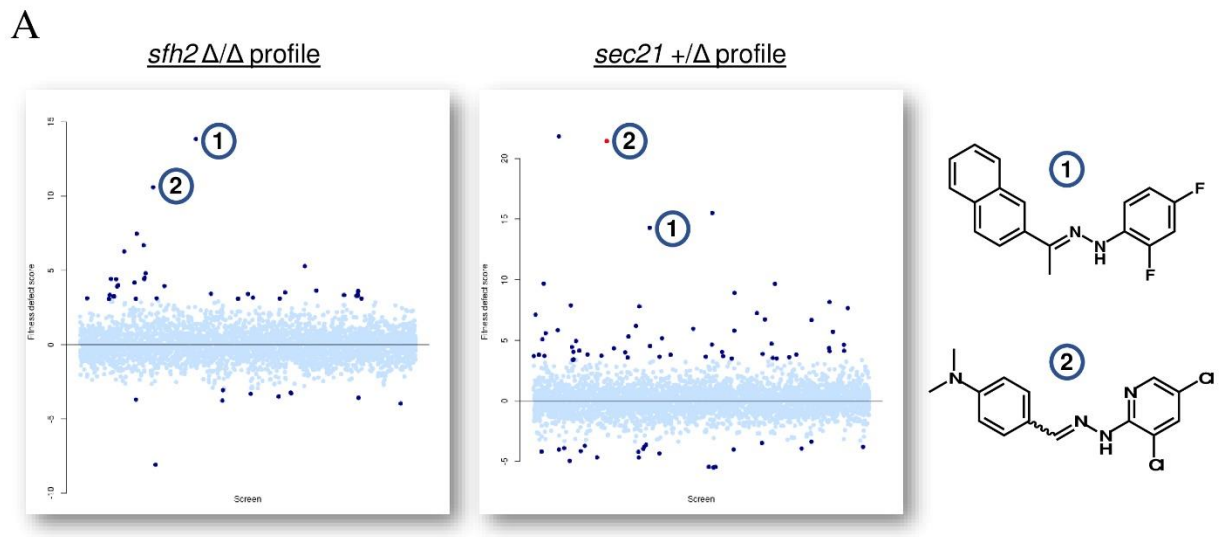

Figure 2-1: Chemogenomic profiles highlight functional interaction between Sfh2 and Sec21

(A) Chemogenomic profiles of *sfh2Δ/Δ* homozygous and *sec21Δ*/SEC21 heterozygous diploid yeast. The compound library screen is plotted on the x-axis against the strain fitness defect score (y-axis). Database highlights molecule 2 as a putative inhibitor of Sec21p function (orange dot in *sec21 +/* Δ profile). Chemogenomic profiles share significant similarity in response to compound screen; correlation value of 0.211, p-value: 3.70E-35 (estimated significance of profile similarity). Molecules 1 and 2 share several chemical moieties.

Sfh2 deletion demonstrated synthetic lethality with both the s*ec12*^{ts} and *sec14*^{ts} alleles for growth on YPD plates at semi-restrictive temperatures (Figure 2-2). However, no significant genetic interaction was observed with *cop1*^{ts} (the alpha COPI coatomer subunit) and *sec21*^{ts} alleles (Figure 2-2).

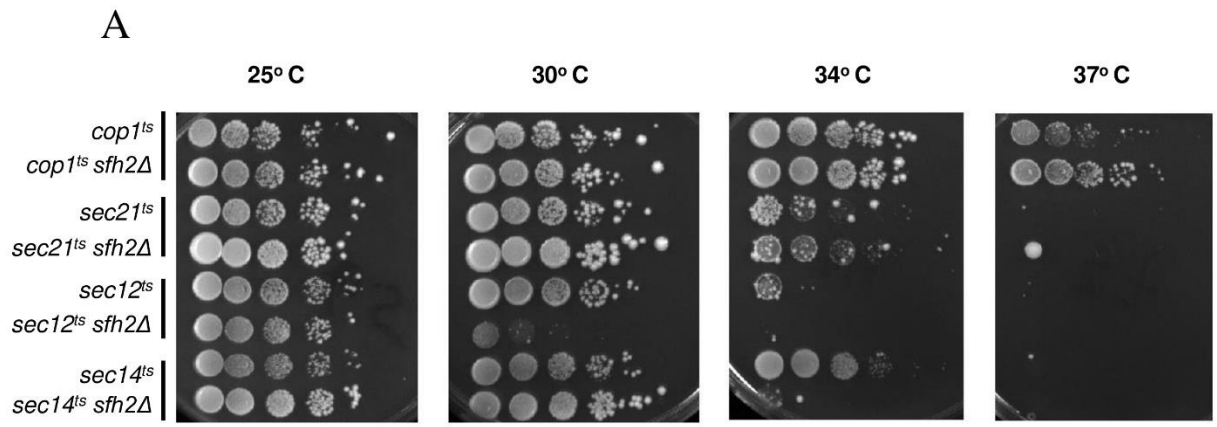

Figure 2-2: Sfh2 is required for growth when anterograde trafficking is defective

Growth data showing that *SFH2* deletion exacerbates the growth defects of s*ec12*^{ts} and *sec14*^{ts} yeast at semi-restrictive temperatures. The deletion of *SFH2* does not exacerbate *cop1*^{ts} and *sec21*^{ts} growth defects at restrictive temperatures. Equivalent numbers of cells were spotted in 10-fold dilution series onto YPD agar plates and grown at temperatures indicated. Images were taken after 3 days.

Pulse-chase radiolabeling analyses that monitored carboxypeptidase Y (CPY) transit through the yeast secretory pathway to the vacuole yielded similar conclusions. Although Sfh2 deletion does not affect CPY trafficking relative to WT and *sec21*^{ts} yeast in a time-course experiment, CPY processing is severely diminished when Sfh2 is abrogated in a Sec12^{ts} genetic background at semi-permissive temperatures (Figure 2-3A-C). Consistent with growth data, Sfh2 deletion induces a moderate effect on CPY processing in the Sec14^{ts} background at a semi-restrictive temperature (Figure 2-3C). This data demonstrates that Sfh2 function is required for CPY processing and cellular viability when anterograde trafficking is defective.

To rule out the possibility that Sfh2 functions in endocytic pathways, trafficking of the bulk endocytic tracer FM4-64 was observed in WT and *sfh2Δ* yeast. Normally, FM4-64 is internalized from the plasma membrane into endosomal compartments within 5 min of chase, with a significant fraction detected in the vacuole by that time point. The remaining FM4-64 pool chases from endosomes to vacuoles during the remainder of the time course (Mousley et. al., 2012). This analysis therefore probes two steps of membrane trafficking: plasma membrane (PM) to endosomes and endosomes to vacuole. The deletion of Sfh2 did not appear to affect FM4-64 trafficking to the vacuole relative to WT (data not shown).

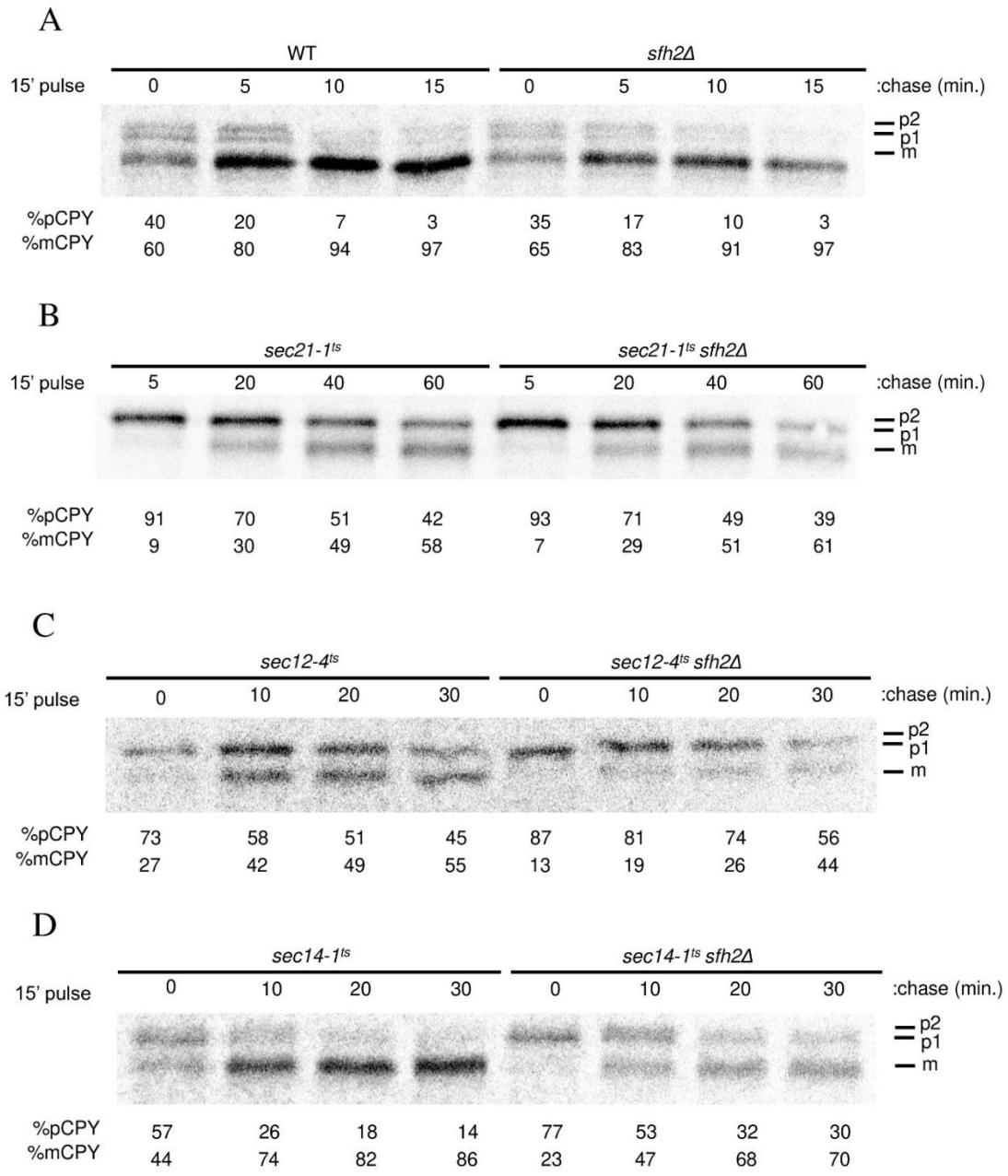

Figure 2-3: Sfh2 is required for CPY processing when anterograde trafficking is defective

Yeast strains with and without SFH2 were grown to mid-logarithmic phase in minimal media lacking methionine and cysteine. Yeast were shifted from 25ºC to 33.5ºC for 2 hours to induce semi-restrictive conditions of temperature sensitive strains. Cells were radiolabeled with [35S]-amino acids for indicated pulse and chase times. Samples were processed, and immunoprecipitates evaluated by SDS-PAGE and autoradiography (see Methods). Precursor p1CPY and p2CPY forms and the fully processed vacuolar mCPY forms are identified. Quantification of pCPY forms (p1 + p2) as percentages of total CPY species are given at the bottom of each condition. (A) Time-course experiment comparing CPY trafficking in WT and *sfh2Δ* yeast. (B) Time-course experiment comparing CPY trafficking in *sec21-1^{ts}* and *sec21-1^{ts} sfh2Δ* yeast. (C) Time-course experiment comparing CPY trafficking in *sec12-4^{ts}* and *sec12-4^{ts} sfh2Δ* yeast. (D) Time-course experiment comparing CPY trafficking in *sec14-1^{ts}* and *sec14-1^{ts} sfh2Δ* yeast.

Sfh2 shares functional homology with a component of ERAD

To investigate the biological role of Sfh2 more thoroughly, chemogenomic data was revisited to refine the hypothesis for its function. The specific database that was utilized provides a computed correlated fitness value termed "*cofitness"* (Pearson correlation coefficient) for every pair of gene-deletion strains. This value corresponds to the measure of the similarity in the importance of the genes in the cellular responses to the chemical perturbations. As a result, cofitness can be considered a measure of functional similarity between gene-pairs.

Sfh2 function correlates with a ubiquitin ligase due to their regulation of sterol homeostasis

The chemogenomic profile of the *sfh2Δ/Δ* strain shared the highest correlation with the *ssm4Δ/Δ* strain (correlation: 0.462; p-value: 1.07 E-176). Ssm4 is a multispanning membrane bound ubiquitin ligase involved in endoplasmic reticulum associated degradation (ERAD; Swanson et. al. 2001). Ssm4p targets cytosolic proteins and membrane proteins with misfolded cytosolic domains, such as the Matα2 repressor and squalene monooxygenase (Erg1), respectively, to the cytosolic 26S proteasome for degradation (Swanson et. al., 2001; Foresti et. al., 2013). As Ssm4 regulates the sterol metabolic pathway by the turnover of squalene monooxygenase, we determined whether Sfh2 function is involved in either sterol homeostasis or the degradation of the Ssm4 substrate, Erg1.

Consistent with a role for Sfh2 in regulating sterol biosynthesis, previous work in our lab demonstrated that the overexpression of Sfh2 renders yeast resistant to fenpropimorph, a morpholine antifungal drug that inhibits ergosterol biosynthesis (Li. et. al., 2000). Further, exploration of the *sfh2Δ/Δ* chemogenomic profile revealed that *sfh2Δ/Δ* yeast were hypersensitive to tioconazole and compound 1181-0519, a validated and putative inhibitor of lanosterol 14-alpha-demethylase (Erg11), respectively, and terbinafine, an allylamine inhibitor of

Erg1. The hypersensitivity to terbinafine was validated by a plate drug-sensitivity assay (Figure 2-4B). Interestingly, relative to WT yeast, *sfh2Δ* yeast were not hypersensitive to zaragozic acid, the potent inhibitor of squalene synthase (Erg7; Figure 2-4). This data indicates that *sfh2Δ* yeast are specifically sensitive to Erg1 inhibition and therefore squalene accumulation. As demonstrated by our prior publication, comparison of the Sfh2 ligand binding site to the mammalian squalene-binding PITP Sec14L2 revealed a striking similarity in their physical dimensions and chemical properties (Tripathi et. al., 2019). Sfh2 was thereby discovered to be the sole squalene-binding yeast PITP and likely evolutionary predecessor of Sec14L2 (see chapter three for the full narrative).

To identify whether Sfh2 is required for the degradation of Erg1, cycloheximide shut-off experiments were performed in WT and *sfh2Δ* yeast. Sfh2 was determined not to be required for the turnover of Erg1 as both WT and *sfh2Δ* strains had a half-life of ~50 minutes (Figure 2-5). Turnover of an Ssm4-independent ERAD substrate, CPY*, neither was affected by Sfh2 deletion (data not shown).Therefore, although Sfh2 does not participate in ERAD, it likely shares significant functional homology with Ssm4 because its function regulates the same step of the sterol biosynthetic pathway through its squalene-sensing ability.

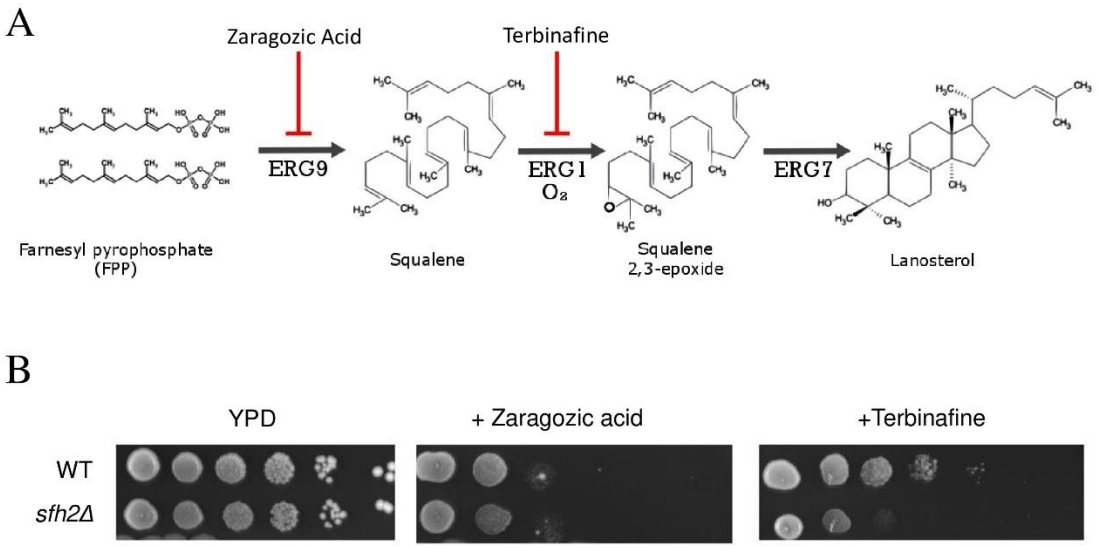

Figure 2-4: *sfh2Δ* cells are hypersensitive to squalene accumulation

(A) Squalene is a metabolic intermediate in the ergosterol biosynthesis pathway and is produced from farnesyl pyrophosphate by the action of the ERG9 gene product squalene synthase. Subsequently, squalene is converted to squalene 2,3-epoxide in a reaction catalyzed by the squalene 2,3-epoxidase (encoded by ERG1) that consumes molecular oxygen. Squalene synthase is inhibited by the natural product zaragozic acid and squalene 2,3-epoxidase is inhibited by the synthetic allylamine terbinafine. (B) Growth data showing that *sfh2Δ* cells are hypersensitive to terbinafine but not to zaragozic acid. 10-fold serial dilutions of WT (CTY182) and *sfh2Δ* cells were spotted on plates containing no drug (YPD) or +Zaragozic acid (5µg/mL), or +Terbinafine (150 µM). Images were taken after 3 days.

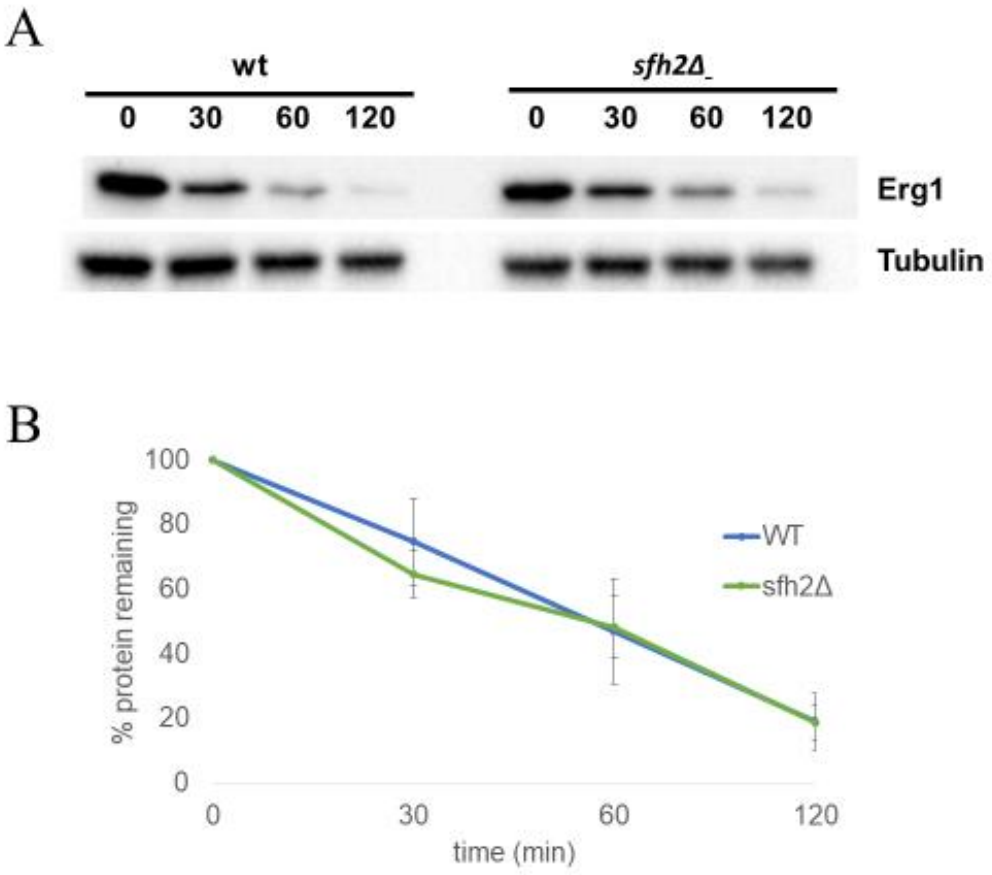

Figure 2-5: *sfh2Δ* cells are not defective in Erg1 degradation

(A) The degradation of endogenous Erg1 was followed after inhibition of protein synthesis by cycloheximide in WT or *sfh2Δ* cells . Whole-cell extracts were analyzed by SDS–PAGE and western blotting. Erg1 was detected with an Erg1 antibody. Tubulin (Tub3; alpha-tubulin) was used as loading control. A representative gel of greater than or equal to three independent experiments is shown. (B) Quantification of greater than or equal to three independent experiments performed as described in (A).

Analysis of Sfh2 cofit genes

Because chemogenomic analysis proved fruitful, a larger-scale analysis of the cofitness list was carried out to deduce more information regarding the possible *in vivo* function of Sfh2. The top ~100 out of 5905 genes (cofit genes) in the cofitness list were classified to discern the biological processes that correlate with Sfh2 function. This list was limited to p-values less than 1.1E-11 and correlation values greater than 0.115. As a result, this list of genes is enriched in functions such as vesicle transport, lipid metabolism, signal transduction pathways, membrane protein insertion and extraction, cell cycle regulation, and translation. ~25 genes were classified as having miscellaneous or unknown functions (Table 1).

Gene	Table 1: Vesicle Transport	Rank in Sfh2 cofitness list	Alias
Ypt52	Rab family GTPase, similar to Ypt51p and Ypt53p and to mammalian rab5; required for vacuolar protein sorting and endocytosis; protein abundance increases in response to DNA replication stress	13	
Sec21	Gamma subunit of coatomer, a heptameric protein complex that together with Arf1p forms the COPI coat; involved in ER to Golgi transport of selective cargo	17	
Apm1	Mu1-like medium subunit of the clathrin-associated protein complex (AP-1); binds clathrin; involved in clathrin-dependent Golgi protein sorting	20	
Exo70	Subunit of the exocyst complex; the exocyst mediates polarized targeting and tethering of post-Golgi secretory vesicles to active sites of exocytosis prior to SNARE-mediated fusion; PtdIns[4,5]P2-binding protein that localizes to exocytic sites in an actin-independent manner, targeting and anchoring the exocyst with Sec3p; involved in exocyst assembly; direct downstream effector of Rho3p and Cdc42p; relocalizes from bud neck to cytoplasm upon DNA replication stress	29	
Sec24	Component of the Sec23p-Sec24p heterodimer of the COPII vesicle coat, required for cargo selection during vesicle formation in ER to Golgi transport; homologous to Sfb2p and Sfb3p	38	
Ptm1	Protein of unknown function; copurifies with late Golgi vesicles containing the v-SNARE Tlg2p; PTM1 has a paralog, YHL017W, that arose from the whole genome duplication	40	
Tvp18	Integral membrane protein localized to late Golgi vesicles along with the v-SNARE Tlg2p; may interact with ribosomes, based on co-purification experiments	45	
Rcy1	F-box protein involved in recycling plasma membrane proteins internalized by endocytosis; localized to sites of polarized growth	48	
Gcs1	ADP-ribosylation factor GTPase activating protein (ARF GAP), involved in ER-Golgi transport; shares functional similarity with Glo3p	52	
Apl2	Beta-adaptin subunit of the clathrin-associated protein (AP-1) complex; binds clathrin; involved in clathrin-dependent Golgi protein sorting; protein abundance increases in response to DNA replication stress	57	
Gyp1	Cis-golgi GTPase-activating protein (GAP) for the Rab family members Ypt1p (in vivo) and for Ypt1p, Sec4p, Ypt7p, and Ypt51p (in vitro); involved in vesicle docking and fusion	63	
Cdc50	Endosomal protein that interacts with phospholipid flippase Drs2p; interaction with Cdc50p is essential for Drs2p catalytic activity; mutations affect cell polarity and polarized growth; similar to Lem3p; CDC50 has a paralog, YNR048W, that arose from the whole genome duplication	73	
Laa1	AP-1 accessory protein; colocalizes with clathrin to the late-Golgi apparatus; involved in TGN-endosome transport; physically interacts with AP-1; similar to the mammalian p200; may interact with ribosomes; YJL207C is a non-essential gene	75	
Exo84	Exocyst subunit with dual roles in exocytosis and spliceosome assembly; subunit of the the exocyst complex which mediates polarized targeting and tethering of post-Golgi secretory vesicles to active sites of exocytosis at the plasma membrane (PM) prior to SNARE-mediated fusion; required for exocyst assembly and targeting the complex to specific sites on the bud tip PM; associates the U1 snRNP; role in pre-mRNA splicing and prespliceosome formation; possible Cdc28 substrate	85	
Ypt31	Rab family GTPase; involved in the exocytic pathway; mediates intra-Golgi traffic or the budding of post-Golgi vesicles from the trans-Golgi; YPT31 has a paralog, YPT32, that arose from the whole genome duplication	87	
YLR171W	(Overlapping APS1 ORF) Aps1: Small subunit of the clathrin-associated adaptor complex AP-1, which is involved in protein sorting at the trans-Golgi network; homolog of the sigma subunit of the mammalian clathrin AP-1 complex	91	Aps1 ORF
Sec22	R-SNARE protein; assembles into SNARE complex with Bet1p, Bos1p and Sed5p; cycles between the ER and Golgi complex; involved in anterograde and retrograde transport between the ER and Golgi; synaptobrevin homolog	96	
Gdi1	GDP dissociation inhibitor, regulates vesicle traffic in secretory pathways by regulating the dissociation of GDP from the Sec4/Ypt/rab family of GTP binding proteins	99	

Table 2-1: Summary of top-ranking Sfh2 cofit genes.

Genes are presented in the functional categories indicated at the top row of the tables. The function of the yeast genes is adapted from Saccharomyces genome database (www.yeastgenome.org). In the right two columns, cofit gene rank and alias is shown.

Gene	Table 1: Lipid Metabolism	Rank in Sfh2 cofitness list	Alias
Srf1	Regulator of phospholipase D (Spo14p); interacts with Spo14p and regulates its catalytic activity; capable of buffering the toxicity of C16:0 platelet activating factor, a lipid that accumulates intraneuronally in Alzheimer's patients	5	
Inp54	Phosphatidylinositol 4,5-bisphosphate 5-phosphatase with a role in secretion, localizes to the endoplasmic reticulum via the C-terminal tail; lacks the Sac1 domain and proline-rich region found in the other 3 INP proteins	8	
Erg25	C-4 methyl sterol oxidase, catalyzes the first of three steps required to remove two C-4 methyl groups from an intermediate in ergosterol biosynthesis; mutants accumulate the sterol intermediate 4,4-dimethylzymosterol	18	
Svf1	Protein with a potential role in cell survival pathways, required for the diauxic growth shift; expression in mammalian cells increases survival under conditions inducing apoptosis; mutant has increased aneuploidy tolerance	21	
Orm2	Evolutionarily conserved protein, similar to Orm1p; required for resistance to agents that induce unfolded protein response; Orm1p and Orm2p together control membrane biogenesis by coordinating lipid homeostasis with protein quality control; protein abundance increases in response to DNA replication stress	23	
Nem1	Probable catalytic subunit of Nem1p-Spo7p phosphatase holoenzyme; regulates nuclear growth by controlling phospholipid biosynthesis, required for normal nuclear envelope morphology and sporulation; homolog of the human protein Dullard	25	
Sec59	Dolichol kinase, catalyzes the terminal step in dolichyl monophosphate (Dol-P) biosynthesis; required for viability and for normal rates of lipid intermediate synthesis and protein N-glycosylation	36	
YCR049C	(Overlapping ARE1 ORF) Are1: Acyl-CoA:sterol acyltransferase; endoplasmic reticulum enzyme that contributes the major sterol esterification activity in the absence of oxygen; ARE1 has a paralog, ARE2, that arose from the whole genome duplication	37	Are1 ORF
Pip2	Autoregulatory oleate-specific transcriptional activator of peroxisome proliferation, contains Zn(2)-Cys(6) cluster domain, forms heterodimer with Oaf1p, binds oleate response elements (OREs), activates beta-oxidation genes; PIP2 has a paralog, OAF1, that arose from the whole genome duplication	39	

Gene	Table 1: Lipid Metabolism (cont.)	Rank in Sfh2 cofitness list	Alias
Csg2	Endoplasmic reticulum membrane protein, required for mannosylation of inositolphosphorylceramide and for growth at high calcium concentrations; protein abundance increases in response to DNA replication stress	43	
Spo7	Putative regulatory subunit of Nem1p-Spo7p phosphatase holoenzyme, regulates nuclear growth by controlling phospholipid biosynthesis, required for normal nuclear envelope morphology, premeiotic replication, and sporulation	46	
Scs3	Protein required for inositol prototrophy; required for normal ER membrane biosynthesis; ortholog of the FIT family of proteins involved in triglyceride droplet biosynthesis and homologous to human FIT2; disputed role in the synthesis of inositol phospholipids from inositol	64	
Vps74	Golgi phosphatidylinositol-4-kinase effector and PtdIns4P sensor; interacts with the cytosolic domains of cis and medial glycosyltransferases, and in the PtdIns4P-bound state mediates the targeting of these enzymes to the Golgi; interacts with the catalytic domain of Sac1p, the major cellular PtdIns4P phosphatase, to direct dephosphosphorylation of the Golgi pool of PtdIns4P; tetramerization required for function; ortholog of human GOLPH3/GPP34/GMx33	66	GOLPH3
Erg11	Lanosterol 14-alpha-demethylase; catalyzes the C-14 demethylation of lanosterol to form 4,4"-dimethyl cholesta-8,14,24-triene-3-beta-ol in the ergosterol biosynthesis pathway; member of the cytochrome P450 family; associated and coordinately regulated with the P450 reductase Ncp1p	68	
Cdc50	Endosomal protein that interacts with phospholipid flippase Drs2p; interaction with Cdc50p is essential for Drs2p catalytic activity; mutations affect cell polarity and polarized growth; similar to Lem3p; CDC50 has a paralog, YNR048W, that arose from the whole genome duplication	73	
Spo14	Phospholipase D; catalyzes the hydrolysis of phosphatidylcholine, producing choline and phosphatidic acid; involved in Sec14p-independent secretion; required for meiosis and spore formation; differently regulated in secretion and meiosis; participates in transcription initiation and/or early elongation of specific genes; interacts with foot domain of RNA polymerase II; deletion results in abnormal CTD-Ser5 phosphorylation of RNA polymerase II at specific promoter regions	82	
Ecm22	Sterol regulatory element binding protein; regulates transcription of sterol biosynthetic genes; contains Zn[2]-Cys[6] binuclear cluster; relocates from intracellular membranes to perinuclear foci on sterol depletion; ECM22 has a paralog, UPC2, that arose from the whole genome duplication	95	
UPC2	Sterol regulatory element binding protein; induces transcription of sterol biosynthetic genes and of DAN/TIR gene products; relocates from intracellular membranes to perinuclear foci on sterol depletion; UPC2 has a paralog, ECM22, that arose from the whole genome duplication	103	

Gene	Table 1: Signal Transduction Pathways	Rank in Sfh2 cofitness list	Alias
Izh2	Plasma membrane protein involved in zinc homeostasis and osmotin-induced apoptosis; transcription regulated by Zap1p, zinc and fatty acid levels; similar to mammalian adiponectins; deletion increases sensitivity to elevated zinc	4	
Rho5	Non-essential small GTPase of the Rho/Rac subfamily of Ras-like proteins, likely involved in protein kinase C (Pkc1p)-dependent signal transduction pathway that controls cell integrity	28	
Cnb1	Calcineurin B; the regulatory subunit of calcineurin, a Ca++/calmodulin-regulated type 2B protein phosphatase which regulates Crz1p (a stress-response transcription factor), the other calcineurin subunit is encoded by CNA1 and/or CMP1; protein abundance increases in response to DNA replication stress	31	
YLL007C	Homolog of mammalian ELMO (Engulfment and celL MOtility); upstream component for regulation through the small GTPase Rho5p; may form a complex with Dck1p that acts as a GEF for Rho5p; cytoplasmic protein that relocates to mitochondria under oxidative stress; implicated in mitophagy; not an essential protein	42	Lmo1
Ckb1	Beta regulatory subunit of casein kinase 2 (CK2), a Ser/Thr protein kinase with roles in cell growth and proliferation; CK2, comprised of CKA1, CKA2, CKB1 and CKB2, has many substrates including transcription factors and all RNA polymerases	55	
Asc1	G-protein beta subunit and guanine nucleotide dissociation inhibitor for Gpa2p; ortholog of RACK1 that inhibits translation; core component of the small (40S) ribosomal subunit; regulates P-body formation induced by replication stress; represses Gcn4p in the absence of amino acid starvation	59	
Gpa2	Nucleotide binding alpha subunit of the heterotrimeric G protein that interacts with the receptor Gpr1p, has signaling role in response to nutrients; green fluorescent protein (GFP)-fusion protein localizes to the cell periphery	60	
Ira1	GTPase-activating protein; negatively regulates RAS by converting it from the GTP- to the GDP-bound inactive form, required for reducing cAMP levels under nutrient limiting conditions, mediates membrane association of adenylate cyclase; IRA1 has a paralog, IRA2, that arose from the whole genome duplication	86	
Ckb2	Beta' regulatory subunit of casein kinase 2 (CK2), a Ser/Thr protein kinase with roles in cell growth and proliferation; CK2, comprised of CKA1, CKA2, CKB1 and CKB2, has many substrates including transcription factors and all RNA polymerase	94	
Gpr1	Plasma membrane G protein coupled receptor (GPCR) that interacts with the heterotrimeric G protein alpha subunit, Gpa2p, and with Plc1p; sensor that integrates nutritional signals with the modulation of cell fate via PKA and cAMP synthesis	97	
Gal83	One of three possible beta-subunits of the Snf1 kinase complex, allows nuclear localization of the Snf1 kinase complex in the presence of a nonfermentable carbon source; contains glycogen-binding domain	100	
Snf3	Plasma membrane low glucose sensor, regulates glucose transport; contains 12 predicted transmembrane segments and a long C-terminal tail required for induction of hexose transporters; also senses fructose and mannose; SNF3 has a paralog, RGT2, that arose from the whole genome duplication	101	

Gene	Table 1: Membrane Protein Extraction	Rank in Sfh2 cofitness list	Alias
Ssm4	Ubiquitin-protein ligase involved in ER-associated protein degradation; located in the ER/nuclear envelope; ssm4 mutation suppresses mRNA instability caused by an rna14 mutation	2	
Ubc7	Ubiquitin conjugating enzyme, involved in the ER-associated protein degradation pathway; requires Cue1p for recruitment to the ER membrane; proposed to be involved in chromatin assembly	6	
YER084W	(ORF overlapping Get2 promoter) Get2: Subunit of the GET complex; involved in insertion of proteins into the ER membrane; required for the retrieval of HDEL proteins from the Golgi to the ER in an ERD2 dependent fashion and for meiotic nuclear division	11	Get2 promote
Cue1	Ubiquitin-binding protein; endoplasmic reticulum membrane protein that recruits the ubiquitin-conjugating enzyme Ubc7p to the ER where it functions in protein degradation; contains a CUE domain that binds ubiquitin to facilitate intramolecular monoubiquitination; CUE1 has a paralog, CUE4, that arose from the whole genome duplication	27	
Cdc48	AAA ATPase involved in multiple processes; subunit of polyubiquitin-selective segregase complex involved in ERAD, cell wall integrity during heat stress, mitotic spindle disassembly; subunit of complex involved in mitochondria-associated degradation; role in mobilizing membrane bound transcription factors by regulated ubiquitin/proteasome-dependent processing; roles in macroautophagy, PMN, RAD, ribophagy, and homotypic ER membrane fusion; functional ortholog of human p97/VCP	34	
Pre9	Alpha 3 subunit of the 20S proteasome, the only nonessential 20S subunit; may be replaced by the alpha 4 subunit (Pre6p) under stress conditions to create a more active proteasomal isoform	41	
Ubx4	UBX domain-containing protein that interacts with Cdc48p; involved in degradation of polyubiquitinated proteins via the ERAD (ER-associated degradation) pathway; modulates the Cdc48p-Nplp-Ufd1p AAA ATPase complex during its role in delivery of misfolded proteins to the proteasome; protein abundance increases in response to DNA replication stress	44	
Usa1	Scaffold subunit of the Hrd1p ubiquitin ligase that also promotes ligase oligomerization; involved in ER-associated protein degradation (ERAD); interacts with the U1 snRNP-specific protein, Snp1p	76	
YML012C-A	(Overlapping UBX2 ORF) Ubx2: Bridging factor involved in ER-associated protein degradation (ERAD); bridges the cytosolic Cdc48p-Npl1p-Ufd1p ATPase complex and the membrane associated Ssm4p and Hrd1p ubiquitin ligase complexes; contains a UBX (ubiquitin regulatory X) domain and a ubiquitin-associated (UBA) domain; redistributes from the ER to lipid droplets during the diauxic shift and stationary phase; required for the maintenance of lipid homeostasis	50	Ubx2 ORF
Ste24	Highly conserved zinc metalloprotease that functions in two steps of a-factor maturation, C-terminal CAAX proteolysis and the first step of N-terminal proteolytic processing; contains multiple transmembrane spans	53	

Gene	Table 1: Membrane Protein Insertion	Rank in Sfh2 cofitness list	Alias
YDR186C	Protein involved in SRP-independent targeting of substrates to the ER; component of an alternative ER targeting pathway that has partial functional redundancy with the GET pathway; preference for substrates with downstream transmembrane domains; interacts with Env10p/Snd2p and Pho88p/Snd3p; can compensate for loss of SRP; co-purifies with ribosomes; GFP-fusion protein localizes to the cytoplasm	3	Snd1
Get3	Guanine nucleotide exchange factor for Gpa1p; amplifies G protein signaling; subunit of the GET complex, which is involved in Golgi to ER trafficking and insertion of proteins into the ER membrane; has low-level ATPase activity; protein abundance increases in response to DNA replication stress	10	
Sec65	Subunit of the signal recognition particle (SRP), involved in protein targeting to the ER; interacts with Srp54p; homolog of mammalian SRP19	24	
Pho88	Protein involved in SRP-independent targeting of substrates to the ER; component of an alternative ER targeting pathway that has partial functional redundancy with the GET pathway; preference for substrates with downstream transmembrane domains; interacts with Snd1p, Env10p/Snd2p, and Sec61p-translocon subunits; can compensate for loss of SRP; role in phosphate transport, interacting with Pho88p, and in the maturation of secretory proteins	47	Snd3
Srp68	Core component of the signal recognition particle (SRP) complex; SRP complex functions in targeting nascent secretory proteins to the endoplasmic reticulum (ER) membrane; relocalizes from cytoplasm to the nuclear periphery upon DNA replication stress	56	
Get2	Subunit of the GET complex; involved in insertion of proteins into the ER membrane; required for the retrieval of HDEL proteins from the Golgi to the ER in an ERD2 dependent fashion and for meiotic nuclear division	77	

Gene	Table 1: Cell Cycle	Rank in Sfh2 cofitness list	Alias
YDR199W	(Overlapping Vps64 ORF) Vps64:Protein required for cytoplasm to vacuole targeting of proteins; forms a complex with Far3p and Far7p to Far11p involved in recovery from pheromone-induced cell cycle arrest; mutant has increased aneuploidy tolerance	9	Vps64 ORF
Far7	Protein involved in recovery from pheromone-induced cell cycle arrest; acts in a Far1p-independent pathway; interacts with Far3p, Far8p, Far9p, Far10p, and Far11p; protein abundance increases in response to DNA replication stress	14	
Far8	Protein involved in recovery from cell cycle arrest in response to pheromone, in a Far1p-independent pathway; interacts with Far3p, Far7p, Far9p, Far10p, and Far11p	15	
Cdc20	Activator of anaphase-promoting complex/cyclosome (APC/C); APC/C is required for metaphase/anaphase transition; directs ubiquitination of mitotic cyclins, Pds1p, and other anaphase inhibitors; cell-cycle regulated; potential Cdc28p substrate; relative distribution to the nucleus increases upon DNA replication stress	16	
Far3	Protein of unknown function; involved in recovery from cell cycle arrest in response to pheromone, in a Far1p-independent pathway; interacts with Far7p, Far8p, Far9p, Far10p, and Far11p; localizes to the endoplasmic reticulum; protein abundance increases in response to DNA replication stress	32	
YMR052C-A	(Overlapping Far3 ORF) Far3:Protein of unknown function; involved in recovery from cell cycle arrest in response to pheromone, in a Far1p-independent pathway; interacts with Far7p, Far8p, Far9p, Far10p, and Far11p; localizes to the endoplasmic reticulum; protein abundance increases in response to DNA replication stress	30	Far3 ORF
Clb3	B-type cyclin involved in cell cycle progression; activates Cdc28p to promote the G2/M transition; may be involved in DNA replication and spindle assembly; accumulates during S phase and G2, then targeted for ubiquitin-mediated degradation; relative distribution to the nucleus increases upon DNA replication stress	71	
Far10	Protein involved in recovery from cell cycle arrest in response to pheromone, in a Far1p-independent pathway; interacts with Far3p, Far7p, Far8p, Far9p, and Far11p; potential Cdc28p substrate	84	
Pcl6	Pho85p cyclin of the Pho80p subfamily; forms the major Glc8p kinase together with Pcl7p and Pho85p; involved in the control of glycogen storage by Pho85p; stabilized by Elongin C binding	74	
Vps64	Protein required for cytoplasm to vacuole targeting of proteins; forms a complex with Far3p and Far7p to Far11p involved in recovery from pheromone-induced cell cycle arrest; mutant has increased aneuploidy tolerance	19	Far9

Gene	Table 1: Translation	Rank in Sfh2 cofitness list	Alias
Nop14	Nucleolar protein, forms a complex with Noc4p that mediates maturation and nuclear export of 40S ribosomal subunits; also present in the small subunit processome complex, which is required for processing of pre-18S rRNA	7	
Trm9	tRNA methyltransferase; catalyzes modification of wobble bases in tRNA anticodons to 2, 5-methoxycarbonylmethyluridine and 5-methoxycarbonylmethyl-2-thiouridine; may act as part of a complex with Trm112p; deletion mutation increases translational infidelity, including amino acid misincorporation and -1 frameshifting, and also confers resistance to zymocin; null mutant displays activation of stress responses	33	
YGR054W	Eukaryotic initiation factor (eIF) 2A; associates specifically with both 40S subunits and 80 S ribosomes, and interacts genetically with both eIF5b and eIF4E; homologous to mammalian eIF2A	72	eIF2A
Pub1	Poly (A)+ RNA-binding protein; abundant mRNP-component protein that binds mRNA and is required for stability of many mRNAs; component of glucose deprivation induced stress granules, involved in P-body-dependent granule assembly; protein abundance increases in response to DNA replication stress	90	
Not1	Component of the CCR4-NOT complex, which has multiple roles in regulating mRNA levels including regulation of transcription and destabilizing mRNAs by deadenylation; basal transcription factor	92	

Gene	Table 1: Miscellaneous Functions	Rank in Sfh2 cofitness list	Alias
Mnl2	Putative mannosidase involved in ER-associated protein degradation; localizes to the endoplasmic reticulum; sequence similarity with seven-hairpin glycosidase (GH47) family members, such as Mns1p and Mnl1p, that hydrolyze 1,2-linked alpha-D-mannose residues; non-essential gene	12	
Env9	Protein proposed to be involved in vacuolar functions; mutant shows defect in CPY processing and defects in vacuolar morphology; has similarity to oxidoreductases, found in lipid particles; required for replication of Brome mosaic virus in S. cerevisiae, a model system for studying replication of positive-strand RNA viruses in their natural hosts	26	
Tom7	Component of the TOM (translocase of outer membrane) complex responsible for recognition and initial import steps for all mitochondrially directed proteins; promotes assembly and stability of the TOM complex	51	
Cbf1	Dual function helix-loop-helix protein; binds the motif CACRTG present at several sites including MET gene promoters and centromere DNA element I (CDEI); affects nucleosome positioning at this motif; associates with other transcription factors such as Met4p and Isw1p to mediate transcriptional activation or repression; associates with kinetochore proteins and required for efficient chromosome segregation; protein abundance increases in response to DNA replication stress	54	
Yml037C	Putative protein of unknown function with some characteristics of a transcriptional activator; may be a target of Dbf2p-Mob1p kinase; GFP-fusion protein co-localizes with clathrin-coated vesicles; YML037C is not an essential gene	58	
Rbd2	Possible rhomboid protease, has similarity to eukaryotic rhomboid proteases including Pcp1p	61	
Mge1	Mitochondrial matrix cochaperone, acts as a nucleotide release factor for Ssc1p in protein translocation and folding; also acts as cochaperone for Ssq1p in folding of Fe-S cluster proteins; homolog of E. coli GrpE	62	
Fsf1	Putative protein, predicted to be an alpha-isopropylmalate carrier; belongs to the sideroblastic-associated protein family; non-tagged protein is detected in purified mitochondria; likely to play a role in iron homeostasis	65	
Yml6	Mitochondrial ribosomal protein of the large subunit, has similarity to E. coli L4 ribosomal protein and human mitoribosomal MRP-L4 protein; essential for viability, unlike most other mitoribosomal proteins	67	
Dal80	Negative regulator of genes in multiple nitrogen degradation pathways; expression is regulated by nitrogen levels and by Gln3p; member of the GATA-binding family, forms homodimers and heterodimers with Gzf3p; DAL80 has a paralog, GZF3, that arose from the whole genome duplication	70	
Mca1	Ca2+-dependent cysteine protease; may cleave specific substrates during the stress response; regulates apoptosis upon H2O2 treatment; required for clearance of insoluble protein aggregates during normal growth; implicated in cell cycle dynamics; undergoes autocatalytic processing; similar to mammalian metacaspases, but exists as a monomer due to an extra pair of anti-parallel beta-strands that form a continuous beta-sheet, blocking potential dimerization	78	
Trr1	Cytoplasmic thioredoxin reductase; key regulatory enzyme that determines the redox state of the thioredoxin system, which acts as a disulfide reductase system and protects cells against both oxidative and reductive stress; protein abundance increases in response to DNA replication stress; TRR1 has a paralog, TRR2, that arose from the whole genome duplication	80	
Msn1	Transcriptional activator; involved in regulation of invertase and glucoamylase expression, invasive growth and pseudohyphal differentiation, iron uptake, chromium accumulation, and response to osmotic stress; localizes to the nucleus; relative distribution to the nucleus increases upon DNA replication stress	93	

Gene	Table 1: Unknown Function	Rank in Sfh2 cofitness list	Alias
Pin2	Protein that induces appearance of [PIN+] prion when overproduced; predicted to be palmitoylated	22	
Gdt1	Putative protein of unknown function; expression is reduced in a gcr1 null mutant; GFP-fusion protein localizes to the vacuole; expression pattern and physical interactions suggest a possible role in ribosome biogenesis	35	
Acf4	Protein of unknown function, computational analysis of large-scale protein-protein interaction data suggests a possible role in actin cytoskeleton organization; potential Cdc28p substrate	49	
YHL045W	Putative protein of unknown function; not an essential gene	69	Pxp3
YPR089W	Protein of unknown function; exhibits genetic interaction with ERG11 and protein-protein interaction with Hsp82p	79	
Mtc4	Protein of unknown function, required for normal growth rate at 15 degrees C; green fluorescent protein (GFP)-fusion protein localizes to the cytoplasm in a punctate pattern; mtc4 is synthetically sick with cdc13-1	81	
YJR018W	Dubious open reading frame unlikely to encode a functional protein, based on available experimental and comparative sequence data	83	
YGL114W	Putative protein of unknown function; predicted member of the oligopeptide transporter (OPT) family of membrane transporters	88	
Dlt1	Protein of unknown function, mutant sensitive to 6-azauracil (6AU) and mycophenolic acid (MPA)	89	
Erg29	Protein of unknown function that may be involved in iron metabolism; mutant bm-8 has a growth defect on iron-limited medium that is complemented by overexpression of Yfh1p; shows localization to the ER; highly conserved in ascomycetes	98	

Vesicle transport

Cofit genes that were classified as being involved in vesicle transport were predominantly associated with post-Golgi/endocytic trafficking. These include a Rab5-like GTPase involved in endocytosis (Ypt52; Cabrera et. al., 2013), regulators of Ypt/rab GTP binding proteins involved in the secretory pathway (Gdi1 and Gyp1; Garrett et. al., 1994, Segev 2001), members of the AP-1 clathrin-associated protein complex (Apm1, Apl2, Laa1; Liu et. al., 2008), proteins involved in endocytic recycling (Cdc50, Rcy1, Ypt31; Furuta et. al., 2007), exocyst complex members involved in exocytosis at the bud tip (Exo70, Exo84; Mei et al., 2018), and proteins involved in ER/Golgi transport (Gcs1, Sec21, Sec22, Sec24; Duden 2003, Xu et. al., 2013) (Figure 2-6).

Lipid Metabolism

Cofit genes in the lipid metabolism category included those that regulate phospholipids, sterols, and sphingolipids (Figure 2-7; see also discussion). PIP-modulating genes include a phosphatidylinositol 4,5-bisphosphate 5-phosphatase (Inp54) and a Golgi phosphatidylinositol-4-kinase effector/phosphatidylinositol-4-phosphate (PtdIns4P) sensor (Vps74/GOLPH3). Phosphatidylcholine (PtdCho) effectors include the PtdCho-hydrolyzing phospholipase D, Spo14, and its regulator, Srf1. Spo7 and Nem1 are two cofit genes that together regulate phospholipid homeostasis through the activation of the diacylglycerol (DAG)-producing phosphatidic acid (PtdOH) phosphatase (Pah1), a key regulatory step that modulates the ratio between phospholipids and triacylglycerol (TAG; Su et. al., 2018). Cofit genes that act in sterol metabolism include Erg11 and Erg25 which both use molecular oxygen to demethylate lanosterol, and a dubious genomic region (YCR049C) overlapping the Are1 acyl-CoA:sterol acyltransferase responsible for the major sterol esterification activity in the absence of oxygen (Valachovič et. al., 2001).

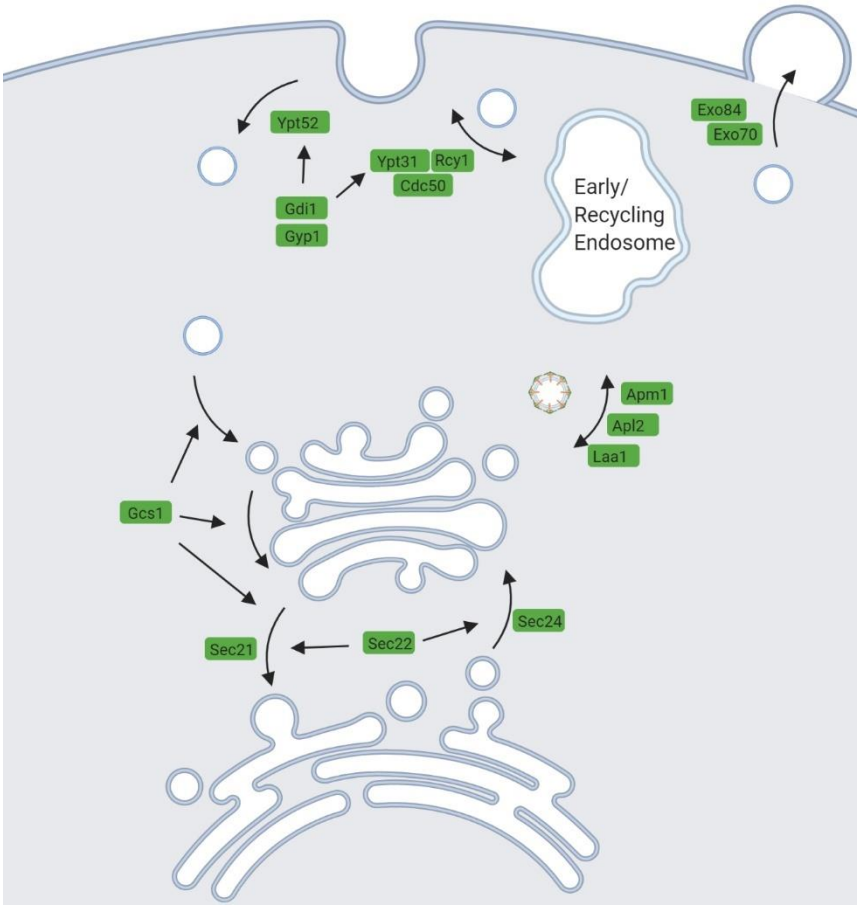

Figure 2-6: Sfh2 cofit genes involved in vesicle transport

This category includes proteins involved in post-Golgi processes such as exocytosis (Exo70, Exo84), endocytosis (Ypt52), endosome recycling to the plasma membrane (Ypt31, Rcy1, Cdc50), effectors of Ypt/rab GTPases (Gdi1, Gyp1), and TGN-endosome transport (Apm1, Apl2, Laa1). This list also includes components of ER-Golgi transport (Gcs1, Sec21, Sec22, Sec24).

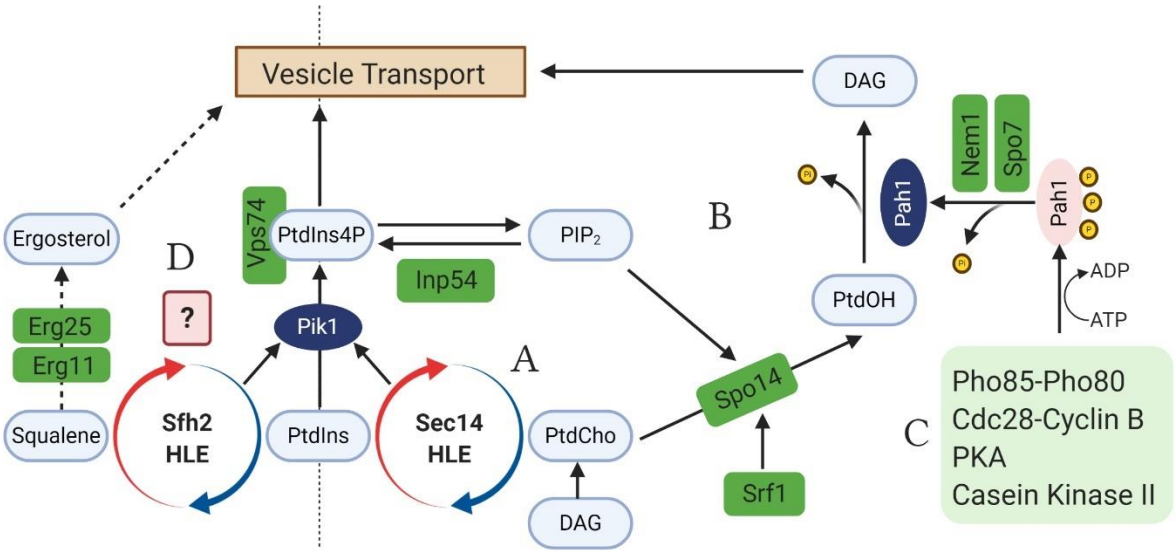

Figure 2-7: Sfh2 lipid metabolism cofit genes in the context of Sec14 function

(A) Sec14 coordinates lipid metabolism with membrane trafficking by potentiating PtdIns4P production. PtdCho binding (sensing) serves as a proxy for the consumption of diacylglycerol (DAG), a lipid required for promoting vesicle formation. This metabolic information is translated into a phosphoinositide signaling event through heterotypic ligand exchange (HLE) of PtdCho and PtdIns within the Sec14 protein. HLE stimulates PtdIns4P production by the Pik1p PtdIns 4-OH kinase (PIK). PtdIns4P substitutes for DAG in promoting vesicle budding.
(B) Sfh2 cofit genes (green rectangles) are involved in lipid metabolic pathways that regulate vesicle transport. (C) Kinases that phosphorylate and inactivate Pah1 are either members or are regulated by Sfh2 cofit genes (light green box; see discussion). (D) Much like Sec14, Sfh2 may be sensing squalene as a proxy for sterol metabolic information and translating this into a PIP signal. Sterol homeostasis may be required for proper vesicle formation and transport.

This list also includes both yeast sterol regulatory element binding protein (SREBP) transcription factors Ecm22 and Upc2 which induce the transcription of sterol biosynthetic genes. Cofit genes that coordinate sphingolipid synthesis include Svf1, Orm2, and Csg2 (Brace et. al., 2007; Breslow et. al., 2010).

Membrane protein insertion and extraction

The next category of cofit genes are involved in both the recruitment of membrane proteins and the degradation of misfolded membrane proteins. Most proteins destined for insertion into a membrane or the secretory pathway are escorted to the ER membrane by the signal recognition particle (SRP) and channeled through the Sec61 translocon (Wild et. al., 2004). Further, certain tail-anchored (TA) proteins cannot utilize the SRP because their single transmembrane domain (TMD) is located at the C-terminus and therefore incompatible with SRP. For this reason, Get1, Get2, and Get3 are responsible for the insertion of C-terminal TA proteins into the ER membrane (Schuldiner et. al., 2008). Finally, a subset of membrane proteins that are neither escorted by the GET proteins or SRP are targeted to the ER by a third route via the three SRP-independent targeting (SND) proteins (Aviram et. al., 2016). In this category of cofit genes, two subunits of the SRP, Sec65 and Srp68, Get2 and Get3, and Snd1 and Snd3 are identified as Sfh2 cofit genes.

Conversely, when membrane proteins misfold, the cell requires their extraction and degradation through a process mediated by ERAD, Cdc48, and the proteasome (Wolf et. al. 2012). With respect to this process, proteins required for the ubiquitination of misfolded membrane proteins (Ssm4, Ubc7, Cue1), the Cdc48 AAA ATPase that extracts misfolded substrates from the ER, Cdc48 interacting proteins (Ubx4 and YML012C-A; a genomic region

overlapping Ubx2), an ERAD scaffold protein (Usa1), and the alpha 3 subunit of the 20S proteasome (Pre9) were identified as Sfh2 cofit genes.

Furthermore, an additional layer of regulation is required for proteins that prematurely misfold during translocation into the ER resulting in "clogged" translocons. Ste24 is a metalloprotease that engages clogged translocons and cleaves the lodged proteins which are then degraded by the proteasome (Ast et. al., 2016). Ste24 is a Sfh2 cofit gene.

Signal transduction pathways

Cofit genes involved in signal transduction pathways are here defined as proteins that respond to extrinsic signals and participate in a known signaling relay. In this analysis, genes were identified that comprise components of nutrient-sensing signaling pathways in yeast. Each of these three signaling pathways initiate with the stimulation of a plasma membrane receptor by extrinsic signals.

Most strikingly, several vital components of a G-protein coupled receptor (GPCR) signaling pathway were identified. In yeast, transition from a non-fermentable carbon source to glucose triggers a signaling cascade that activates adenylyl cyclase and cAMP production, a second messenger that activates protein kinase A (PKA), a kinase that promotes growth and cell cycle progression among other biological processes (Thevelein et. al., 1999). This signaling pathway is mediated by the glucose-sensing GPCR (Gpr1), its associated Gα subunit (Gpa2) and two GTPases (Ras1/2) which collectively stimulate the adenylyl cyclase (Cyr1; Figure 2- Kim et. al., 2013). Gpr1, Gpa2 and its nucleotide dissociation inhibitor Asc1, and Ira1, the GTPase activating protein (GAP) of Ras1/2, were identified as cofit genes (Zeller et. al., 2007; Tanaka et. al., 2006). An additional, non-redundant plasma membrane glucose sensor, Snf3, also ranked among the top 100 Sfh2 cofit genes (Kim et. al., 2013).

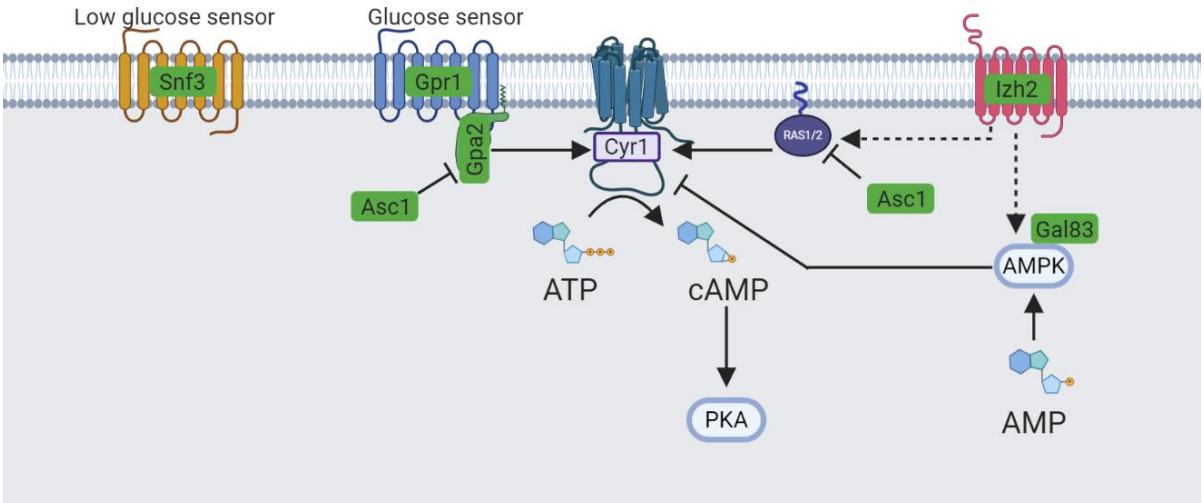

Figure 2-8: Signal transduction Sfh2 cofit genes are involved in nutrient sensing pathways

Nutrient sensing pathways are enriched in the signal transduction category of Sfh2 cofit genes (green rectangles). Under low glucose conditions, ATP levels drop, and AMP levels rise. AMP activates the AMP kinase (AMPK/Snf1) which activates catabolic processes and inhibits anabolic processes to maintain cellular energy homeostasis. AMPK also inactivates adenylyl cyclase (Cyr1) under these conditions. Localization of AMPK to the nucleus and its nuclear target proteins requires binding to Gal83. Under high glucose conditions, glucose binding to Gpr1 initiates a signaling cascade that activates PKA which activates growth-promoting processes. Izh2 is a plasma membrane receptor that functions upstream of both AMPK and Ras2. Snf3 is a non-redundant plasma membrane glucose sensor involved in a separate signaling cascade.

Further, two genes involved in the AMP-activated protein kinase (AMPK) pathway were identified, Izh2 and Gal83. AMPK is a heterotrimeric complex and master regulator in the response to nutrient-limiting conditions (Herzig and Shaw, 2018). AMPK is activated by sensing low cellular ATP levels via AMP binding. AMPK phosphorylation activates catabolic processes and inhibits anabolic processes to maintain cellular energy homeostasis. Izh2 is the plasma membrane receptor yeast homolog of the mammalian Progestin and AdipoQ Receptor family (mammalian AdipoR1/AdipoR2; PAQR) known to regulate glucose and lipid metabolism by stimulating and enhancing AMPK activity in mammalian cells (Yamauchi et. al., 2002, Narasimhan et. al., 2005; Kubota et. al., 2007). Interestingly, Izh2 can also functions upstream of Ras2 in the programmed cell death signaling pathway activated by the antimicrobial protein osmotin (Figure 2-8; Narasimhan et. al., 2005). Gal83 is the primary regulatory β-subunit of AMPK (Snf1) which is required for the nuclear localization of Snf1 in response to glucose starvation (Hedbacker et. al., 2006). It was also discovered that Snf1 (the AMPK catalytic subunit) phosphorylates and inactivates the adenylyl cyclase under conditions of low glucose (Figure 2-8; Nicastro et. al., 2015).

Cell cycle

Strikingly, the cell cycle category of Sfh2 cofit genes consisted of nearly every member of a protein complex involved in cell cycle arrest in response to pheromone (Far3, Far7, Far8, Far9/Vps64, and Far10; Kemp and Sprague, 2003). Although it did not meet the requirements as a Sfh2 cofit gene, the remaining member of this complex (Far11) ranked only 116th in the Sfh2 cofitness list. Cells lacking in this complex recover from the G_1-arrest of the cell cycle induced by exposure to pheromone whereas WT cells cannot. However, the precise means by which this complex regulates the cell cycle is still unknown.

This category also included, Clb3, a mitotic B cyclin that activates the Cdc28 cyclin-dependent kinase (CDK) to progress through G_2/M, Cdc20, the activator of anaphase-promoting complex/cyclosome (APC/C) at mitotic exit, and Pcl6, a cyclin of the Pho85 CDK (Mendenhall and Hodge, 1998; Visintin et. al., 1997; Conrad et. al., 2014). Interestingly, Cdc20-APC/C targets mitotic B cyclins for degradation which promotes progression through mitosis (Lara-Gonzalez et. al 2019).

Translation

Cofit genes characterized as being involved in translation include Nop14, an architectural protein involved in 40S ribosome assembly and maturation; Trm9, a tRNA methyltransferase of uridine at the wobble position that is involved in translational fidelity and proteostasis; eIF2A (YGR054W), an alternative initiation factor that catalyzes translation under stressful environmental conditions which inhibit the activity of the canonical initiation factor eIF2α; Pub1, a poly-A RNA binding protein involved in the formation of messenger ribonucleoprotein (mRNP) stress granules in energy-depleted yeast; and Not1, the scaffold protein of the Ccr4-Not complex that promotes mRNA decay by deadenylation in mRNP P-bodies (Chaker-Margot et. al., 2017; Pereira et. al., 2018; Starck et. al., 2016; Kroschwald et. al., 2018; Parker et. al., 2007).

Terbinafine profiling

Because terbinafine induces the accumulation of squalene in yeast (Garaiová et. al., 2014), we interpret that this accumulation is what makes *sfh2Δ* yeast sensitive to terbinafine. To discern what biological functions rely on the squalene-sensing function of Sfh2, the HIPHOP chemogenomic database was mined to identify genes required for terbinafine resistance. The identification of Sfh2 cofit genes that are critical for resistance to squalene accumulation narrowed down possibilities for the specific biological function of Sfh2 in vivo.

Sfh2 cofit genes that were required for resistance to terbinafine included those involved in lipid metabolism, protein insertion into the membrane, and post-Golgi/endocytic vesicle sorting. Cofit genes that regulate phospholipid homeostasis include the Nem1/Spo7 protein phosphatase while cofit genes involved in the de novo sphingolipid synthesis pathway include Csg2 and Orm2. Surprisingly, Get1, Get2, and Get3 deletion strains were all identified as significantly sensitive to terbinafine. Finally, Rcy1, Cdc50, Apl2, Apm1, and Laa1 were Sfh2 cofit genes involved in vesicle sorting to and from the Golgi and early endosomes that were required for resistance to terbinafine and/or squalene accumulation (Liu et. al., 2008).

Discussion

Sec14-like PITPs are predicted to integrate the lipid metabolome with PIP signaling and a specific biological function (Bankaitis et. al., 2010). In Sec14, membrane trafficking from the TGN is mediated through the exchange of PtdIns and a unique secondary ligand within the Sec14 hydrophobic cavity (heterotypic ligand exchange; detailed in chapter one). Sfh2 is a yeast PITP with an enigmatic biological function yet its secondary ligand has been identified as squalene, an intermediate of sterol biosynthesis. Chemogenomic databases are powerful resources that can be used to generate and test hypotheses about a gene of interest in *S. cerevisiae*. The chemogenomic analysis of Sfh2 revealed several biological processes that overlap with Sfh2 function.

Chemogenomic data indicates that the loss of Sfh2 resembles defects in post-Golgi/endocytic vesicle sorting pathways. Sfh2 ablation also resembles defects in membrane lipid composition, particularly, phospholipid, sphingolipid, and sterol homeostasis. The loss of Sfh2 function also seems to affect the cell as if membrane protein homeostasis is aberrant. The effect of Sfh2 deletion also seems to resemble the inability to properly sense nutrient availability

signals and relay them to the cell. Further, the deletion of Sfh2 resembles the inability to regulate certain cell cycle checkpoints, specifically those controlled in response to pheromone. Finally, the deletion of Sfh2 shares some similarity to defects in the regulation of translation under stressed conditions.

Some chemogenomic functional interactions were validated. Sfh2 is required for the optimal function of anterograde trafficking from the ER and TGN. Functional overlap with sterol metabolic enzymes is supported because Sfh2 presumably senses the membrane composition or localization of its ligand, squalene. Further, the association of lipid metabolism, vesicle trafficking, and cell cycle regulation has precedent when we consider the case of the Sec14 antagonist and oxysterol-binding protein, Kes1. It too links membrane trafficking, PtdIns4P signaling, and sterol sensing with the ability to regulate cell proliferation (Mousley et. al., 2012). Most significantly, many members of this cohort of Sfh2 cofit genes are involved in known Sec14-associated pathways that are integral to its function (Figure 2-7A); namely, PIP and DAG metabolic pathways, lipids required for vesicle formation and transport. Spo14 encodes the sole phosphatidylinositol-4,5-bisphosphate-activated phospholipase D which produces PtdOH by the hydrolysis of PtdCho (Figure 2-7A). The normally non-essential Spo14 becomes essential under conditions that bypass the function of Sec14 to ensure that DAG pools crucial for TGN/endosomal trafficking are not exhausted by PtdCho biosynthesis (Figure 2-7A; Xie et. al., 1998; Bankaitis et. al., 2010). Further, the Nem1-Spo7 phosphatase heterodimer that activates Pah1 (the PtdOH phosphatase that generates DAG) are both Sfh2 cofit genes and required for resistance to terbinafine (Figure 2-7B). Several other Sfh2 cofit genes converge around this highly regulated metabolic step. Pah1 is phosphorylated and inactivated by Pho85-Pho80, Cdc28-cyclin B, PKA, and casein kinase II (Su et. al. 2018). Each of those kinases are either

members of or are regulated by Sfh2 cofit genes (See signal transduction cofit genes: Pcl6, Clb3, the GPCR pathway members, Ckb1 and Ckb2; Figure 2-7C). Based off chemogenomic data alone, a model for Sfh2 function could be described that mirrors Sec14 (Figure 2-7D). In response to perturbations in squalene and/or sterol homeostasis, Sfh2 may promote PtdIns4P production to restore membrane conditions that are conducive for vesicle formation and transport. Therefore, this analysis suggests that Sfh2 preserves the primary Sec14 function of coordinating lipid metabolism with membrane trafficking by potentiating PtdIns4P production.

This analysis provides a systematic approach to navigating chemogenomic data to provide functional information about a gene of interest. Chemogenomic data mining elucidated the complex biological function of Sfh2, gave evidence to support the Sec14-based model of PITP function, and shed light on the significance of squalene in the eukaryotic cell. This approach can be used for any gene in the database and may reveal novel insights about both well-established and uncharacterized genes.

CHAPTER III - FUNCTIONAL DIVERSIFICATION OF THE CHEMICAL LANDSCAPES OF YEAST SEC14-LIKE PHOSPHATIDYLINOSITOL TRANSFER PROTEIN LIPID-BINDING CAVITIES[*]

Summary

Phosphatidylinositol-transfer proteins (PITPs) are key regulators of lipid signaling in eukaryotic cells. These proteins both potentiate the activities of phosphatidylinositol (PtdIns) 4-OH kinases and help channel production of specific pools of PtdIns-4-phosphate (PtdIns4P) dedicated to specific biological outcomes. In this manner, PITPs represent a major contributor to the mechanisms by which the biological outcomes of phosphoinositide are diversified. The two-ligand priming model proposes that the engine by which Sec14-like PITPs potentiate PtdIns kinase activities is a heterotypic lipid exchange cycle where PtdIns is a common exchange substrate among the Sec14-like PITP family, but the second exchange ligand varies with the PITP. A major prediction of this model is that second-exchangeable ligand identity will vary from PITP to PITP. Thus, we used structural, computational and biochemical approaches to probe the diversities of the lipid binding cavity microenvironments of the yeast Sec14-like PITPs. Using Sfh2 and Sfh3 as models, we demonstrate these represent PtdIns/squalene and PtdIns/ergosterol exchange proteins, respectively. The collective data report that yeast Sec14-like PITP lipid-binding pockets indeed define diverse chemical microenvironments that translate into differential ligand binding specificities across this protein family.

[*] Reprinted with permission from Tripathi, Ashutosh, et al. "Functional diversification of the chemical landscapes of yeast Sec14-like phosphatidylinositol transfer protein lipid-binding cavities." *Journal of Biological Chemistry* 294.50 (2019): 19081-19098.

Introduction

Lipids play central roles in cell signaling in addition to their critical involvements in maintaining intracellular compartmentation. A significant aspect of lipid signaling involves the action and metabolism of phosphorylated derivatives of PtdIns. These phosphoinositides modulate an impressively wide range of cellular processes, including regulation of G-protein coupled receptor and receptor tyrosine kinase signaling at plasma membranes, actin dynamics, transcription and membrane trafficking (Strahl and Thorner, 2007). Although the basic involvements of specific lipid kinases in generating specific phosphoinositide species are well appreciated, recent studies indicate that the regulation of phosphoinositide production for specific signaling events is far more complicated. PtdIns kinases, particularly the PtdIns 4-OH kinases, are biologically insufficient enzymes that by themselves cannot produce enough PtdIns4P to overcome the activities of negative regulators of PtdIns4P signaling to promote productive signaling events (Schaaf et. al., 2008; Bankaitis et. al., 2010; Nile et. al., 2010; Grabon et. al., 2015). Rather, these enzymes require the activities of Sec14-like PtdIns transfer proteins (PITPs) to potentiate the robust synthesis of PtdIns4P so that the actions of PtdIns4P signaling antagonists are overcome in a precisely regulated manner.

Sec14-like PITPs are founding members of the large Sec14 protein superfamily, and the common unifying element of this superfamily is a conserved Sec14 (or CRAL-TRIO) fold (Schaaf et. al., 2008, Sha et. al., 1998; Yang et. al., 2013; Ren et. al., 2014). In that regard, while broad conservation of fold can provide indications of protein functional properties, functional diversification within a single fold class is manifested by virtue of finer structural features embedded within individual proteins. Such is the case within the Sec14 protein superfamily as exemplified by the fact that Sec14-like PITPs channel PtdIns 4-OH kinase activities to specific

yet diverse biological outcomes (Figure 3-1A) (Schaaf et. al., 2008; Bankaitis et. al., 2010; Nile et. al., 2010; Grabon et. al., 2015). The engine for doing so is proposed to be a heterotypic lipid exchange cycle where exchange of a 'second' ligand for PtdIns renders the PtdIns molecule a superior substrate for the lipid kinase (Figure 3-1B). The available data project that this primed 'PtdIns presentation' regime is a major mechanism for functionally specifying diverse biological outcomes for PtdIns4P signaling -- even in simple eukaryotic cells such as yeast (Wu et. al., 2000; Ren et. al., 2014; Li et. al., 2000; Routt et. al., 2005). The PtdIns presentation model for Sec14-like PITP function is founded upon structural data that project PtdIns-binding as a conserved activity across the Sec14 superfamily, whereas the nature of the second ligand is highly diversified (Schaaf et. al., 2008; Bankaitis et. al., 2010). This marked diversity in ligand binding specificities, together with the flexibility of the Sec14-fold, suggests that evolution has: (i) taken advantage of the fundamental architecture of this fold to accommodate a large variety of lipid ligands, and (ii) translated that biochemical diversity into a diversity of biological outcomes. Thus, although the general notion of conservation of overall fold across the Sec14 superfamily is an interesting one, it is the specific and differential biological outcome associated with each of these proteins that is central to our understanding of how phosphoinositide signaling is spatially organized and functionally diversified in cells. These underlying mechanisms remain largely uninvestigated, however. It is in this context that integrating primary sequence comparisons with structural properties offers powerful opportunities to glean new insights into how functional diversity is incorporated into an otherwise hardwired Sec14-fold.

Herein, we report systematic investigation of the structural features of yeast Sec14-like PITPs to gain an understanding of molecular mechanisms that generate diversity and specificity

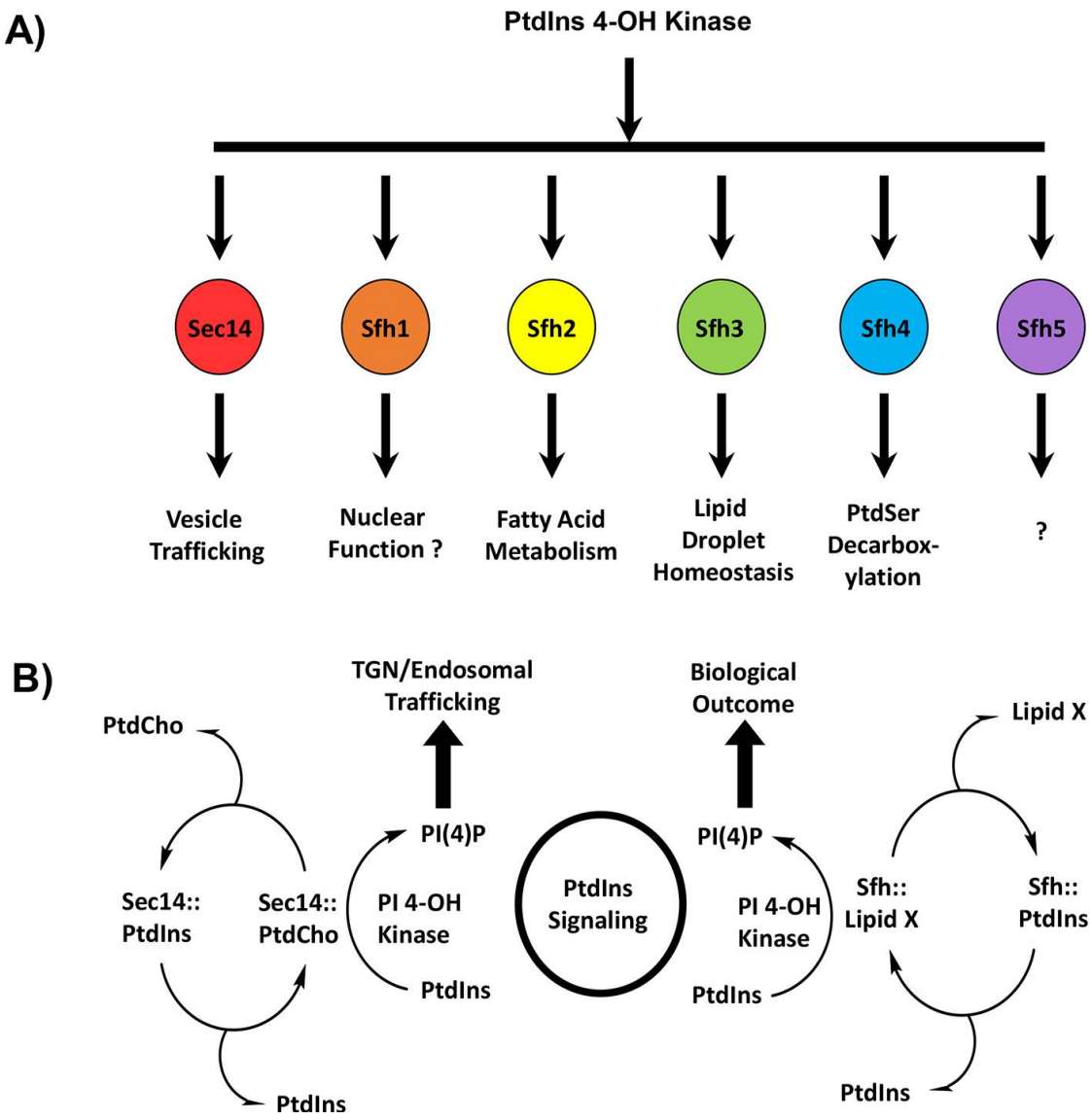

Figure 3-1: Sec14-like PITPs and diversification of PtdIns(4)P signaling.

A illustrates the concept that the biological outcome of PtdIns(4)P signaling in yeast is primarily determined by the Sec14-like PITP that stimulates activity of a PtdIns 4-OH kinase to produce a functionally channeled PtdIns(4)P pool. This strategy is a major mechanism for diversifying PtdIns(4)P signaling. B depicts a heterotypic PtdIns/"second lipid" exchange cycle where the second lipid (lipid X) is a priming lipid that potentiates presentation of PtdIns to the lipid kinase, thereby rendering the PtdIns a superior substrate for the kinase resulting in stimulation of PtdIns(4)P production (3, 4, 6). At left is shown the concept for the Sec14 PtdIns/PtdCho-exchange cycle where PtdIns(4)P is channeled to promotion of membrane trafficking from the TGN/endosomal system. At right is shown the general case proposed for Sec14-like PITPs that fail to bind PtdCho and for whom identification of the exchangeable lipid X is sought.

for lipid substrates across the Sec14 superfamily. The data indicate that the chemical microenvironments of yeast Sec14-like PITP lipid-binding pockets are diverse. Using the Sfh2 and Sfh3 PITPs as experimental models, we show that these structural diversifications translate to differential 'second ligand' lipid-binding specificities.

Materials and Methods

Protein preparation and model building.

The X-ray crystal structures of Sec14, Sfh1, Sfh3 and other mammalian proteins were obtained from PDB repository (www.rcsb.org). The protein models were prepared using the Protein Preparation Wizard panel in the Schrödinger suite. The Prime program (Jacobson et. al., 2002) was used to predict any missing loops and the resulting complete structures were optimized with the OPLS_2005 forcefield in the Schrödinger suite to relieve all atom and bond strains found after adding all missing side chains and/or atoms. The small molecule model structures for cholesterol and ergosterol were prepared and energy minimized in MOE (Molecular Operating Environment; Chemical Computing Group, 2018) and the lowest energy conformations of each were selected for docking.

Homology modeling.

All sequence and structural alignments were carried out within the MOE software package v. 2013.08. Homology models of Sec14 for the fungal species were generated with the MOE 2013.08 modeling package. The Sec14 and homolog sequences to be modeled were aligned to the Sec14 (target) crystal structure sequences in: i) its open conformation (pdb id: 1aua; 2.50 Å resolution), ii) Sfh1 bound with PtdIns (pdb id: 3b7n; 1.86 Å resolution) and iii) Sfh1 bound with PtdCho (pdb id: 3b7q; 2.03 Å resolution). The latter two Sfh1 crystal structures, with the PtdIns and PtdCho ligands, were included in the environment to facilitate generating

induced-fit homology models of Sec14-PtdIns/PtdCho complexes. By default, ten independent intermediate models were generated. These different intermediate homology models were generated as a result of permutational selection of different loop candidates and side chain rotamers. The intermediate model, which scored best according to the Amber99 forcefield, was chosen as the final model and was then subjected to further optimization.

Docking studies.

Computational docking was carried out using the genetic algorithm-based ligand docking program GOLD 5.2 (Jones et. al., 1997). GOLD 5.2 includes algorithms that provide limited flexibility to protein side chains with hydroxyl groups by reorienting the hydrogen bond donor and acceptor groups. The active site was defined by manually generating a centroid in the LBD of Sfh3 surrounded by a volume with a radius of 10 Å around that centroid created with the GOLD cavity detection algorithm. GOLD docking was carried out without using any constraints or biases to explore all possible solutions. In this study, we carried out 3 separate 10, 100 and 1000 GOLD genetic algorithm runs with early termination turned off. In order to explore all the possible binding modes, docking was carried out to generate diverse solutions. All other parameters were as defaults. To evaluate and validate GOLD performance, the co-crystallized substrate PtdIns was extracted and docked. GOLD, using our protocol, accurately reproduced the experimentally observed binding mode of PtdIns in Sfh3, and squalene in Sec14L2. Cholesterol and ergosterol were then docked to Sfh3 and squalene docked to homology model of Sfh2 and scored using the CHEMPLP scoring function within GOLD. CHEMPLP was used because it gives the highest success rates for both pose prediction and virtual screening experiments against diverse validation test sets (Liebeschuetz et. al., 2012).

Surface electrostatics.

ICM-Pro was used to calculate the electrostatic potentials of the molecules in this study using the boundary element algorithm (Abagyan et. al., 1994), and from that generate a 3D surface skin model colored by potential. The ICM-Pro Rapid Exact-Boundary Electrostatics (REBEL) methodology allows solutions of the Poisson equation for a molecule without a grid and with exact positions of electric charges (Totrov et. al., 2001). The energies so calculated consisted of terms representing the intramolecular Coulomb energy and solvation energy, and those terms were plotted as colors on the surface elements according to potentials from red (most negative) to blue (most positive).

Cavity identification.

Binding pockets of Sec14 and Sec14-like homologues were detected using the Vectorial Identification of Cavity Extents (VICE) algorithm (Tripathi et. al., 2010) that is an option in HINT (Kellogg and Abraham, 2000) implemented as a local module within SYBYL 8.1. The VICE algorithm is a grid-based method that propels vectors in directions that are defined by integer numbers of grid cubes, e.g., (0,0,1), (0,1,0), (1,0,0), (0,1,1), (1,0,1), (1,1,0), (1,1,1), (1,1,2), (1,2,1, (2,1,1), etc., rather than in directions defined by angles. These vectors are projected until they either hit a cube occupied by molecule (putatively a cavity wall) or the edge of grid box. For each grid cube, the fraction of vectors finding a cavity wall defines it "cavityness"; cubes with cavityness > ~0.5 are thus inside a cavity. Two cleanup phases finish the algorithm: 1) cubes with few adjacent neighbors also within the cavity are discarded as small crannies; 2) closed surfaces with volumes smaller than a default are also discarded. VICE was used to search for pockets within the Lipid-binding Domains (LBDs) of Sec14 and Sfh proteins in PtdIns/PtdCho complexes, where the LBD was defined to include all amino acid residues

within 10 Å of the bound ligand. The grid resolution was set at 0.5 Å and the minimum closed contour value was set to be 60 Å3. The default cavity definition was set to 0.45 and the contour value was set to 0.4. All other variables were kept at their default values.

Cavity mapping.

HINT 3D complement maps were calculated for the cavity regions within the region of interest nominally defined as the molecular (dimensional) extents of the substrate within the binding cavity. This HINT algorithm projects the hydropathic character and intensity of the atoms adjacent to unoccupied grid cubes to hypothesize the character and intensity of an "ideal" atom occupying that space; i.e., a Lewis acid would be ideal for interacting with Lewis base neighbors, etc. (Tripathi et. al., 2010; Tripathi et. al., 2011; Kellogg and Abraham, 2000). Its distance to these other atoms mediates its hydropathic intensity. In practice, this is accomplished with map pairs – a hydrophobic/polar map where positive field values represent hydrophobic regions of space, and negative field values represent polar (hydrophilic) regions. The second map, acid/base, depicts the acidic polar and basic polar regions of space with positive and negative field values, respectively. The VICE cavity map, represented as a Boolean (1=inside cavity; 0=outside cavity), was then multiplied by each of the complement maps in the map pair to focus the representation within the cavity. The final, overall display of these contoured maps showed regions of the active site most hospitable to hydrophobic groups (green contours) and differentiates between the two types of polar regions (Lewis acid-like in red and Lewis base-like in blue). Generally, contour values were chosen such that their values were ~ 50% of the maximum (or minimum) field value.

Molecular graphics and chemical drawing.

Molecular graphics and analyses were performed with the Schrodinger and MOE software suites. Marvin was used for drawing, displaying and characterizing chemical structures, substructures and reactions (Marvin 5.10.0 and 5.11.4, 2012; ChemAxon, http://www.chemaxon.com. Chemical drawings were also produced using ChemBioDraw Ultra, CambridgeSoft (www.cambridgesoft.com), 11.01.1, 2012.

Lipids and liposomes.

L-α- Phosphatidylcholine, (chicken) egg PtdCho, L- α-phosphatidylinositol (soy) and L-α- phosphatidic acid (chicken) egg of highest available quality were purchased from Avanti Polar Lipids (Alabaster, AL, USA) and used without further purification. 1-palmitoyl-2- decapyrenyl-sn-glycero-3-phospho-choline, [Pyr]-PtdCho and 1-palmitoyl-2-decapyrenyl-snglycero- 3-phosphoinositol, [Pyr]-PtdIns, were generous gifts from Dr. Pentti Somerharju (Helsinki University, Helsinki, Finland), and synthesis of these lipids is described (Gupta et. al., 1977;, Somerharju et. al., 1982). 2,4,6-trinitrophenyl-phosphatidylethanolamine, TNP-PtdEtn was prepared from phosphorethanolamine as described by Gordensky and Marinetti (Gordesky et. al., 1973) and purified by silica gel column chromatography. Cholestatrienol (CTL) was a generous gift from Dr. J. Peter Slotte (Åbo Akademi University, Turku, Finland). [^{3}H]- cholesterol (1 mCi/ml) was obtained from American Radiolabeled Chemicals (St. Louis, MO, USA). The concentrations of all phospholipid solutions were determined per Rouser et al. (Rouser et. al., 1970).

[^{3}H]-Squalene transfer assays.

Donor liposomes were comprised of PtdCho/[^{3}H]- squalene (99/1 wt %). For each assay, 40ug of lipid was dried under a stream of N2 gas and resuspended by vortexing in 50uL

phosphate buffer (300 mM NaCl, 25 mM Na2HPO4, 5 mM β-mercaptoethanol, 1 mM NaN3, pH 7.5). Small unilamellar vesicles were then generated from the suspension by sonication in an ice bath. Squalene transfer assays were then conducted using bovine heart mitochondria as acceptor membranes as previously described for PtdChotransfer assays (Schaaf et. al., 2008, Vincent et. al., 2005; Huang et. al., 2016). [12,13-^{3}H] Squalene (0.1 mCi/ml) was obtained from American Radiolabeled Chemicals (St. Louis, MO, USA).

[^{3}H]PtdIns transfer assays

To measure PtdIns transfer, end-point radioactive transfer assays were performed. [^{3}H]PtdIns transport was measured from rat liver microsomes to liposomes (98 mol % PtdCho and 2 mol % PtdIns) to bovine heart mitochondria as described (Bankaitis et. al., 1990).

Expression and purification of recombinant proteins.

The *SFH2* gene was amplified from the yeast genome and integrated into a pET28BHis-6 protein expression plasmid. All mutations were confirmed by DNA sequencing outsourced to the Eton Biosciences service. Recombinant Sfh2^{His6} and mutant variants were purified as described by Ren et. al. using an *E.coli* BL21 (RIL/DE3; New England Biolabs Inc., Ipswich, MA) expression system. Protein mass was quantified by SDS-PAGE.

Results

Sec14 PtdIns/PtdCho-transfer proteins conserve both the general fold and protein surface electrostatics.

Sec14 PtdIns- and PtdCho-transfer proteins from evolutionarily divergent fungal species (C. albicans, C. glabrata, K. lactis, C. dubliniensis, A. nidulans and S. pombe) share 53-87% primary sequence identity and 71-92% sequence similarity to S. cerevisiae Sec14. The high sequence homologies shared by these Sec14 proteins permitted the construction of 3D homology

models using high-resolution crystal structures of PtdIns-bound Sfh1 (1.86 Å, pdb id, 3B7N; 3), PtdCho-bound Sfh1 (2.00 Å; pdb id, 3B7Q; 3) and β-octylglucoside-bound Sec14 (2.50 Å; pdb id, 1AUA; 20) as templates. As expected, all homology models conformed to a two-domain structure with an N-terminal tripod motif and a C-terminal lipid-binding domain (LBD), and an overall fold consisting of eleven α-helices, eight 3_{10}-helices, and six β-strands (Figure 3-2A). An equally prominent feature of all of the Sec14 proteins was a β-sheet floor of the large hydrophobic lipid-binding cavity with a hybrid α/3_{10}-helix gating access to that cavity. A composite superimposition of all of these models emphasizes the structural conservation at the level of the α-carbon fold in this protein class (Figure 3-2A).

The impressive structural conservation amongst this protein class was further reflected in the general similarities of the molecular surface properties of these PITPs. Evaluation of the electrostatic surface maps of Sec14 and its orthologs from widely divergent fungi illustrated that these proteins are in effect dipoles. While a significant portion of the exposed surface area of these Sec14 proteins is electronegative, conspicuous regions of electropositive potential are apparent at the solvent-exposed surfaces of substructures that form the helical gate and floor of the lipid-binding cavity in en face views of these molecules (Figure 3-2B). Electronegative and electropositive charges are distributed similarly across those surfaces of the other Sec14s from widely divergent fungal species (Figure 3-2B). These asymmetric surface charge distributions are most likely involved in orienting the Sec14 molecules in such a way that the electropositive regions are directed towards interactions with the electronegative membrane surface – thereby forecasting potential orientations by which Sec14 and its orthologs dock onto membranes.

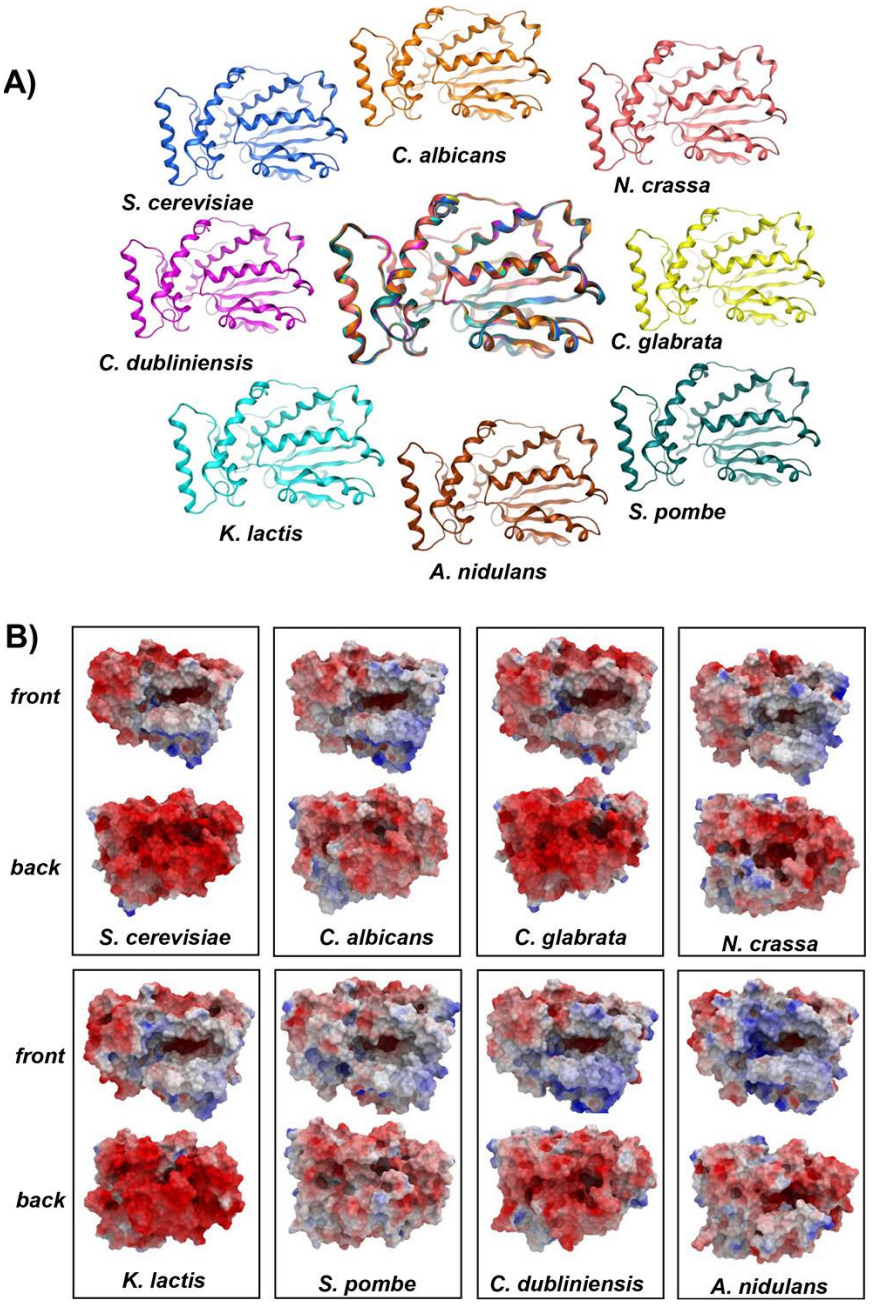

Figure 3-2: Structural features of Sec14 orthologs.

(A) α-carbon backbones of the basic folds of open conformers of Sec14 orthologs from the indicated fungal species: *S. cerevisiae* (*blue*); *C. albicans* (*orange*); *Neurospora crassa* (*pink*); *C. dubliniensis* (*magenta*); *C. glabrata* (*yellow*); *K. lactis* (*cyan*); *A. nidulans* (*brown*); and *S. pombe* (*teal*). At center is a structural overlay of the collective α-carbon backbones onto that of Sec14 that highlights the high overall conservation of the basic fold across large evolutionary distances. (B) Electrostatic potential surfaces of open conformers Sec14 and Sec14 orthologs from the indicated fungal species are shown. The *en face* orientation illustrates the open gating helices and the exposed lipid-binding cavities. Surfaces with electropositive potential are rendered *blue*, and electronegative surfaces are highlighted in red.

Divergent Sec14 homologs conserve the general fold but not protein surface electrostatics.

S. cerevisiae expresses five other Sec14-like PITPs in addition to Sec14 (Li et. al., 2000). These proteins are designated Sec Fourteen Homologs (Sfh) 1-5. The Sfh proteins share ~25-78% primary sequence similarity to Sec14, and high-resolution crystal structures are available for PtdIns- and PtdCho-bound Sfh1 (3B7N, 3B7Q, 3B7Z) (Schaaf et. al., 2008), and for apo-Sfh3 (4J7Q,4M8Z) (Yang et. al., 2013; Ren et. al., 2014). Inspection of those structures, and of 3D homology models created by threading of the primary sequences of the Sfh2, Sfh4 and Sfh5 (i.e. proteins whose crystal structures are not yet solved) onto the structure of S. cerevisiae Sec14 (pdb id: 1AUA; Sha et. al., 1998), demonstrated all of these Sfh proteins similarly shared a typical Sec14-fold with minor differences in detail (primarily in the loops; Figure 3-3A).
The conservation of fold notwithstanding, evaluation of the electrostatic surface maps of the Sfh proteins showed the protein surface properties to be distinct from those of Sec14 and its orthologs. Although Sfh1 exhibited a Sec14-like dipole pattern of surface charge distribution, the electropositive charge was further expanded onto the protein surface covering the structural elements perpendicular to the side of the lipid binding cavity (Figure 3-3B). Sfh2 also showed electropositive character but it was concentrated on the tripod motif surface rather than at the helical gate surface and the floor of the cavity. Sfh3 presented strong electropositive character, whereas Sfh4 exhibited more diffusely distributed areas of electropositive charge over its molecular surface (Figure 3-3B). Sfh5 was an extreme case where the LBD surface was highly electropositive throughout. The distinct surface charge distributions and surface electrostatics of Sec14 and Sfh proteins likely contribute to the distinguishing molecular recognition determinants that help specify the diverse biological functions of these proteins.

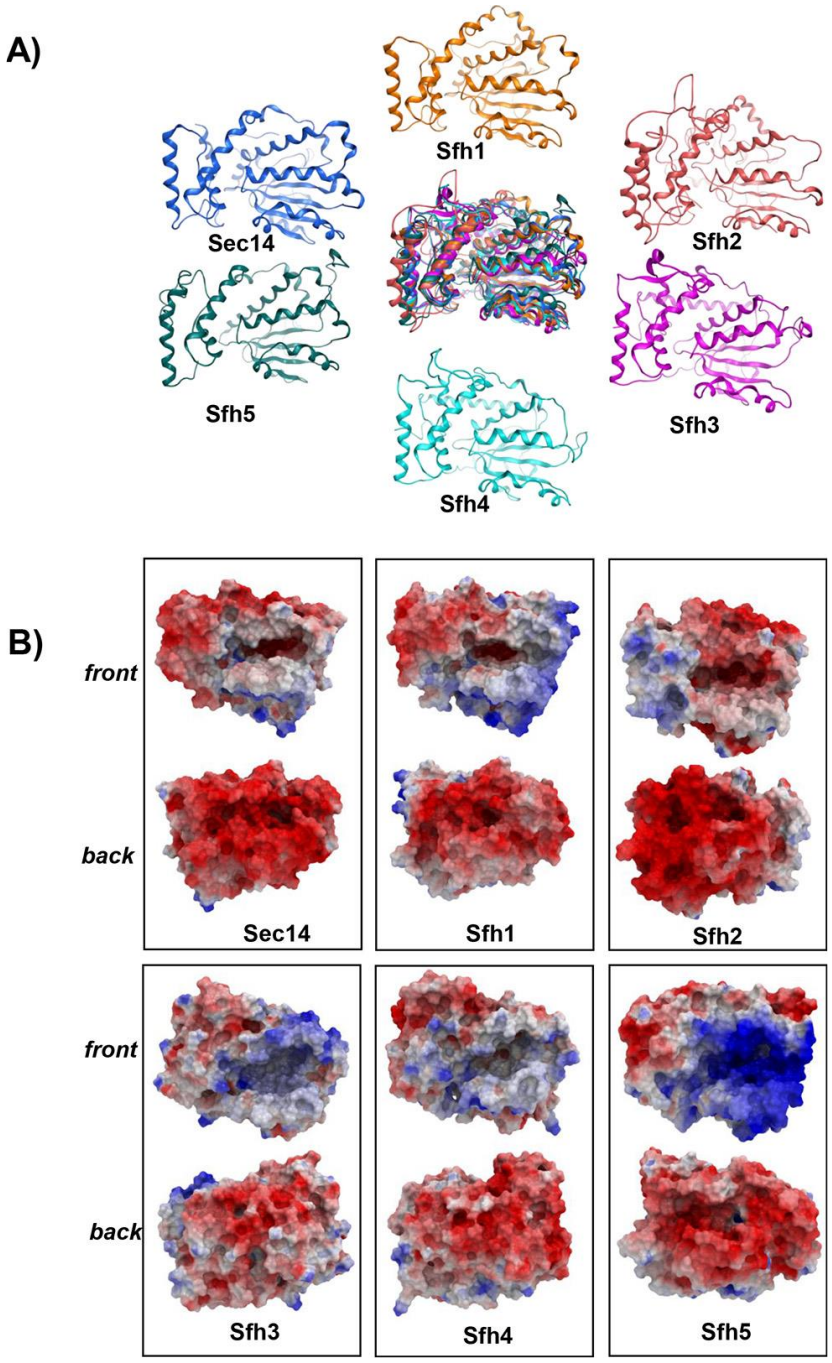

Figure 3-3: Structural features of Sec14 paralogs, the Sec14-like Sfh proteins.

(A) α-carbon backbones of the basic folds of open conformers of Sec14 and the Sec14-like Sfh PITPs from *S. cerevisiae*: Sec14 (*blue*); Sfh1 (*orange*); Sfh2 (*pink*); Sfh3 (*magenta*); Sfh4 (*cyan*); and Sfh5 (*teal*). At center is a structural overlay of the collective α-carbon backbones superimposed onto that of Sec14 that highlights the overall conservation of the basic Sec14-fold across the yeast Sfh1 family. (B) Electrostatic potential surfaces of open conformers Sec14 and indicated Sfh PITPs are shown. The *en face* orientation illustrates the open-gating helices and the exposed lipid-binding cavities and is labeled as "front," and the opposite side of the molecule is identified as "*back*." Surfaces with electropositive potential are rendered *blue*, and the electronegative surfaces are highlighted in *red*.

Inferred heterogeneities in lipid-binding specificity.

A second significant property proposed to contribute to functional diversification of Sec14-like PITPs is diversity in the nature of the second 'ligand' bound by these proteins even with conserved PtdIns-binding activity. Evidence for this comes from sequence and structural alignments of divergent Sec14 orthologs that identify residues engaged in specific lipid headgroup binding (i.e., binding bar-codes). Both primary sequence alignments and 3D homology models of fungal Sec14 orthologs show highly conserved PtdIns- and PtdCho-binding bar-codes (Figure 3-7A; Figure 3-4A, left panel). When compared to S. cerevisiae Sec14, the structural elements that coordinate binding of the inositol and choline headgroups are highly conserved as are the hydrophobic residues that lie within 4.5 Å of the fatty acyl chains. The PtdIns-binding barcode is comprised of highly conserved Arg, Lys, Glu and Asp residues that engage in H-bond interactions with the headgroup inositol ring, and Pro, Thr and Lys residues that coordinate the PtdIns phosphate moiety via H-bonds. In addition, an essentially invariant Thr within the LBD engages in H-bond interactions with the PtdIns glycerol backbone while a conserved Arg residue contacts the PtdIns glycerol backbone and phosphate moieties via side-chain and backbone H-bonds, respectively. Similarly, the PtdCho bar-code is also conserved in the 3D homology models of divergent fungal Sec14 orthologs. Those bar-code residues coordinate PtdCho binding via a network of hydrogen bonds and water bridges and cation-π interactions between Tyr/Phe residues and the choline methyl groups.

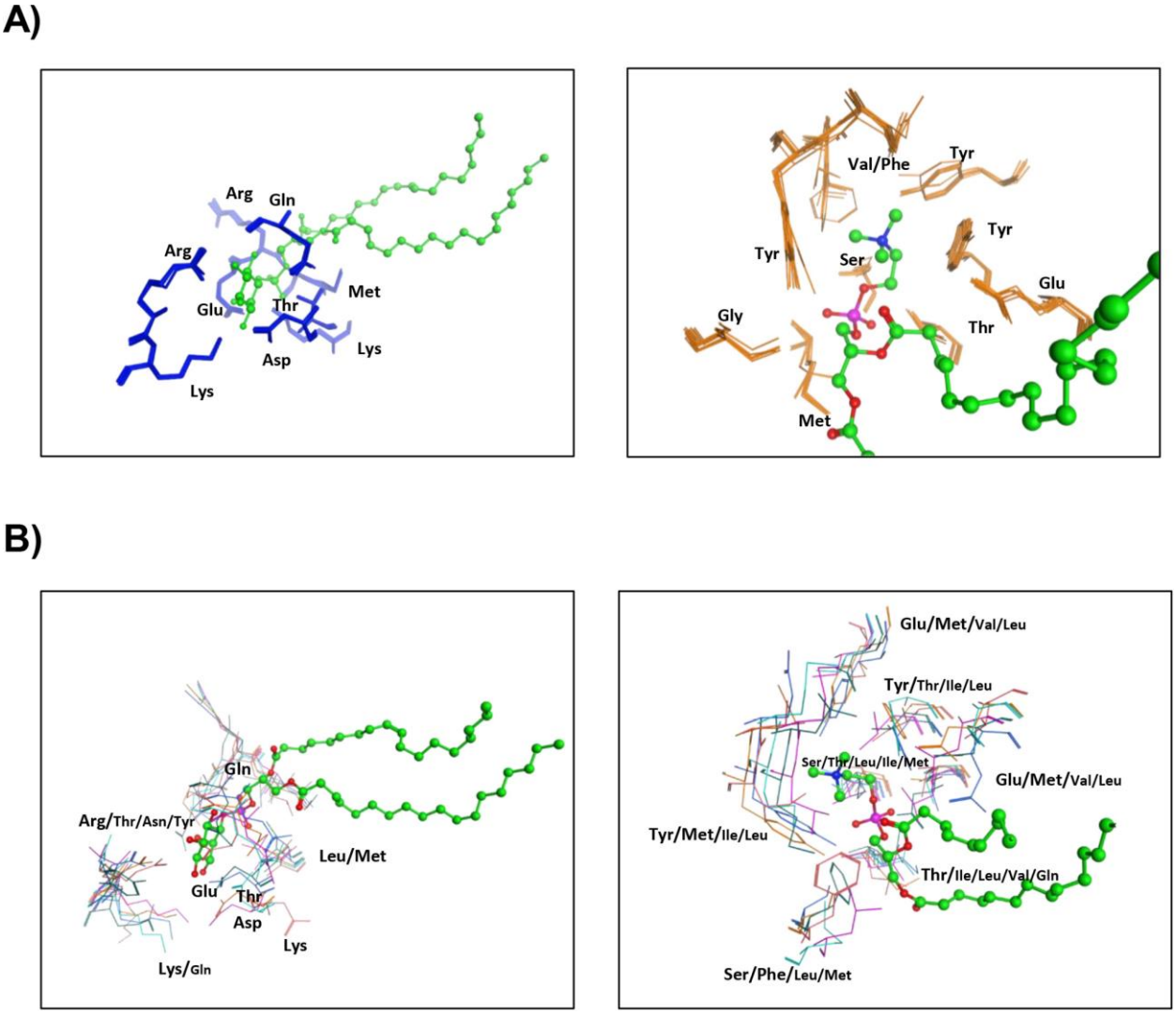

Figure 3-4. Structural barcodes for PtdIns- and PtdCho-binding in Sec14 orthologs and Sec14-like Sfh proteins.

(A) structural overlay of the PtdIns-binding (*left panel*) and PtdCho-binding barcode residues (*right panel*) from Sec14 orthologs superimposed onto those of Sec14. PtdIns-binding barcode residues are shown in *blue stick model* with PtdIns rendered in *green ball* and *stick*. The PtdCho-binding barcode residues are shown in *orange stick model*, and PtdCho is rendered in *green ball* and *stick*. Both barcodes are structurally preserved in Sec14 orthologs across large evolutionary distances. (B) Structural overlay of the PtdIns-binding (*left panel*) and PtdCho-binding barcode residues (*right panel*) from the indicated Sec14-like Sfh PITPs superimposed onto those of Sec14. PtdIns- and PtdCho-binding barcode residues are shown in a *stick model* using the color code of Fig. 3*A* to identify residues of individual Sfh proteins. PtdIns is rendered in *green ball* and *stick*. The PtdCho-binding barcode regions are shown using the color code of Fig. 3*A* to identify residues of individual Sfh proteins. PtdCho is rendered in *green ball* and *stick*. Although the PtdIns-binding barcodes are structurally well-preserved in the Sfh proteins, the PtdCho barcode is highly divergent (with the exception of Sfh1).

In Sec14, the PtdCho phosphate oxygen engages in a hydrogen bond network involving Tyr, Ser and Thr residues to further stabilize the complex (Figure 3-7A; Figure 3-4A, right panel). Sec14 and Sfh1 share an identical PtdCho-binding bar-code, and this conservation is of functional relevance. Both proteins bind/transfer PtdCho in vitro (Schaaf et. al., 2008, Bankaitis et. al., 1990; Schaaf et. al., 2011), and PtdCho-binding is an essential property required for these proteins to potentiate PtdIns 4-OH kinase activity in vivo (Schaaf et. al., 2008, Schaaf et. al., 2011).

With regard to the functionally divergent Sfh proteins, the key PtdIns headgroup-binding bar-code residues are conserved in the Sec14-like Sfh PITPs (Figure 3-7B, Figure 3-4B, left panel). This conservation reflects a functional property of these Sfh proteins as all exhibit PtdIns-binding/ transfer activity in vitro (Schaaf et. al., 2008, Schaaf et. al., 2011).

However, there was a clear departure from the PtdCho-binding bar-code in the other Sfh proteins as indicated by both primary sequence divergences (Figure 3-7B), and by inspection of the analogous PtdCho headgroup coordinating regions of these proteins (Figure 3-4B, right panel). For Sfh2, Sfh3, Sfh4, and Sfh5, the corresponding cavity microenvironment was distinct for each member and the divergences in the amino acids corresponding to PtdCho-binding bar-code residues are incompatible with PtdCho binding. Indeed, none of these Saccharomyces Sfh proteins bind/transfer PtdCho in vitro (Li et. al., 2000). Those sequence divergences forecast distinct ligand specificities that confer differential ligand binding properties, and therefore distinct functional properties, to each Sfh protein (Figure 3-7B, Figure 3-4B, right panel).

Comparative PtdIns-binding topographies of Sec14 and Sfh lipid-binding cavities.

As the chemical landscape of the PITP lipid-binding cavity suggests a chemistry that governs ligand recognition/selectivity, a detailed structural and physiochemical characterization of each lipid-binding cavity was warranted. To that end, we determined the dimensions and extents of each cavity, and then characterized each cavity with respect to its three-dimensional hydropathic properties. The first step was application of the cavity search and characterization algorithm (Vectorial Identification of Cavity Extents, VICE) which we described previously (Tripathi et. al., 2010). VICE offers a complete set of metrics, including the cavity's volume, entrance opening size and surface area. The resulting Boolean cavity extent maps were integrated with hydropathic "complement" property maps calculated by HINT (Tripathi et. al., 2011; Kellogg and Abraham, 2000). The complement map represents the physical and chemical environments within the lipid-binding cavities in terms of the hydropathic properties of the ideal "complement" to a site -- i.e., mapping where a complementary molecule should be hydrophobic, acidic or basic (see Materials and Methods). We were thus able to obtain detailed fingerprints of Sec14/Sfh lipid-binding cavity micro-environments in terms of their polar and hydrophobic character (Figure 3-5A). The integration of VICE and HINT maps, which is simply a point-by-point multiplication of the two maps, allowed extraction of unique information as to what the general features of a ligand might be; such that the extracted parameters of Sec14 and Sfh lipid-binding cavities could be translated to physical/chemical/spatial (rather than primary sequence) bar-codes for ligand-binding activity. As PtdIns-binding is a conserved property of all fungal Sec14 PtdIns/PtdCho-transfer proteins, and of the S. cerevisiae Sfh proteins, comparative analyses of the PtdIns-binding topographies of the various lipid-binding pockets served as test case for assessing the suitability of this general approach. The cavity properties of Sec14-like

PITPs were characterized (i.e., volume, surface area, hydropathic character, entrance cross sectional surface area, etc.; Figure 3-5B). In these terms, the PtdIns-binding cavities were similar with respect to volume and surface area in all fungal Sec14s – even though PtdIns is a flexible molecule. The PtdIns headgroup was consistently bound in these cavities at the interfaces of the LBD and tripod motifs. As a detailed PtdIns-binding fingerprint, the inositol headgroup and glycerol backbone-binding region (defined as the proximal end of the lipid-binding cavity) was landmarked by distinct polar patches ideal for engagement of these chemical moieties. As expected, the acyl chains were hosted by the hydrophobic LBD. However, the distal end of the PtdIns-binding pocket (towards helices α7- α 8 and α 9) was again landmarked by a patch of polar residues (Fig. 3-5A). Conservation of this general PtdIns-binding topography was evident for the Sfh proteins as well, and the Sec14-like PtdIns-binding microenvironment fingerprint was also nicely conserved in Sfh1, Sfh2, Sfh3 and Sfh4. By contrast, Sfh5 provided an exception in that it exhibited a rather polar and strikingly basic LBD environment – even though the fingerprint of the Sfh5 PtdIns headgroup binding region conformed to the PtdIns-binding fingerprints calculated for Sec14 and the other Sfh proteins. Taken together, these data validated the integrated VICE/HINT mapping approach as a reliable tool with which to produce spatial fingerprints of the physical/chemical parameters of individual Sec14/Sfh lipid-binding cavities for comparative analyses.

Comparative PtdCho-binding topographies of Sec14 and Sfh protein lipid-binding pockets.

Sfh protein divergences from the PtdCho-binding primary sequence bar-code are consistent with the idea that these proteins are able to prime PtdIns 4-OH kinase activity by heterotypic exchange of their distinct second ligands for PtdIns (Schaaf et. al., 2008; Bankaitis et. al., 2010; Nile et. al., 2010; Grabon et. al., 2015). The detailed fingerprinting of individual Sfh

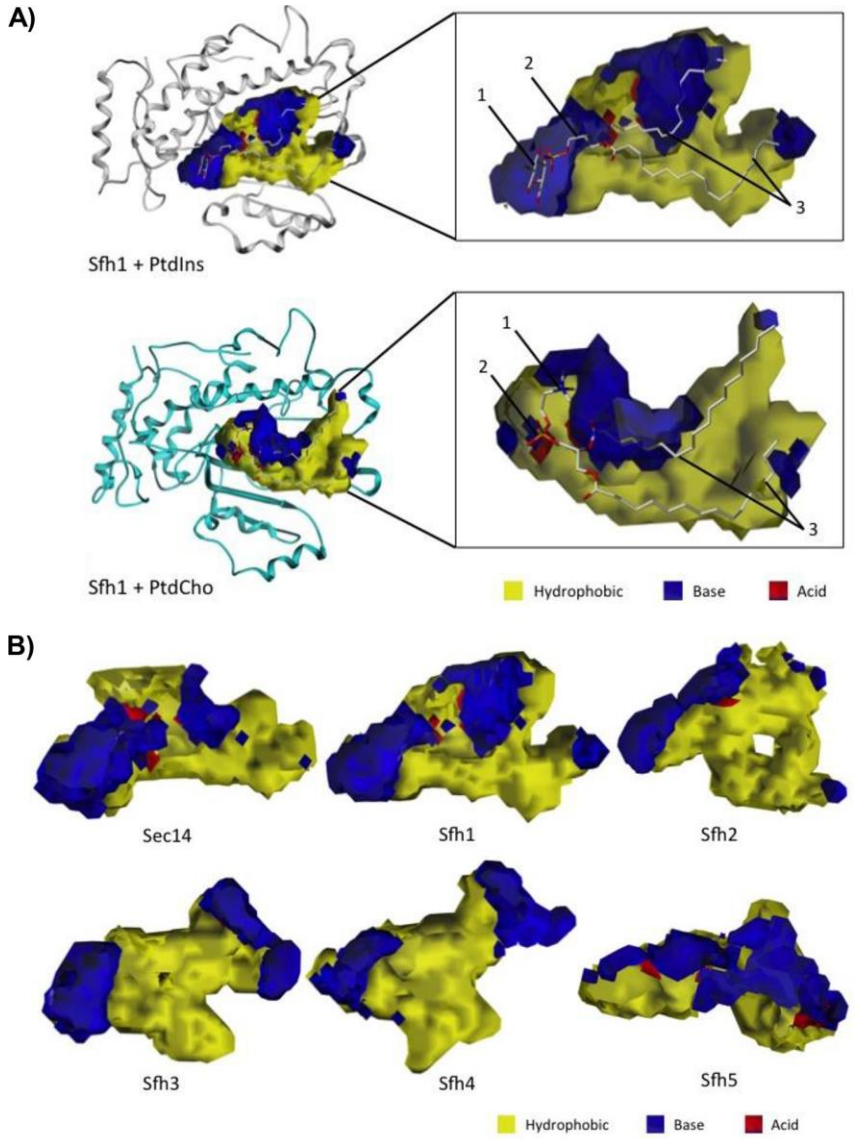

Figure 3-5: VICE/HINT mapping of the Sec14 and Sfh PITP lipid-binding cavities.

(A) VICE-calculated binding cavity of Sfh1 was mapped with HINT complementary maps, and the PtdIns (top) and PtdCho (bottom) headgroup-binding regions are illustrated. PtdIns is bound in the cavity at the interface between the LBD and tripod motifs. The inositol headgroup (1) and glycerol backbone-binding region (2) are localized in distinctive polar microenvironments of the cavity surface. The acyl chains (3) pack into the largely hydrophobic LBD. PtdCho binds the cavity at the interface between the LBD and tripod motifs. The choline headgroup (1) is located in a hydrophobic area in the near vicinity of an extensive polar region. The PtdCho phosphate moiety (2) is coordinated in a polar surface, and the acyl chains (3) pack into the largely hydrophobic LBD. The Sfh1 α-carbon backbone is rendered in ribbon style, and the lipid ligands are rendered with ball and stick. In HINT complementary maps, yellow contours identify hydrophobic regions, and blue and red contours identify polar electropositive and electronegative surfaces, respectively. (B) Lipid-binding cavity maps for Sec14 and the Sfh PITPs are shown. Binding cavities were mapped by the VICE cavity detection algorithm and HINT complementary maps. In HINT complementary maps, yellow contours depict hydrophobic regions, and blue and red contours identify polar electropositive and electronegative cavity surfaces, respectively.

lipid-binding cavities, as described above, was applied to determine whether divergences in the primary sequence bar-codes translated to unique physical/chemical properties of Sfh lipid-binding cavities. Of special interest were distinguishing polar microenvironments identified by HINT/VICE mapping within individual (and largely hydrophobic) ligand-binding cavities because it is those features that likely contribute to the second-ligand binding specificities of Sec14-like proteins

While the polar microenvironment associated with PtdIns headgroup binding was conserved throughout the Sec14 and Sfh protein cavity maps, the nature and distributions of other polar microenvironments in the lipid-binding cavities were unique to each Sfh protein (Figure 3-5B). Interestingly, very similar PtdCho headgroup-binding microenvironments were shared by the two PtdCho-binding members of this family (Sec14 and Sfh1), but the cavities of other Sfh proteins showed very different chemical properties in their corresponding microenvironments. Sfh2 exhibited unique polar character in the area of helix α9 and the loop connecting α9 to β-strand β4, while the large distal region of the lipid-binding cavity was hydrophobic – unlike the corresponding regions of the Sec14 and Sfh1 cavities (Figure 3-5B). The Sfh3 cavity was characterized by a deeply buried cleft that was both larger and more hydrophobic than that of Sec14 or Sfh1, while the binding pocket shapes and topographies of Sfh4 and Sfh5 diverged significantly from those of Sec14, Sfh1, Sfh2 and Sfh3 (Figure 3-5B).

Sfh2 is a PtdIns- and squalene-exchange protein.

The identification of second ligands for a Sec14-like PITP would afford an opportunity to relate the chemical/physical fingerprint of the corresponding lipid-binding cavity to binding of that second ligand. It is from this perspective that the remainder of this work focuses on the Sec14-like Sfh2 and Sfh3.

The most unexpected result from the VICE/HINT pocket mapping experiments was the altogether unique toroid-shaped topography of the Sfh2 binding pocket (Figure 3-5B). Although Sfh2 is a PITP that shares 30-35% homology with Sec14 and Sfh1 (Li et. al., 2000), and the Sec14 and Sfh1 structures were used as templates to generate the Sfh2 homology model, the highly divergent pocket topography projected Sfh2 bound an unusual second ligand. In that regard, the first clue was derived from the structural homology of Sfh2 with the mammalian Sec14L2 protein. This mammalian member of the Sec14 superfamily has been crystallized bound to squalene and 2,3-oxidosqualene (Christen et. al., 2015). These two metabolites are sterol precursors and squalene is converted to 2,3-oxidosqualene by the action of the terbinafine target squalene 2,3-epoxidase (ERG1 gene product; Figure 3-6A) Indeed, structural overlay representations indicated that Sfh2 and Sec14L2 shared toroid-shaped and hydrophobic binding cavities within the LBDs (Figure 3-6B). Those data suggested these two Sec14-like proteins provide similar binding microenvironments for their respective ligands, and strongly implicated squalene as a bona fide ligand for Sfh2.

To investigate in more detail the suitability of squalene as putative second binding ligand for Sfh2, the molecule was computationally docked in the binding pocket of Sfh2 and the dock pose optimized. The docked squalene models showed binding poses similar to that observed for squalene in the Sec14L2 lipid-binding cavity (Figure 3-6C). Bound squalene, which describes an open hydrocarbon chain, was primarily coordinated by hydrophobic residues Phe268, Ile271, Trp272, Leu279 and V283 positioned on the helical gate and lining the interior of the lipid-binding cavity. Residues comprising the floor of hydrophobic lipid-binding cavity also contributed to squalene binding and these included Ile224, Phe226, Leu228, Leu256, Leu259, Leu260, and Ile261. Significant contributions for the hydrophobic micro-environment supporting

squalene binding were also provided by residues on helix α9 which constitutes part of the cavity ceiling. Those residues included Pro240, Val241, Phe243, Leu244, Ile245, and Phe248.
We also note that, in addition to the largely hydrophobic character of the Sfh2 lipid-binding cavity, the distal and interior end of the cavity included hydrophilic residues (Glu157, Thr158, Asn177, Arg185, His189, Gln194, Thr195, Glu198 and Lys201. Thus, the Sfh2 cavity exhibited significant amphipathic character. Interestingly, these features recapitulated the chemical landscape of the Sec14L2 lipid-binding cavity (Figure 3-6D). Moreover, molecular modeling data further projected that squalene binding space closely overlaps with that of the sn-2 acyl chain of PtdIns.

To directly determine whether squalene is an exchangeable ligand for Sfh2, an assay was developed to measure Sfh2-mediated transfer of [^{3}H]-squalene from donor liposomes to acceptor bovine heart mitochondria in vitro (see Materials and Methods). Indeed, Sfh2 showed robust squalene transfer activity in this assay (Figure 3-6E). A fixed amount of Sfh2 (10μg) typically catalyzed transfer of ~40% of the [^{3}H]-squalene from donor liposomes to acceptor membranes in a 30 min incubation at 37°C. Those results came with a signal:background ratio of approximately four, and squalene transfer exhibited Sfh2 concentration dependence (Figure 3-6E). Moreover, Sfh2-mediated [^{3}H]-squalene transfer was a specific activity from the perspective that neither Sec14, nor any of the other Sfh proteins, effected any significant squalene transfer above background (Figure 3-6F). This level of transfer is notable as maximal achievable transfer in ~50%. That squalene binding by Sfh2 is of physiological relevance is supported by our finding that Sfh2-deficient yeast cells exhibit enhanced sensitivity to terbinafine (Figure 3-6G).

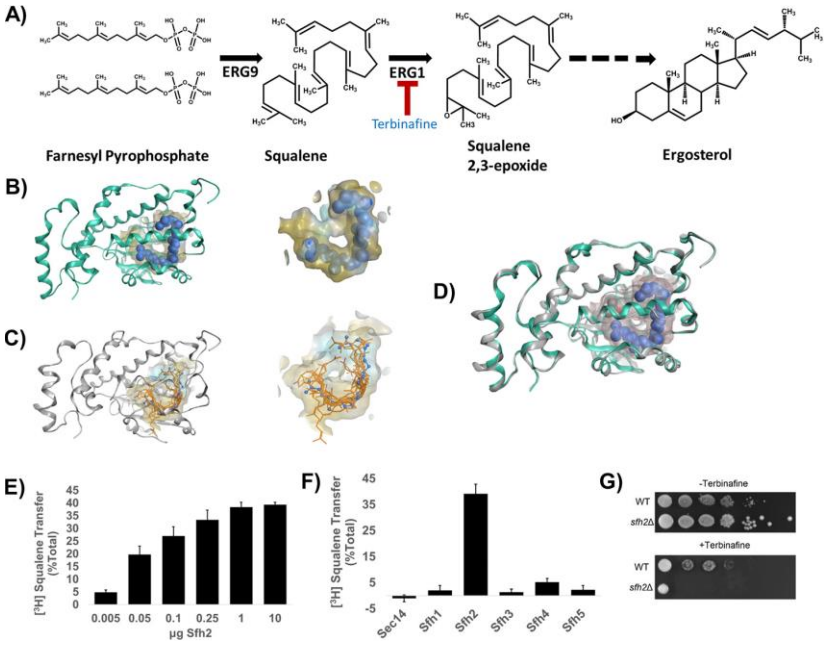

Figure 3-6: Sfh2 is squalene-binding/exchange PITP.

(A) Squalene is a metabolic intermediate in the ergosterol biosynthesis pathway and is produced from farnesyl pyrophosphate by the action of the ERG9 gene product squalene synthase. Subsequently, squalene is converted to squalene 2,3-epoxide in a reaction catalyzed by the squalene 2,3-epoxidase (encoded by ERG1) that consumes molecular oxygen. Squalene 2,3-epoxidase is inhibited by the synthetic allylamine terbinafine. (B) Left, Sec14L2::squalene structural model is shown with the protein α-carbon backbone in ribbon style (green) with squalene as a space-filled model (blue) in a yellow translucent binding cavity. Right, close-up view of squalene within the Sec14L2-binding pocket is shown. The data were extracted from PDB code 4OMK (29). (C) Left shows the Sfh2 homology model (gray ribbon) with squalene (orange stick) docked into the lipid-binding cavity. The 10 highest scoring dock poses are shown. Right shows a close-up view of the model Sfh2 lipid-binding pocket with the 10 highest scoring squalene dock poses. The blue ball and stick model is a superimposition of the squalene pose extracted from Sec14L2 for comparison (PDB code 4OMK). (D) Structural overlay of the Sec14L2::squalene crystal structure (green ribbon, squalene rendered as a blue space-filled model) and a homology model of Sfh2 (gray ribbons). (E) Sfh2-dependent [^{3}H]squalene transfer. Squalene transfer is expressed as the fraction of total input of squalene transferred from donor liposomes to bovine heart mitochondria acceptor in 30 min at 37 °C after subtraction of background. [^{3}H]Squalene input in these assays ranged from 21 to 27x10^3 cpm, and background ranged from 4 to 5x10^3 cpm. The mass amounts of Sfh2 assayed in these titration experiments are shown at the bottom. The values represent the averages of three independent determinations performed in triplicate. Error bars represent standard deviations. (F) Clamped amount (10 µg) of each of the indicated Sec14-like PITPs was assayed for squalene transfer as in E. Under those conditions, Sfh2 catalyzed ~40% transfer of input [^{3}H]squalene after subtraction of background. [^{3}H]Squalene input in these assays ranged from 18 to 24x10^3 cpm and background ranged from 4 to 6 x 10^3 cpm. The values represent averages of triplicate determinations from three independent experiments. Error bars represent standard deviations. (G) Sfh2-deficient yeast exhibit increased sensitivity to terbinafine. Isogenic WT and *sfh2Δ* yeast strains were spotted in 10-fold dilution series onto YPD plates without or with the squalene 2,3-epoxidase inhibitor terbinafine (250 µM), as indicated. Plates were incubated at 30 °C for 72 h.

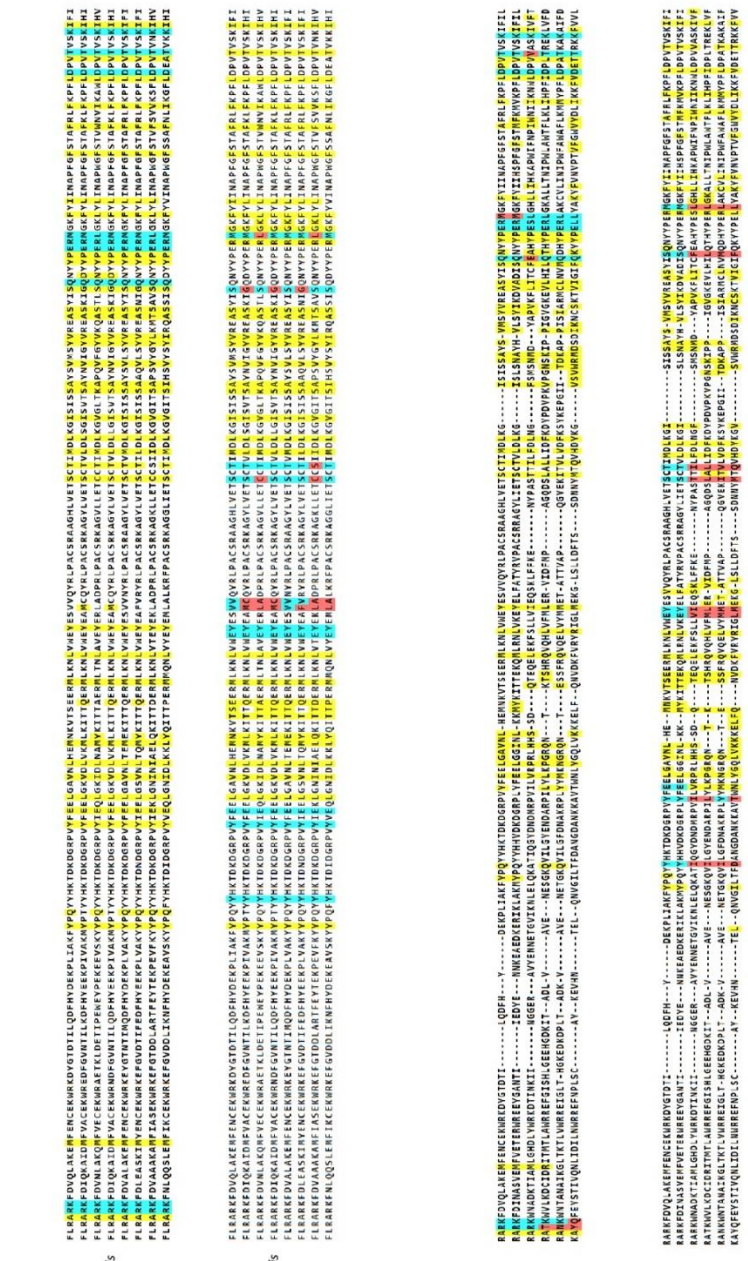

Figure 3-7: Primary sequence barcodes for PtdIns- and PtdCho-binding in Sec14 orthologs and Sec14-like Sfh proteins.

(A) Primary sequence alignment that depicts conservation of the PtdIns (top) and PtdCho barcodes (bottom), respectively, for Sec14 orthologs from the indicated fungal species. Key coordinating residues are in cyan and divergences within that barcode are highlighted in red. Binding pocket residues are highlighted in yellow. (B) Primary sequence alignment that depicts conservation of the PtdIns (top) and divergence of PtdCho barcodes (bottom), respectively, for the indicated Sec14-like PITPs. Key coordinating residues are in cyan and divergences within that barcode are highlighted in red. Binding pocket residues are highlighted in yellow.

Discussion

Herein, we report a systematic investigation of structural features of Sec14-like PITPs including their surface electrostatic properties, and the diverse shapes and chemical microenvironments of lipid-binding cavities, to gain an understanding of molecular mechanisms that generate diversity and specificity for lipid substrates across the Sec14 superfamily. Using integrated X-ray crystallographic and computational-based approaches, the conservation and evolution of the diverse functionalities in Sec14-like PITPs were interrogated. Particular focus was trained on defining the comparative anatomies of the Sec14-like PITP LBDs in terms of the physical and chemical microenvironments that these structural elements provide for lipid-binding. Using the functionally enigmatic Sfh2 and the lipid droplet-associated Sec14-like PITP Sfh3 as experimental foci, we identify squalene and sterols as exchangeable second lipid-binding ligands for Sfh2 and Sfh3, respectively. Taken together, the collective data indicate that the Sec14-like PITP lipid-binding pockets define diverse chemical microenvironments, that these diversifications reflect differential ligand binding specificities across this protein family, and that these ligand binding specificities are associated with functional diversification.

Selective conservation of physical properties across the Sec14-protein superfamily.

A remarkable feature of Sec14-like proteins in yeast is their ability to diversify the biological outcomes of PtdIns-4-P signaling in cells. These available data suggest that Sec14-like PITPs instruct biological outcomes for PtdIns 4-OH kinase activity, and current ideas are these PITPs do so via a regulated metabolic channeling of PtdIns-4-P production to dedicated effectors of PtdIns-4-P signaling (Bankaitis et. al., 2010; Ghosh et. al., 2015). In that regard, we find that, while the structural fold of Sec14-like PITPs (as defined by the α-carbon backbone) was highly conserved across widely diverged fungal species (S. cerevisiae and S. pombe diverged from each

other ~350 million years ago; 35), proteins of this family differed in at least two general respects. The first involved protein surface chemistry where the electrostatic surface properties of Sec14 orthologs were impressively preserved across wide evolutionary distances. These PITPs showed highly asymmetric distributions of negative and positive surface charge with the basic regions concentrated in the vicinity of the helical gate element that controls access to the lipid-binding pocket. By contrast, four of the five Sec14 homologs of S. cerevisiae presented very different surface charge distributions. Sfh1, the protein most similar in primary sequence to Sec14, was the single exception.

The second general area of divergence involved the nature of the lipid-binding cavity. An integrated VICE/HINT cavity mapping approach indicated that the dimensions and the chemical environments of the lipid-binding cavities of Sec14, its homologs from distant fungal species, and of Sfh1 were again highly conserved -- as were the ligand-binding/ exchange properties of those PITPs. The Sec14 proteins from S. cerevisiae and S.pombe are PtdIns/PtdCho-transfer proteins in vitro as is Sfh1 (Schaaf et. al., 2008, Schaaf et. al., 2011; Nakase et. al., 2001). By contrast, not only did the PtdCho-binding bar-code regions deviate from those of Sec14 in the other four yeast Sfh proteins, but the general shapes and chemical fingerprints of their corresponding lipid-binding cavities were also distinct from those of Sec14 and from each other. Those features further reinforce the concept that Sec14-like proteins have diverged to accommodate the binding of a wide variety of lipids/lipophilic molecules while preserving the features critical for PtdIns-binding/ exchange.

Squalene as second ligand for a Sec14-family protein.

The most unusual yeast Sec14-like PITPs from the standpoint of the VICE/HINT analyses were Sfh2 and Sfh5. Whereas Sfh5 exhibited distinct electropositive character, Sfh2

was characterized by its unique toroid-shaped hydrophobic cavity. This property of a toroid shaped lipid-binding cavity is also shared by the mammalian Sec14-like squalene-binding protein Sec14L2, and we demonstrate that Sfh2 is a robust PtdIns and squalene exchange protein – thereby identifying squalene as a bona fide second-ligand for this Sec14-like PITP.

There are two satisfying aspects of those results. First, the unique topology of the Sfh2 lipid-binding cavity among the yeast Sec14-like PITPs translated to a specific ability to bind and exchange squalene validated the basic premise of using the VICE/HINT approach to predict ligand-binding diversification in these proteins. Second, the data promise to inform downstream analyses of Sfh2 function in vivo. Sfh2 is a functionally enigmatic PITP that has been indirectly implicated, on the basis of genetic interactions, to be involved in a number of in vivo activities such as regulation of oxidative stress, hypoxia-related fatty acid synthesis, DNA replication stress, etc. (Cha et. al., 2003; Desfougères et. al., 2008; Régnacq et. al., 2002; Tkach et. al., 2012). Our collective data, including the demonstration that Sfh2- deficient cells are sensitized to terbinafine challenge, a condition expected to elevate intracellular squalene levels, now suggest that Sfh2 activity is functionally linked either to squalene homeostasis or in potentiating a squalene-induced stress response.

Implications for interpretation and exploitation of lipid-binding bar-codes.

High resolution crystal structures of closed Sfh1 conformers individually bound to PtdIns or PtdCho provided the startling demonstration that the motifs that coordinate headgroup-binding for these phospholipids were physically and spatially distinct in Sec14-like PtdIns/PtdChotransfer proteins (Schaaf et. al., 2008). Those data, in turn, permitted the recognition of physically discrete PtdIns- and PtdCho headgroup-specific binding bar-codes at the level of primary sequence (Schaaf et. al., 2008; Bankaitis et. al., 2010; Nile et. al., 2010;

Grabon et. al., 2015). The definition of PtdIns- and PtdCho-binding bar-codes, in turn, provide useful guides for generating headgroup-specific binding mutants for as yet poorly characterized Sec14-like proteins. This is particularly true for the PtdIns-binding bar-code as it is conserved across the Sec14 protein superfamily. The ability to generate specific headgroup-binding mutants in Sec14-like PITPs that do not exchange PtdCho suggests experimental avenues for rigorous interrogation of the 'second' ligand model for priming PITP-dependent presentation of PtdIns to the PtdIns 4-OK kinase (Schaaf et. al., 2008, Wu et. al., 2000; Huang et. al., 2016; Ren et. al., 2014; Li et. al., 2000; Routt et. al., 2005).

The results reported herein, however, discourage tacit extrapolation of the biochemical specificities of defects that come with altered PtdIns-binding bar-codes for Sec14-like PITPs where the second ligand remains unknown. Two recent studies of Sfh3 function in vivo provide a case in point. Both studies assumed that perturbation of the Sfh3 PtdIns-binding barcode would result in specific inactivation of PtdIns-binding/exchange activity (Ren et. al., 2014; Holič et. al., 2014). One of those studies directly confirmed that PtdIns binding/ exchange activity and the ability to stimulate PtdIns 4-OH kinase activity in vivo was indeed ablated by such perturbations (Ren et. al., 2014), and both studies found that such perturbations completely abolished Sfh3 biological function. Those phenotypic data were taken as evidence that PtdIns-binding/exchange is an essential functional property of Sfh3 (Ren et. al., 2014; Holič et. al., 2014). While that conclusion may yet prove correct, the data reported herein demonstrate that neither of the PtdIns-binding mutants used in those studies inactivated Sfh3 PtdIns-binding activity specifically. Rather, both PtdIns- and sterol exchange were compromised.

Unlike the case of the PtdIns and PtdCho binding bar-codes, which might yet prove exceptional in their discreteness, the Sfh3 data indicate substantial overlap of lipid-binding bar-

codes might prove a common scenario in Sec14-like PITPs. Indeed, this also appears to be the case for Sfh2. The squalene binding space in the Sfh2 lipid-binding cavity overlaps extensively with that of PtdIns. Consistent with such an assignment, we have to date failed to generate mutants selectively ablated for squalene binding/exchange that retain uncompromised PtdIns-binding/exchange activity.

Taken together, the data herein clearly demonstrate that the hydrophobic lipid-binding cavities of Sec14-like PITPs present chemically diverse landscapes that translate to functional diversities for 'second ligand'-binding. This property fulfills one prediction of the 'second-ligand priming' model for how Sec14-like PITPs stimulate the activities of PtdIns 4-OH kinases and identifies Sec14-like PITPs as particularly well-suited to contribute to the remarkable diversification of the biological outcomes of phosphoinositide signaling. In that regard, these studies identify Sfh5 as a genuinely unique Sec14-like protein given its hydrophilic and highly basic surface and cavity properties. Those unusual properties suggest the interesting possibility that the ligand-binding properties of Sfh5 and other Sec14-like proteins extend beyond lipids.

CHAPTER IV – UNCOUPLING OF THE DUAL SFH2 LIGAND-BINDING FUNCTIONS GUIDED BY LIGAND-BINDING BARCODES AND STRUCTURAL ANALYSIS

Summary

Sec14-like phosphatidylinositol transfer proteins (PITPs) translate metabolic information into phosphoinositide signals that promote a specific biological function. This intrinsic function is possible in Sec14p due to its unique ability to perform heterotypic ligand exchange (HLE) reactions between phosphatidylinositol (PtdIns) and its secondary ligand, phosphatidylcholine (PtdCho). We have previously reported that Sec14-homolog 2 (Sfh2) is a yeast PITP whose secondary ligand is squalene, a metabolic intermediate in sterol biosynthesis. However, its biophysical mechanism has yet to be characterized. In this study, we identified a putative "squalene-binding barcode" that is conserved from yeast to humans in Sfh2-like PITPs. We observe that mutations of these residues translate to defects in squalene transfer in vitro. As a result, a PtdIns-binding defective and a squalene-binding defective Sfh2 mutant were generated. Design of these mutants was guided by conserved ligand-binding barcodes and the comparison of a Sfh2 homology model to crystal structures of orthologous PITPs. We further provide evidence that supports that the ability of Sfh2 to fully compensate for the loss of Sec14 in yeast depends on its PtdIns-binding ability and proper squalene content in the yeast cell. This work serves to test the canonical Sec14-based model of PITP function and determine whether sterol metabolism and PIP signaling are integrated to induce a specific biological function by the squalene-binding PITP, Sfh2.

Introduction

Biological membranes carry out essential operations in the eukaryotic cell that depend upon the functional competence of the membrane. This functional competence is determined by its lipid composition. However, lipid composition is highly dynamic and responsive to environmental conditions such as temperature, oxygen and nutrient availability. Therefore, the cell needs to spatially and temporally determine whether membranes are competent for a specific function. For this reason, one role of membrane-embedded signaling lipids called phosphoinositides (PIPs) is to inform the cell of the competence of a membrane so that a specific membrane function is performed. However, phosphatidylinositol (PtdIns) kinases are engineered to be biologically incompetent and require being informed of when and where to generate PIP pools (Bankaitis et. al. 2010). In this context, PtdIns kinase ability to generate PIPs is dependent upon a phosphatidylinositol transfer protein (PITP), like Sec14 in yeast, that can simultaneously sense the lipid composition of a membrane and present PtdIns to its kinase in an interfacial manner (Schaaf et. al., 2008). In the case of Sec14, the production of this specific pool of PIP potentiates the essential function of vesicle formation and trafficking from the trans-Golgi network (Bankaitis et. al. 2010).

The concept that PITPs can both sense specific aspects of lipid metabolism and transmit that information to PIP synthesis is based upon Sec14's unique ability to perform heterotypic ligand exchange reactions (HLE; detailed in chapter one). The fact that the eukaryotic cell contains a multiplicity of Sec14-like PITPs - even in simple cells such as *S. cerevisiae* - and that they do not all share the secondary ligand of Sec14, implies that there are many aspects of lipid metabolism being monitored and coordinated with PIP signaling by the various Sec14-like proteins.

Sfh2 is a yeast Sec14-homolog whose secondary ligand is squalene, a metabolic precursor to all sterols in eukaryotic cells (Tripathi et al., 2019). The identity of this secondary ligand indicates that Sfh2 coordinates sterol metabolism with PIP signaling and a specific biological function according to the Sec14-based model. To confirm this hypothesis, it must be determined whether Sfh2 performs HLE reactions in the likeness of Sec14. The means to test the HLE model is by generating individual ligand-binding mutants of Sfh2 and testing them for functionality in vitro and in vivo. Using this approach, Sfh2 serves to determine whether sterol and PIP metabolic pathways are integrated by a PITP and whether the Sec14 model of PITP function is preserved in Sfh2. Unfortunately, mutations that completely uncouple PtdIns- and squalene-binding were unable to be generated, which impedes the validation of the HLE model. However, future analysis supported by data obtained in this work will help identify mutations that can adequately test the HLE model in vivo.

Materials and Methods

Sequence alignment and Homology modeling

Protein coding sequences were extracted, and alignment was generated utilizing Clustal Omega (Madeira et. al. 2019). Homology model of *S. cerevisiae* Sfh2 was generated with the MOE software package version 2013.08. The Sfh2 sequence was threaded to the Sfh1 (Sec14-homolog 1) crystal structure bound with PtdIns (PDB ID 3B7N; 1.86 Å resolution). The bound PtdIns ligand was included in the procedure to facilitate generating induced-fit homology models of a Sfh2-PtdIns complex. By default, 10 independent intermediate models were generated. These different intermediate homology models were generated as a result of permutational selection of different loop candidates and side-chain rotamers. The intermediate model, which

scored best according to the Amber99 force field, was chosen as the final model and was then subjected to further optimization.

Expression and purification of recombinant proteins.

The *SFH2* gene was amplified from the yeast genome and integrated into a pET28BHis-6 protein expression plasmid. All mutations were confirmed by DNA sequencing outsourced to the Eton Biosciences service. Recombinant $Sfh2^{His6}$ and mutant variants were purified as described by Ren et. al. using an *E.coli* BL21 (RIL/DE3; New England Biolabs Inc., Ipswich, MA) expression system. Protein mass was quantified by SDS-PAGE.

[^{3}H]PtdIns transfer assays

To measure PtdIns transfer, end-point radioactive transfer assays were performed. [^{3}H]PtdIns transport was measured from rat liver microsomes to liposomes (98 mol % PtdCho and 2 mol % PtdIns) to bovine heart mitochondria as described (Bankaitis et. al., 1990).

[^{3}H]Squalene transfer assays

Donor liposomes were composed of PtdCho/[^{3}H]squalene (99/1 weight %). For each assay, 40μg of lipid was dried under a stream ofN2 gas and resuspended by vortexing in 50μl of phosphate buffer (300mM NaCl, 25mM Na2HPO4, 5 mM β-mercaptoethanol, 1mM NaN3, pH 7.5). Small unilamellar vesicles were then generated from the suspension by sonication in an ice bath. Squalene transfer assays were then conducted using bovine heart mitochondria as acceptor membranes as described previously for PtdCho-transfer assays (Schaaf et. al., 2008). [12,13-^{3}H] Squalene (0.1 mCi/ml) was obtained from American Radiolabeled Chemicals (St. Louis, MO).

Results

Design strategy for Sfh2 mutants with defects in ligand binding

Several resources were employed to design Sfh2 derivatives defective in ligand binding. In the absence of a Sfh2 crystal structure, a homology model of Sfh2 threaded to the Sec14-homolog 1 (Sfh1) crystal structure (PDB ID: 3B7N) was utilized (Tripathi et al., 2019). The squalene-bound crystal structure of Sec14L2 (the human squalene-binding PITP and potential Sfh2 homolog; PDB ID: 4OMK) was referenced to guide this design (Christen et. al. 2015). Candidate residues for mutagenesis were also selected by comparing sequences from the yeast Sec14 family and highly divergent Sfh2 orthologs.

Sfh2 Residue E249 was mutated to Phe to sterically obstruct the coordination of the PtdIns headgroup and prohibit the ability of Sfh2 to bind PtdIns. The rationale for this mutation is that although residue E249 is a member of the "PtdIns-binding barcode" residues conserved among all Sec14-like PITPs, its identity as glutamate is unique to Sfh2 (Figure 4-1A; residue highlighted in red). However, this amino acid is absolutely conserved at this location in all Sfh2 orthologs in divergent yeast and in Sec14L2 (Figure 4-1B; boxed residues). In comparison to the cognate residue in the crystal structure of PtdIns-bound Sfh1 (PDB ID: 3B7N), this barcode residue is involved in the coordination of the PtdIns headgroup. This residue retains this orientation in our Sfh2 homology model when PtdIns is superimposed into the Sfh2 binding cavity (Figure 4-1C).

Sfh2 squalene-binding residues for mutagenesis were selected by analyzing Sec14L2 residues which resided within the hydrophobic cavity and contacted squalene in the crystal structure. Candidate residues were restricted to those that are conserved across Sfh2 orthologs in divergent yeast (Figure 4-1B).

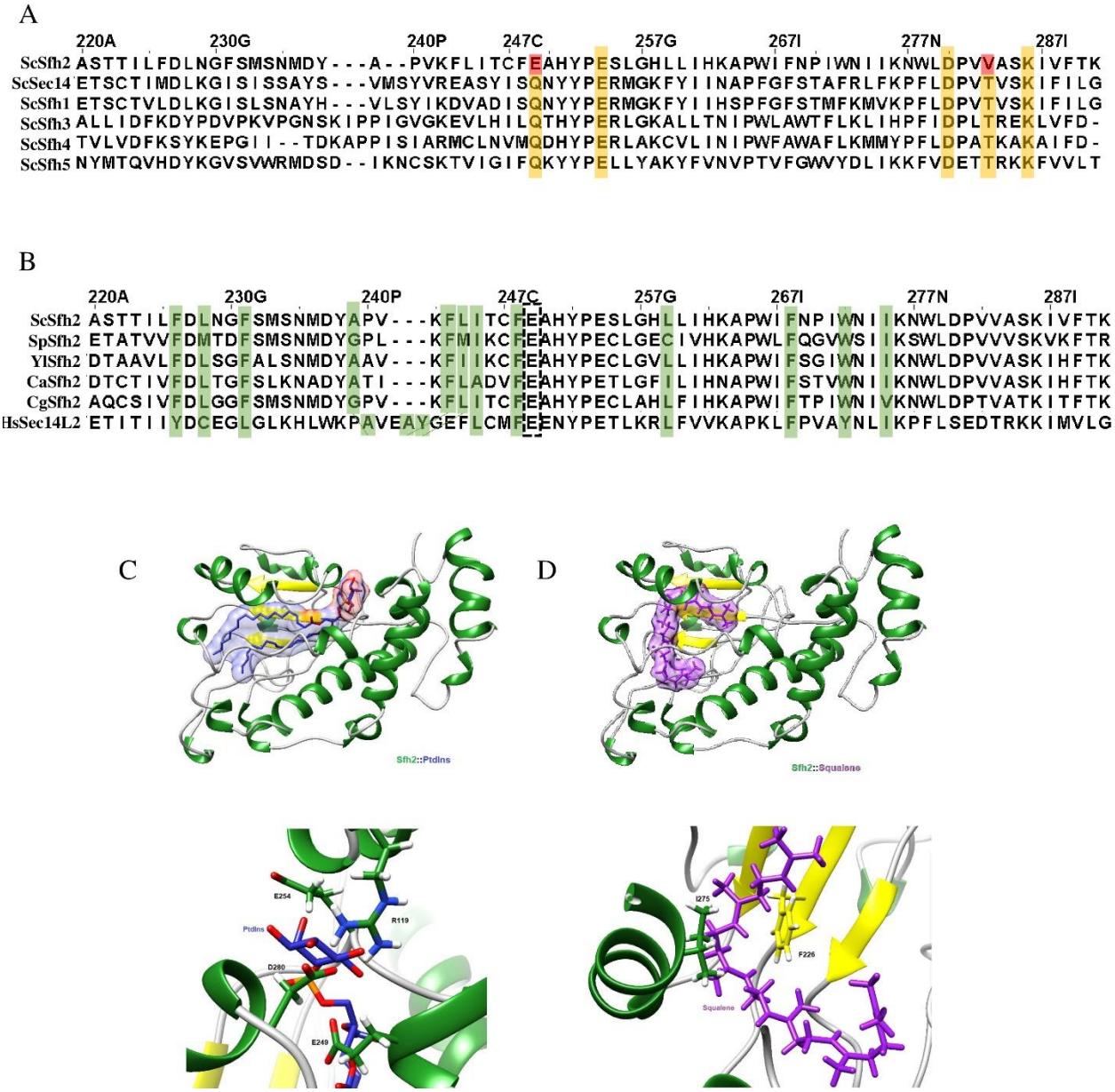

Figure 4-1: Sfh2 ligand-binding barcodes and residues

(A) Sequence alignment of the yeast PITPs. "PtdIns-binding barcode" residues highlighted in yellow. Barcode residues distinct to Sfh2 highlighted in red. Sc= Saccharomyces cerevisiae; Sp=Schizosaccharomyces pombe; Yp=Yarrowia lipolytica; Ca= Candida albicans; Cg=Candida glabrata; Hs=Homo sapiens. (B) Sequence alignment of Sfh2 orthologs in divergent organisms. "Squalene-binding barcode" highlighted in green. Sfh2 residue E249 and orthologous residues boxed in dashed line. (C) Homology model of Sfh2 with PtdIns (extracted from Sfh1 crystal structure; PDB ID: 3B7N) superimposed into ligand binding cavity (above). Orientation of "PtdIns-binding barcode" residues and E249 relative to PtdIns headgroup (below). (D) Homology model of Sfh2 with squalene (extracted from Sec14L2 crystal structure, PDB ID: 4OMK) superimposed into ligand binding cavity (above). Orientation of residues F226 and I275 relative to squalene.

These residues included Y153, C155, L158, A167, A170, Y171, L175, F178, L189, F198, Y202, I205 in Sec14L2 and are analogous to Sfh2 residues F226, L228, F231, A239, F243, L244, I245, F248, L259, F268, W272, and I275 respectively. These residues can be considered as the putative "squalene-binding barcode". Several mutations affected squalene binding, however, mutating both residues F226 and I275 to alanine demonstrated the greatest decrease in squalene binding ability without compromising PtdIns-binding (Figure 4-2). The cognate residues in Sec14L2 (Y153 and I205) reside within an average of about 3Å from the squalene ligand in the crystal structure (PDB ID: 4OMK). The orientation of F226 and I275 towards squalene is maintained in the Sfh2 homology model and can be observed when squalene is extracted from the Sec14L2 crystal structure and superimposed into the Sfh2 homology model (Figure 4-1D).

Ligand-transfer activities of mutant Sfh2 derivatives

The mutants described above exhibited the specific ligand-binding defects that were predicted by the design strategy. Recombinant $Sfh2^{E249F}$ (PtdIns-binding mutant; PIBM) and $Sfh2^{F226A,\ I275A}$ (squalene-binding mutant; SQBM) were purified and assayed for both PtdIns and squalene transfer activity *in vitro*. The $Sfh2^{E249F}$ PtdIns-binding mutant demonstrated the loss of ~90% of wild-type PtdIns transfer activity while retaining wild-type levels of squalene transfer (Figure 4-3). The $Sfh2^{F226A,\ I275A}$ squalene-binding mutant lost ~60% of its squalene transfer activity while retaining wild-type levels of PtdIns transfer (Figure 4-3). *SFH2*, $SFH2^{E249F}$ $SFH2^{F226A,\ I275A}$ were modified with a C-terminal HA-tag and integrated into the native locus of *SFH2* in our parental wild-type *S. cerevisiae* strain (CTY 182) and were determined to be expressed equivalently at steady-state in vivo (Figure 4-3C).

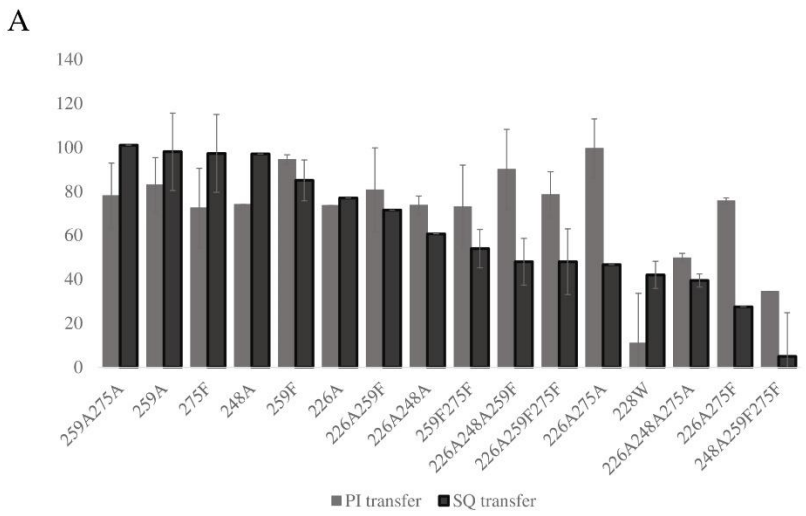

Figure 4-2. Screening of squalene-binding barcode mutants

(A) Several mutations were assessed for the loss of squalene-transfer activity. PtdIns- and squalene-transfer data for 10 μg protein represented as percentage of wild type. Data presented in descending order of squalene transfer activity. Average values and standard deviations are given when possible (i.e. when experiments were performed more than once). Each mutant is assayed in triplicate in every experiment.

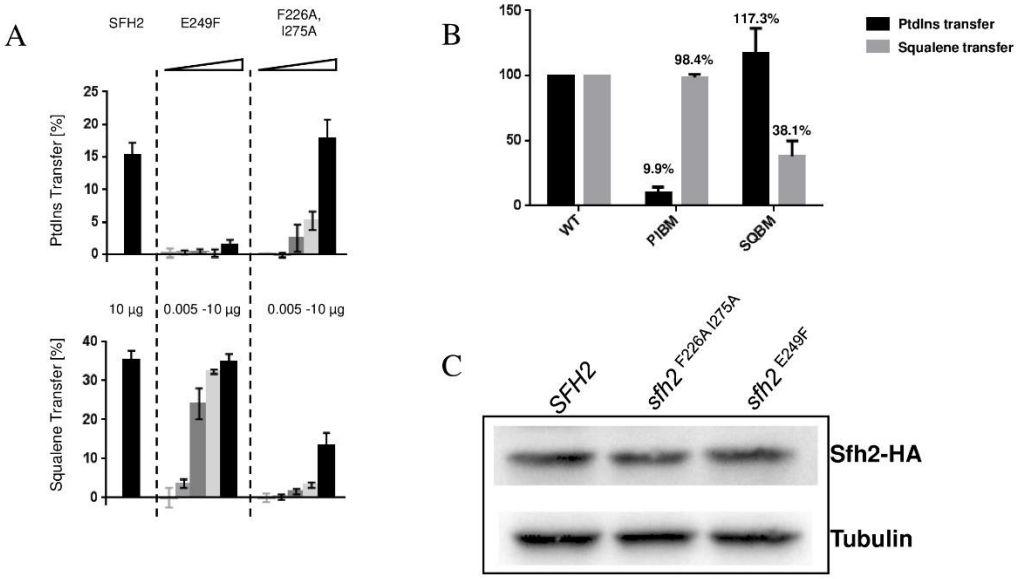

Figure 4-3. Biochemical validation of Sfh2 ligand-binding mutants

(A) PtdIns- and squalene- transfer assay data are presented. Purified recombinant Sfh2 proteins were assayed in a step series of 0.005, 0.025, 0.25, 1, and 10 µg for PtdIns- and squalene-transfer activity. Average values and standard deviations are given ($n \geq 3$ for each condition). (B) PtdIns- and squalene-transfer data for 10 µg condition represented as percentage of wild type. PIBM (PtdIns-binding mutant) and SQBM (squalene-binding mutant) are Sfh2E249F and Sfh2F226A I275A, respectively. (C) HA-tagged versions of SFH2 mutants were integrated into the native genomic locus of Sfh2 to determine their steady-state levels in vivo. Immunoblotting was performed with an anti-HA monoclonal antibody. Tubulin (Tub3) was evaluated as a control for proper normalization.

SFH2^{E249F} and SFH2$^{F226A\ I275A}$ ligand-binding mutants are still functional in vivo

A Sec14 rescue assay was employed to assess the biochemical functionality of the Sfh2 ligand-binding derivatives. Overexpression of *SFH2* phenotypically rescues the conditional lethality associated with the *sec14-1^{ts}* mutation (Routt et al., 2005). Further, biochemical measurements demonstrate that this is accompanied with an increase in phosphatidylinositol-4-phosphate (PtdIns4P; Routt et al. 2005). These data demonstrate that Sfh2p can potentiate the same essential PtdIns4P pool as Sec14. We show here that even a low dose of WT Sfh2 expressed from the *SFH2* promoter on a centromeric plasmid complements Sec14 function (Figure 4-4A). The phenotypic data report that Sfh2^{E249F} is moderately compromised in rescuing *sec14-1^{ts}*-associated growth defects relative to WT Sfh2 (Figure 4-4A). However, Sfh2$^{F226A\ I275A}$ still robustly rescued Sec14 defects.

Cellular threshold for Sfh2-mediated rescue of Sec14-deficient yeast is very low

The Sec14-based model of PITP function holds explanatory power superior to classical lipid transfer protein models because the observation that the functional threshold for Sec14-dependent cellular viability is extremely low indicates that the relationship between Sec14 and PtdIns goes beyond merely supply/transfer (Bankaitis et. al.; 2010). That Sfh2^{E249F} still retained residual ability to rescue Sec14 defects on a low-copy centromeric plasmid even though it only retains ~10% of WT Sfh2 PtdIns-transfer activity supported the observation that the threshold for rescuing Sec14-mediated PtdIns4P production is quite low. For this reason, the native copy of *SFH2* in the *sec14-1^{ts}* strain was deleted to remove its potential contribution to Sec14 rescue. In this strain, WT Sfh2, Sfh2^{E249F}, and Sfh2$^{F226A\ I275A}$ could still rescue Sec14-defects (Figure 4-4B). This demonstrates that even a low copy number of severely defective Sfh2 variants can complement Sec14 function.

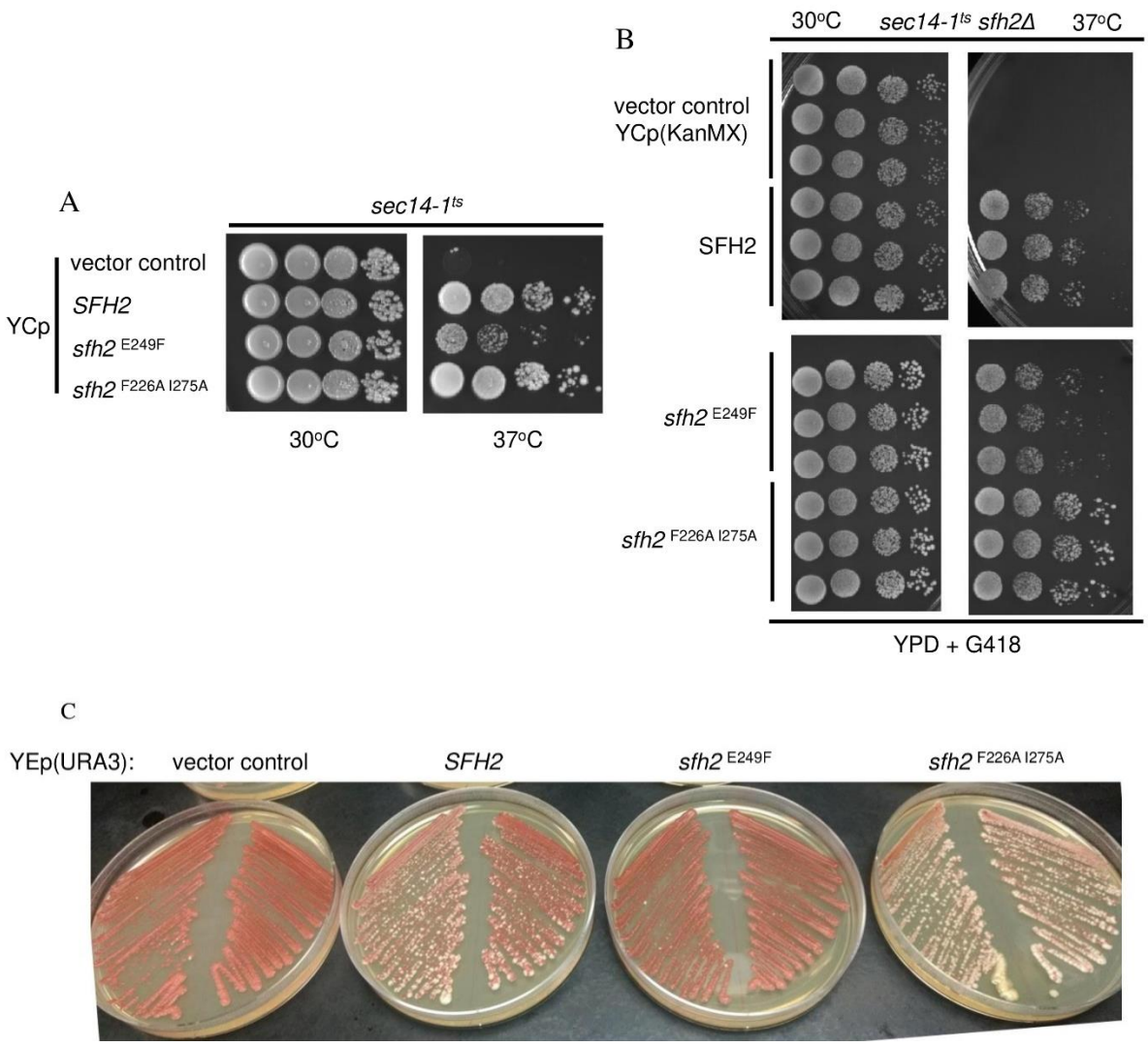

Figure 4-4. Functional validation of Sfh2 ligand-binding mutants

(A) *Sec14-1*^{ts} transformed with YCp plasmids carrying the designated Sfh2 alleles (indicated at left) were spotted in 10-fold dilution series onto YPD agar plates and incubated at 30ºC and 37ºC. Rescue of growth defect reports functionality. YCp(*URA3*) served as vector (negative) control. (B) Experiment done as in (A) except that *Sec14-1*^{ts} *sfh2Δ* are transformed with the indicated plasmids. YCp plasmids contain the *KanMX* marker as *SFH2* is deleted using the *URA3* selection marker. Three independent colonies were tested for each strain. Plasmids were retained using YPD agar supplemented with G418. (C) An *ade2 ade3 sec14Δ*/YEp(*SEC14, LEU2, ADE3*) yeast strain (strain CTY558) was transformed with the indicated high-copy YEp(*sfh2, URA3*) plasmids and two independent colonies of each indicated strain were streaked onto YPD agar. Functionality of mutant *sfh2* product is manifested as appearance of white segregant colonies that acquire leucine and histidine auxotrophies, signifying loss of parental YEp(*SEC14, LEU2, ADE3*). Retention of parental plasmid (i.e., nonfunctionality of the mutant *sfh2*) is reported by red colony color (Schaaf et. al. 2008).

Plasmid shuffle assays also demonstrate Sfh2^{E249F} functional insufficiency

Alternatively, plasmid shuffle assays were utilized to discern whether the Sfh2 variants can fulfill the essential Sec14 function *in vivo*. Episomal plasmids bearing the WT and SQBM variants of Sfh2 expressed by a the *SFH2* promoter were able to shuffle and thereby able to fulfill the essential role of Sec14 function in vivo (Figure 4-4). However, the Sfh2 PIBM is unable to generate the PIP pool necessary to compensate for the loss of the essential Sec14 PtdIns4P pool *in vivo* as determined by lack of plasmid shuffle.

Squalene depletion prevents WT Sfh2, but not Sfh2$^{F226A\ I275A}$, from rescuing Sec14

A pillar of the Sec14 model of PITP function is that the simultaneous exposure of a PITP to both of its ligands is required for HLE to occur. For this reason, the abundance of squalene was chemically modulated to determine whether this perturbation will influence the ability of Sfh2 to complement Sec14-mediated PIP production. This was achieved by using the chemical inhibitors zaragozic acid and terbinafine to deplete or accumulate squalene levels, respectively. Depleting squalene levels using zaragozic acid prevented both WT and Sfh2^{E249F} from rescuing Sec14-deficient growth (Figure 4-5A). Surprisingly, this had a negligible effect on the ability of Sfh2$^{F226A\ I275A}$ to complement Sec14. Further, this phenotype was not recapitulated when inducing squalene accumulation using terbinafine. To ensure that this phenotype was not due to squalene sequestration by WT Sfh2 and Sfh2^{E249F}, Sfh2 was expressed on a high-copy plasmid in the *sec14-1^{ts}* strain and grown in the presence of zaragozic acid at restrictive temperatures (Fig 4-5B). Under these conditions, overexpression of Sfh2 was still able to rescue the growth of Sec14-deficient cells. This data indicates that Sfh2 on a low copy plasmid is unable to overcome the threshold of Sec14 rescue when squalene levels are depleted. However, it is unclear why the functional competence of Sfh2$^{F226A\ I275A}$ is not similarly affected by squalene depletion.

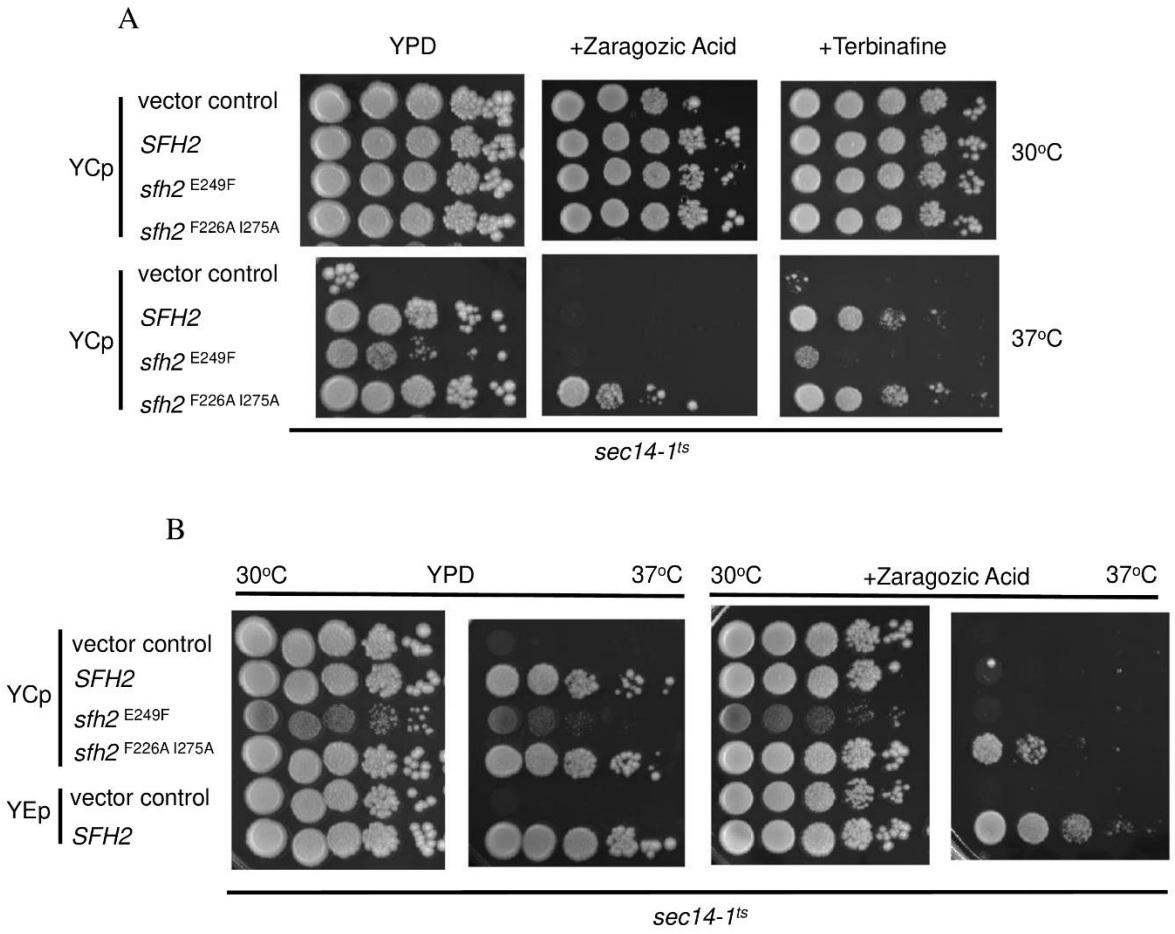

Figure 4-5. In vivo ligand binding dynamics of Sfh2

(A) Sec14-1ts transformed with YCp plasmids carrying the designated Sfh2 alleles (indicated at left) were spotted in 10-fold dilution series onto YPD agar plates and incubated at 30oC and 37oC. Rescue of growth defect reports functionality. YCp(URA3) served as vector (negative) control. YPD was supplemented with either 3.5 μg/mL zaragozic acid or 150μM terbinafine in drug containing plates. (B) Experiment performed as in (A); includes Sec14-1ts transformed with YEp plasmids (indicated at left; bottom two rows).

Discussion

Understanding how sterol metabolism is integrated with PIP signaling to ensure that cellular membranes remain functionally competent will be facilitated by the biophysical characterization of Sfh2. This work takes the first steps at attaining that goal by producing two Sfh2 mutants that separate its two ligand-binding functions ($Sfh2^{E249F}$ and $Sfh2^{F226A\ I275A}$) and determining their in vivo functionality. This research presents: (1) a putative "squalene-binding barcode" that is conserved from yeast to humans in Sfh2-like PITPs (2) mutation of these barcode residues translates to defects in squalene transfer in vitro, (3) although $Sfh2^{E249F}$ and $Sfh2^{F226A\ I275A}$ lose a significant amount of PtdIns- and squalene-transfer activity in vitro, respectively, they are still functional PITPs in vivo, (4) data that indicates that the threshold for Sec14 functional complementation is extremely low, and (5) that squalene availability may influence WT Sfh2 function. This work demonstrates that Sfh2 is a readily exploitable protein to both test the Sec14 paradigm of PITP function and thereby identify a mediator between sterol metabolism, PIP signaling, and a distinct biological function.

One hurdle that was faced in the design of squalene-binding mutants was that nearly every mutation that affected squalene binding also perturbed PtdIns binding (Figure 4-2). This is because PtdIns and squalene occupy the same ligand binding region in the hydrophobic pocket of Sfh2, notably, in the region that binds the PtdIns acyl chains. This is analogous to the way the PtdIns- and PtdCho-binding regions overlap in Sec14 and gives structural evidence to support that Sfh2 ligands undergo HLE reactions in the same manner as Sec14.

A parameter was imposed in designing squalene-binding mutants that required any mutation that affected squalene transfer in vitro left PtdIns transfer activity intact. This was implemented so that the inability of squalene-binding mutants to rescue Sec14 in vivo would not

be attributed to PtdIns-transfer defects. However, because the results that demonstrate that Sfh2^{E249F} expressed on a centromeric plasmid, at ~10% WT activity, even when the native copy of *SFH2* is ablated from the genome, is still able to complement Sec14 function, Sfh2 PtdIns-transfer activity can be significantly reduced before losing complete functionality as a PITP in vivo. For this reason, more severe squalene-binding mutants should be tested even at the expense of PtdIns-transfer activity. One candidate mutant is Sfh2$^{F248A\ L259F\ I275F}$ which displayed 5% squalene- and 34.5% PtdIns- transfer activity relative to WT Sfh2 (preliminary data). The same approach can be applied to find more severe PtdIns-binding mutants.

Without observing that the loss of both squalene- and PtdIns-binding ability renders Sfh2 incapable of functioning as a PITP in vivo (as determined by Sec14 rescue), the HLE model for Sfh2 cannot be supported. However, if the precise biological function of Sfh2 is deduced, the HLE model can be revisited in this context. If successful, the biophysical characterization of Sfh2 will serve to demonstrate how other members of the Sec14-like PITP family integrate lipid metabolic pathways and specific membrane functions such as vesicle formation and transport.

CHAPTER V – CONCLUSIONS AND FUTURE DIRECTION

The characterization of individual members of the yeast Sec14 PITP family will reveal more about the individual biological functions they regulate; especially in terms of the lipid composition the functions require. The overarching aim of this research was to elucidate the functional and biophysical characteristics of the yeast Sec14-like PITP, Sfh2. This aim is attained by determining the biological function of Sfh2, identifying its secondary ligand, and characterizing its ligand-binding dynamics. The analysis of chemogenomic data revealed that Sfh2 is involved in vesicle formation/transport and potentially in the endosome/trans-Golgi network (TGN) system in response to perturbed lipid metabolism under nutrient deprived conditions. Identification of its secondary ligand as squalene implies that squalene is acting as metabolic information to be translated into a phosphoinositide signal and cellular function; according to the Sec14-based model of PITP function. Finally, the data demonstrates that Sfh2 ligand-binding abilities can be uncoupled. However, better ligand-binding mutants need to be designed before the canonical heterotypic ligand exchange model can be validated in vivo. This final aim will establish that squalene metabolism is indeed coupled to PIP synthesis by Sfh2. Herein we discuss pending experiments and preliminary data that can direct Sfh2 research moving forward.

Chapter two of this dissertation revolved around the chemogenomic analysis of *sfh2Δ/Δ* homozygous deletion yeast to identify genes and biological functions that overlapped with Sfh2 function. This analysis led to the discovery that Sfh2 function is essential when there are defects in anterograde membrane trafficking at the ER-to-Golgi and TGN steps of the secretory pathway. These findings can be more fully characterized if we determine whether a PtdIns- or squalene-binding mutant is able to phenocopy Sfh2 ablation in the parental strains (s*ec12*^{ts} and *sec14*^{ts}) in

both the temperature-sensitive growth assay and pulse-chase CPY trafficking assays. This will determine whether Sfh2-mediated squalene-sensing and/or PIP signaling are required for these vesicle transport events.

The chemogenomic analysis of Sfh2 described in chapter two appears to be substantiated in light of a recent report about the in vivo function of Sec14l3, the functional homolog of the human Sec14-like PITP, Sec14L2, in zebrafish. Because Sfh2 and Sec14L2 both bind and transfer squalene in vitro and are structurally homologous, it is very likely that they are functionally homologous as well. Indeed, Gong et. al. report that Sec14l3/Sec14L2 promote vascular endothelial growth factor receptor 2 (VEGFR2) internalization from the plasma membrane and return from endosomal pools to maximize signaling strength upon ligand stimulation (Gong et. al., 2019). This signaling pathway regulates endothelial cell proliferation, differentiation, migration, and position via the PLCγ/ERK and PI3K/AKT pathways (Gong et. al., 2019). Importantly, the signaling output of the VEGFR2 pathway is significantly regulated by the intracellular trafficking and endocytic kinetics of the receptor (Gong et. al., 2019). Strikingly, Sec14L2 was also found to physically interact with RAB5A, which is the human homolog of the Sfh2 cofit gene Ypt52. Furthermore, VEGFR2 displays a distinct distribution in lipid rafts, ordered membrane microdomains characterized by high concentrations of cholesterol and glycosphingolipids (Caliceti et. al. 2014). This paper reiterated nearly every biological process identified in the chemogenomic analysis of Sfh2. That is, a process that involves lipid-dependent endomembrane recycling of a plasma membrane receptor that initiates a signal transduction pathway that regulates the cell cycle in response to extracellular signals/nutrient availability.

Although FM4-64 trafficking experiments indicated that there were no endocytic defects, increasing signal resolution by using confocal microscopy may help to quantify subtle but significant trafficking defects; especially if Sfh2 deletion induces kinetic defects at specific endocytic transit steps. Further, recycling of Snc1 must be analyzed in the Sfh2 deletion strain. Snc1 is a v-SNARE that drives fusion of exocytic vesicles with the plasma membrane which then recycles through the endocytic pathway to the Golgi for reuse in exocytosis (Xu et. al., 2017).

Chemogenomic analysis was thorough but not exhaustive. Many more observations and connections can be made regarding the *sfh2Δ/Δ* cofitness data and the terbinafine chemogenomic profile. For example, genes that code for tryptophan (Trp) biosynthetic enzymes (i.e. Trp3, Trp5, Trp2, Trp4; ranked in descending order) were enriched in the top 10 of 4807 homozygous deletion strains sensitive to terbinafine. Absence of these genes leads to Trp auxotrophy and necessitates that the Trp transporter, Tat2, be trafficked to the plasma membrane so that exogenous Trp can be imported into the cell. Squalene accumulation or an altered sterol composition may be affecting the vesicular sorting of this transporter or is somehow affecting its structure and function. This hypothesis is supported by literature that demonstrated that perturbation of the sterol biosynthetic pathway, by gene deletion or small molecule inhibitors, led to the ubiquitination, missorting, and degradation of the Tat2 transporter (Umbeyashi et. al., 2003; Daicho et. al. 2007). Therefore, the fate of Tat2-GFP will need to be observed in the presence and absence of Sfh2, small molecule inhibitors of ergosterol biosynthesis, and under standard, high, and low Trp media concentrations.

Finally, in regard to the in vivo role of Sfh2, one very possible condition in which Sfh2 function is utilized is under anaerobiosis. Sfh2 was identified with a group of genes that were

significantly up-regulated under hypoxic conditions (Kwast et. al., 2001). In this study, many ergosterol biosynthetic enzymes and cell wall-related proteins were enriched in this set of upregulated genes. The expression of Sfh2 was specifically identified as being likely regulated by both Rox1, a hypoxia transcriptional repressor whose expression and activity is proportional to oxygen availability, and Upc2, a sterol regulatory element binding protein (SREBP) that induces sterol biosynthesis and is repressed by Rox1p under aerobiosis (Figure 5-1; Kwast et. al., 2001). Indeed, both Upc2 and Rox1 target sequences can be found in the Sfh2 promoter using the Yeastract+ database (Monteiro et. al., 2020). Furthermore, five target sequences of Mot3, a hypoxia-related transcription factor (TF) which represses gene transcription under aerobiosis, are also found in the Sfh2 promoter region (Monteiro et. al., 2020). Further, Upc2 and its paralog Ecm22 are both among the highest ranked genes that correlate with Sfh2 function according to chemogenomic database analysis (Lee et al., 2014). In support of these observations, one study demonstrated that Sfh2 expression was induced by the constitutive expression of Sut1, a TF that regulates sterol uptake and hypoxic gene expression under anaerobic conditions (Figure 5-1; Bourot et al., 1995; Régnacq et al., 2008).

The Sfh2 promoter region also contains target sequences of TFs that are activated by the Slt2/Mpk1 mitogen activated protein kinase (MAPK) cell wall integrity (CWI) pathway; these TFs are Skn7, Swi4, and Mcm1 (Figure 5-1). Further, the alias of Sfh2, Csr1, is so named because of its ability to rescue a *chs5 spa2* lethal phenotype; these two genes are implicated in proper cell wall formation (Santos and Snyder, 2000).

Considering the identity of the secondary ligand of Sfh2, squalene, it is interesting and relevant that squalene epoxidation is an essential oxygen requiring step of the sterol biosynthetic pathway. Further, the inhibition of squalene epoxidase function (Erg1) by terbinafine or hypoxia

leads to the accumulation of squalene in yeast (Garaiová et al., 2014; Gleason et al., 2011). Furthermore, chemogenomic data demonstrates that Slt2, the MAPK that regulates the CWI pathway, is required for resistance to terbinafine. This data cumulatively describes a picture where Sfh2 is expressed under hypoxic conditions to sense the accumulation of squalene and prevent cell wall stress.

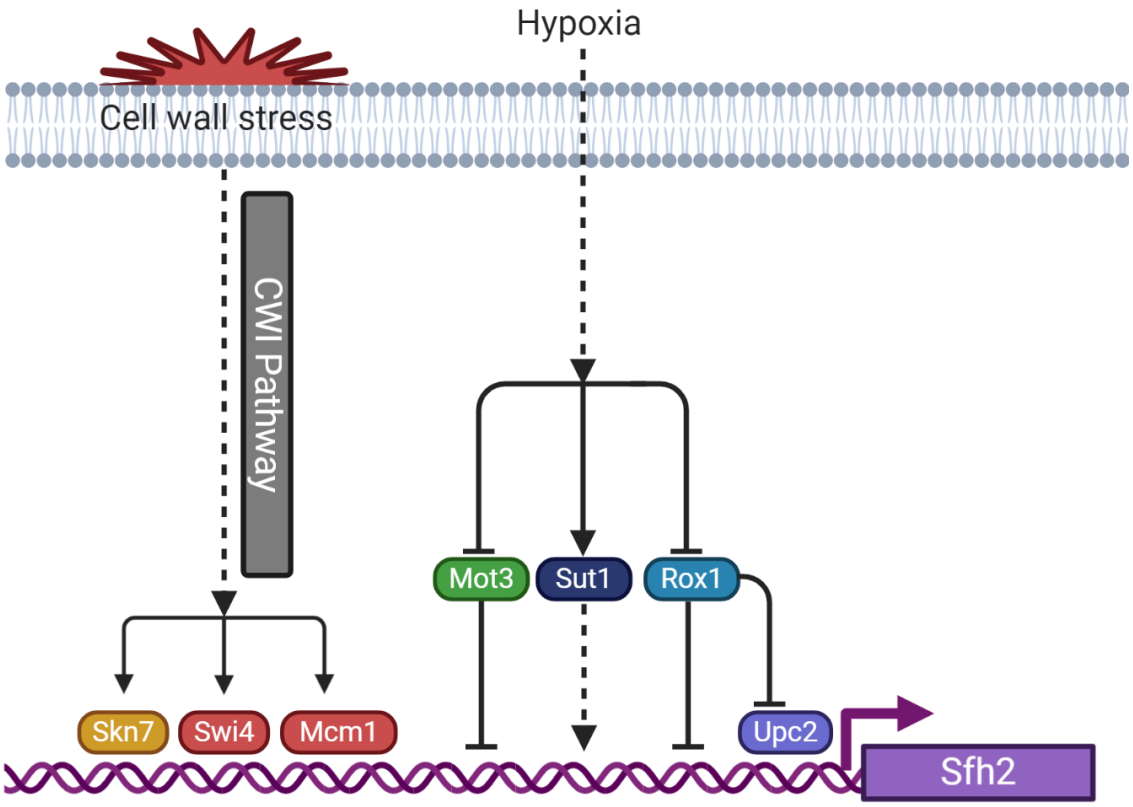

Figure 5-1. Cell wall stress and hypoxia potentially regulate of Sfh2 expression

Sfh2 expression is potentially regulated by transcriptional activators and repressors involved in the Slt2 cell wall integrity (CWI) pathway, the hypoxic response, and sterol regulation (Sut1 and Upc2) based on the presence of target sequences in its promoter region.

Chapter four focused on the functional characterization of Sfh2 ligand-binding mutants. Once optimal ligand-binding mutations are designed, if we observe that both the full loss of squalene- and PtdIns-binding ability renders Sfh2 incapable of functioning as a PITP in vivo, several experiments can be pursued that will validate the HLE model. We need to determine whether these mutations must be housed “in cis” (i.e. in the same molecule) or whether a mixed population of Sfh2::PtdIns and Sfh2::Squalene molecules satisfies the essential requirement for cell viability in the Sec14-rescue assay. Both ligand-binding mutants will be used to determine whether either/both ligand-binding abilities are necessary for resistance to terbinafine. In regard to the role of Sfh2 in lipid metabolism, mass spectrometry (MS)-based “shotgun lipidomics” can be employed to determine the effect of Sfh2 deletion and mutants on the relative levels of phospholipids, sphingolipids, and ergosterol biosynthetic intermediates.

REFERENCES

Abagyan, Ruben, Maxim Totrov, and Dmitry Kuznetsov. "ICM—a new method for protein modeling and design: applications to docking and structure prediction from the distorted native conformation." *Journal of computational chemistry* 15.5 (1994): 488-506.

Ast, Tslil, Susan Michaelis, and Maya Schuldiner. "The protease Ste24 clears clogged translocons." *Cell* 164.1-2 (2016): 103-114.

Aviram, Naama, et al. "The SND proteins constitute an alternative targeting route to the endoplasmic reticulum." *Nature* 540.7631 (2016): 134-138.

Bankaitis, Vytas A., et al. "An essential role for a phospholipid transfer protein in yeast Golgi function." *Nature* 347.6293 (1990): 561-562.

Bankaitis, Vytas A., Carl J. Mousley, and Gabriel Schaaf. "The Sec14 superfamily and mechanisms for crosstalk between lipid metabolism and lipid signaling." *Trends in biochemical sciences* 35.3 (2010): 150-160.

Bourot, Stéphane, and Francis Karst. "Isolation and characterization of the Saccharomyces cerevisiae SUT1 gene involved in sterol uptake." *Gene* 165.1 (1995): 97-102.

Brace, Jennifer L., et al. "SVF1 regulates cell survival by affecting sphingolipid metabolism in Saccharomyces cerevisiae." *Genetics* 175.1 (2007): 65-76.

Breslow, David K., et al. "Orm family proteins mediate sphingolipid homeostasis." *Nature* 463.7284 (2010): 1048-1053.

Cabrera, Margarita, et al. "Functional separation of endosomal fusion factors and the class C core vacuole/endosome tethering (CORVET) complex in endosome biogenesis." *Journal of Biological Chemistry* 288.7 (2013): 5166-5175.

Caliceti, Cristiana, et al. "Role of plasma membrane caveolae/lipid rafts in VEGF-induced redox signaling in human leukemia cells." *BioMed research international* 2014 (2014).

Cha, Mee-Kyung, et al. "The protein interaction of Saccharomyces cerevisiae cytoplasmic thiol peroxidase II with SFH2p and its in vivo function." *Journal of Biological Chemistry* 278.37 (2003): 34952-34958.

Chaker-Margot, Malik, et al. "Architecture of the yeast small subunit processome." *Science* 355.6321 (2017).

Christen, Monika, et al. "Structural insights on cholesterol endosynthesis: Binding of squalene and 2, 3-oxidosqualene to supernatant protein factor." *Journal of structural biology* 190.3 (2015): 261-270.

Cleves, Ann E., et al. "Mutations in the CDP-choline pathway for phospholipid biosynthesis bypass the requirement for an essential phospholipid transfer protein." *Cell* 64.4 (1991): 789-800.

Conrad, Michaela, et al. "Nutrient sensing and signaling in the yeast Saccharomyces cerevisiae." *FEMS microbiology reviews* 38.2 (2014): 254-299.

Daicho, Katsue, et al. "The ergosterol biosynthesis inhibitor zaragozic acid promotes vacuolar degradation of the tryptophan permease Tat2p in yeast." *Biochimica et Biophysica Acta (BBA)-Biomembranes* 1768.7 (2007): 1681-1690.

Desfougères, Thomas, et al. "SFH2 regulates fatty acid synthase activity in the yeast Saccharomyces cerevisiae and is critical to prevent saturated fatty acid accumulation in response to haem and oleic acid depletion." *Biochemical Journal* 409.1 (2008): 299-309.

Dickson, Eamonn James. "Recent advances in understanding phosphoinositide signaling in the nervous system." *F1000Research* 8 (2019).

Duden, Rainer. "ER-to-Golgi transport: Cop I and Cop II function." *Molecular membrane biology* 20.3 (2003): 197-207.

Foresti, Ombretta, et al. "Sterol homeostasis requires regulated degradation of squalene monooxygenase by the ubiquitin ligase Doa10/Teb4." *Elife* 2 (2013): e00953.

Furuta, Nobumichi, et al. "Endocytic recycling in yeast is regulated by putative phospholipid translocases and the Ypt31p/32p–Rcy1p pathway." *Molecular biology of the cell* 18.1 (2007): 295-312.

Garaiová, Martina, et al. "Squalene epoxidase as a target for manipulation of squalene levels in the yeast Saccharomyces cerevisiae." *FEMS Yeast Research* 14.2 (2014): 310-323.

Garrett, M. D., et al. "GDI1 encodes a GDP dissociation inhibitor that plays an essential role in the yeast secretory pathway." *The EMBO journal* 13.7 (1994): 1718-1728.

Ghosh, Ratna, et al. "Sec14-nodulin proteins and the patterning of phosphoinositide landmarks for developmental control of membrane morphogenesis." *Molecular biology of the cell* 26.9 (2015): 1764-1781.

Gleason, Julie E., et al. "Analysis of hypoxia and hypoxia-like states through metabolite profiling." *PloS one* 6.9 (2011): e24741.

Gong, Bo, et al. "Sec14l3 potentiates VEGFR2 signaling to regulate zebrafish vasculogenesis." *Nature communications* 10.1 (2019): 1-16.

Gordesky, Stanley E., and G. V. Marinetti. "The asymmetric arrangement of phospholipids in the human erythrocyte membrane." *Biochemical and biophysical research communications* 50.4 (1973): 1027-1031.

Grabon, Aby, Danish Khan, and Vytas A. Bankaitis. "Phosphatidylinositol transfer proteins and instructive regulation of lipid kinase biology." *Biochimica et Biophysica Acta (BBA)-Molecular and Cell Biology of Lipids* 1851.6 (2015): 724-735.

Gupta, Chhitar M., Ramachandran Radhakrishnan, and H. Gobind Khorana. "Glycerophospholipid synthesis: improved general method and new analogs containing photoactivable groups." *Proceedings of the National Academy of Sciences* 74.10 (1977): 4315-4319.

Hedbacker, Kristina, and Marian Carlson. "Regulation of the nucleocytoplasmic distribution of Snf1-Gal83 protein kinase." *Eukaryotic cell* 5.12 (2006): 1950-1956.

Herzig, Sébastien, and Reuben J. Shaw. "AMPK: guardian of metabolism and mitochondrial homeostasis." *Nature reviews Molecular cell biology* 19.2 (2018): 121.

Holič, Roman, et al. "Phosphatidylinositol binding of Saccharomyces cerevisiae Pdr16p represents an essential feature of this lipid transfer protein to provide protection against azole antifungals." *Biochimica et Biophysica Acta (BBA)-Molecular and Cell Biology of Lipids* 1841.10 (2014): 1483-1490.

Huang, Jin, et al. "Two-ligand priming mechanism for potentiated phosphoinositide synthesis is an evolutionarily conserved feature of Sec14-like phosphatidylinositol and phosphatidylcholine exchange proteins." *Molecular biology of the cell* 27.14 (2016): 2317-2330.

Jacobson, Matthew P., et al. "On the role of the crystal environment in determining protein side-chain conformations." *Journal of molecular biology* 320.3 (2002): 597-608.

Jones, Gareth, et al. "Development and validation of a genetic algorithm for flexible docking." *Journal of molecular biology* 267.3 (1997): 727-748.

Karpichev, Igor V., Lizbeth Cornivelli, and Gillian M. Small. "Multiple regulatory roles of a novel Saccharomyces cerevisiae protein, encoded by YOL002c, in lipid and phosphate metabolism." *Journal of Biological Chemistry* 277.22 (2002): 19609-19617.

Kellogg, Glen Eugene, and Donald J. Abraham. "Hydrophobicity: is LogPo/w more than the sum of its parts?." *European journal of medicinal chemistry* 35.7-8 (2000): 651-661.

Kemp, Hilary A., and George F. Sprague Jr. "Far3 and five interacting proteins prevent premature recovery from pheromone arrest in the budding yeast Saccharomyces cerevisiae." *Molecular and cellular biology* 23.5 (2003): 1750-1763.

Khan, Danish, et al. "A Sec14-like phosphatidylinositol transfer protein paralog defines a novel class of heme-binding proteins." *Elife* 9 (2020): e57081.

Kim, Jeong-Ho, et al. "The glucose signaling network in yeast." *Biochimica et Biophysica Acta (BBA)-General Subjects* 1830.11 (2013): 5204-5210.

Kroschwald, Sonja, et al. "Different material states of Pub1 condensates define distinct modes of stress adaptation and recovery." *Cell reports* 23.11 (2018): 3327-3339.

Kubota, Naoto, et al. "Adiponectin stimulates AMP-activated protein kinase in the hypothalamus and increases food intake." *Cell metabolism* 6.1 (2007): 55-68.

Kwast, Kurt E., et al. "Genomic analyses of anaerobically induced genes in Saccharomyces cerevisiae: functional roles of Rox1 and other factors in mediating the anoxic response." *Journal of Bacteriology* 184.1 (2002): 250-265.

Lara-Gonzalez, Pablo, et al. "The G2-to-M transition is ensured by a dual mechanism that protects cyclin B from degradation by Cdc20-activated APC/C." *Developmental cell* 51.3 (2019): 313-325.

Li, Xinmin, et al. "Analysis of oxysterol binding protein homologue Kes1p function in regulation of Sec14p-dependent protein transport from the yeast Golgi complex." *The Journal of cell biology* 157.1 (2002): 63-78.

Li, Xinmin, et al. "Identification of a novel family of nonclassic yeast phosphatidylinositol transfer proteins whose function modulates phospholipase D activity and Sec14p-independent cell growth." *Molecular Biology of the Cell* 11.6 (2000): 1989-2005.

Liebeschuetz, John W., Jason C. Cole, and Oliver Korb. "Pose prediction and virtual screening performance of GOLD scoring functions in a standardized test." *Journal of computer-aided molecular design* 26.6 (2012): 737-748.

Lingwood, Daniel, and Kai Simons. "Lipid rafts as a membrane-organizing principle." *science* 327.5961 (2010): 46-50.

Liu, Ke, et al. "P4-ATPase requirement for AP-1/clathrin function in protein transport from the trans-Golgi network and early endosomes." *Molecular biology of the cell* 19.8 (2008): 3526-3535.

Lyons, Thomas J., et al. "Metalloregulation of yeast membrane steroid receptor homologs." *Proceedings of the National Academy of Sciences* 101.15 (2004): 5506-5511.

Madeira, Fábio, et al. "The EMBL-EBI search and sequence analysis tools APIs in 2019." *Nucleic acids research* 47.W1 (2019): W636-W641.

McCrea, Heather J., and Pietro De Camilli. "Mutations in phosphoinositide metabolizing enzymes and human disease." *Physiology* 24.1 (2009): 8-16.

Mei, Kunrong, and Wei Guo. "The exocyst complex." *Current Biology* 28.17 (2018): R922-R925.

Mendenhall, Michael D., and Amy E. Hodge. "Regulation of Cdc28 cyclin-dependent protein kinase activity during the cell cycle of the yeast Saccharomyces cerevisiae." *Microbiology and Molecular Biology Reviews* 62.4 (1998): 1191-1243.

ULC, CCG. "Molecular Operating Environment (MOE), 2013.08, 1010 Sherbooke St." *West, Suite* 910 (2018).

Monteiro, Pedro T., et al. "YEASTRACT+: a portal for cross-species comparative genomics of transcription regulation in yeasts." *Nucleic Acids Research* 48.D1 (2020): D642-D649.

Mousley, Carl J., et al. "A sterol-binding protein integrates endosomal lipid metabolism with TOR signaling and nitrogen sensing." *Cell* 148.4 (2012): 702-715.

Nakase, Y., et al. "The S. pombe spo20^{+} gene encoding a homologue of S. cerevisiae Sec14 plays an important role in forespore membrane formation." *Mol. Biol. Cell* 12 (2001): 901-917.

Narasimhan, Meena L., et al. "Osmotin is a homolog of mammalian adiponectin and controls apoptosis in yeast through a homolog of mammalian adiponectin receptor." *Molecular cell* 17.2 (2005): 171-180.

Nemoto, Yasuo, et al. "Functional characterization of a mammalian Sac1 and mutants exhibiting substrate-specific defects in phosphoinositide phosphatase activity." *Journal of Biological Chemistry* 275.44 (2000): 34293-34305.

Nicastro, Raffaele, et al. "Snf1 phosphorylates adenylate cyclase and negatively regulates protein kinase A-dependent transcription in Saccharomyces cerevisiae." *Journal of Biological Chemistry* 290.41 (2015): 24715-24726.

Nile, Aaron H., et al. "PITPs as targets for selectively interfering with phosphoinositide signaling in cells." *Nature chemical biology* 10.1 (2014): 76-84.

Nile, Aaron H., Vytas A. Bankaitis, and Aby Grabon. "Mammalian diseases of phosphatidylinositol transfer proteins and their homologs." *Clinical lipidology* 5.6 (2010): 867-897.

Parker, Roy, and Ujwal Sheth. "P bodies and the control of mRNA translation and degradation." *Molecular cell* 25.5 (2007): 635-646.

Pereira, Marisa, et al. "Impact of tRNA modifications and tRNA-modifying enzymes on proteostasis and human disease." *International journal of molecular sciences* 19.12 (2018): 3738.

Phillips, Scott E., et al. "Yeast Sec14p deficient in phosphatidylinositol transfer activity is functional in vivo." *Molecular cell* 4.2 (1999): 187-197.

Régnacq, Matthieu, et al. "SUT1 suppresses sec14-1 through upregulation of CSR1 in Saccharomyces cerevisiae." *FEMS microbiology letters* 216.2 (2002): 165-170.

Ren, Jihui, et al. "A phosphatidylinositol transfer protein integrates phosphoinositide signaling with lipid droplet metabolism to regulate a developmental program of nutrient stress–induced membrane biogenesis." *Molecular biology of the cell* 25.5 (2014): 712-727.

Rouser, G., Fkeischer, S., and Yamamoto, A. (1970) A two dimensional thin layer chromatographic separation of polar lipids and determination of PLs by phosphorus analysis of spots. *Lipids* 5, 494–496

Routt, Sheri M., et al. "Nonclassical PITPs activate PLD via the Stt4p PtdIns-4-kinase and modulate function of late stages of exocytosis in vegetative yeast." *Traffic* 6.12 (2005): 1157-1172.

Santos, Beatriz, and Michael Snyder. "Sbe2p and sbe22p, two homologous Golgi proteins involved in yeast cell wall formation." *Molecular Biology of the Cell* 11.2 (2000): 435-452.

Schaaf, Gabriel, et al. "Functional anatomy of phospholipid binding and regulation of phosphoinositide homeostasis by proteins of the sec14 superfamily." *Molecular cell* 29.2 (2008): 191-206.

Schaaf, Gabriel, et al. "Resurrection of a functional phosphatidylinositol transfer protein from a pseudo-Sec14 scaffold by directed evolution." *Molecular biology of the cell* 22.6 (2011): 892-905.

Schnabl, Martina, et al. "Subcellular localization of yeast Sec14 homologues and their involvement in regulation of phospholipid turnover." *European journal of biochemistry* 270.15 (2003): 3133-3145.

Schuldiner, Maya, et al. "The GET complex mediates insertion of tail-anchored proteins into the ER membrane." *Cell* 134.4 (2008): 634-645.

Segev, Nava. "Ypt/rab gtpases: regulators of protein trafficking." *Science's STKE* 2001.100 (2001): re11-re11.

Sha, Bingdong, et al. "Crystal structure of the Saccharomyces cerevisiae phosphatidylinositol-transfer protein." *Nature* 391.6666 (1998): 506-510.

Somerharju, Pentti, and Karel WA Wirtz. "Semisynthesis and properties of a fluorescent phosphatidyl-inositol analogue containing a cis-parinaroyl moiety." *Chemistry and Physics of lipids* 30.1 (1982): 81-91.

Starck, Shelley R., et al. "Translation from the 5′ untranslated region shapes the integrated stress response." *Science* 351.6272 (2016).

Strahl, Thomas, and Jeremy Thorner. "Synthesis and function of membrane phosphoinositides in budding yeast, Saccharomyces cerevisiae." *Biochimica et Biophysica Acta (BBA)-Molecular and Cell Biology of Lipids* 1771.3 (2007): 353-404.

Su, Wen-Min, et al. "Protein kinase A phosphorylates the Nem1–Spo7 protein phosphatase complex that regulates the phosphorylation state of the phosphatidate phosphatase Pah1 in yeast." *Journal of Biological Chemistry* 293.41 (2018): 15801-15814.

Swanson, Robert, Martin Locher, and Mark Hochstrasser. "A conserved ubiquitin ligase of the nuclear envelope/endoplasmic reticulum that functions in both ER-associated and Matα2 repressor degradation." *Genes & development* 15.20 (2001): 2660-2674.

Tanaka, Kazuma, et al. "S. cerevisiae genes IRA1 and IRA2 encode proteins that may be functionally equivalent to mammalian ras GTPase activating protein." *Cell* 60.5 (1990): 803-807.

Tkach, Johnny M., et al. "Dissecting DNA damage response pathways by analysing protein localization and abundance changes during DNA replication stress." *Nature cell biology* 14.9 (2012): 966-976.

Totrov, Maxim, and Ruben Abagyan. "Rapid boundary element solvation electrostatics calculations in folding simulations: successful folding of a 23-residue peptide." *Peptide Science: Original Research on Biomolecules* 60.2 (2001): 124-133.

Tripathi, Ashutosh, and Glen E. Kellogg. "A novel and efficient tool for locating and characterizing protein cavities and binding sites." *Proteins: Structure, Function, and Bioinformatics* 78.4 (2010): 825-842.

Tripathi, Ashutosh, J. Andrew Surface, and Glen E. Kellogg. "Using active site mapping and receptor-based pharmacophore tools: prelude to docking and de novo/fragment-based ligand design." *Drug Design and Discovery*. Humana Press, 2011. 39-54.

Tripathi, Ashutosh, et al. "Functional diversification of the chemical landscapes of yeast Sec14-like phosphatidylinositol transfer protein lipid-binding cavities." *Journal of Biological Chemistry* 294.50 (2019): 19081-19098.

Umebayashi, Kyohei, and Akihiko Nakano. "Ergosterol is required for targeting of tryptophan permease to the yeast plasma membrane." *The Journal of cell biology* 161.6 (2003): 1117-1131.

Valachovič, Martin, Lucia Hronská, and Ivan Hapala. "Anaerobiosis induces complex changes in sterol esterification pattern in the yeast Saccharomyces cerevisiae." *FEMS microbiology letters* 197.1 (2001): 41-45.

Van Meer, Gerrit, Dennis R. Voelker, and Gerald W. Feigenson. "Membrane lipids: where they are and how they behave." *Nature reviews Molecular cell biology* 9.2 (2008): 112-124.

Vincent, Patrick, et al. "A Sec14p-nodulin domain phosphatidylinositol transfer protein polarizes membrane growth of Arabidopsis thaliana root hairs." *The Journal of cell biology* 168.5 (2005): 801-812.

Visintin, Rosella, Susanne Prinz, and Angelika Amon. "CDC20 and CDH1: a family of substrate-specific activators of APC-dependent proteolysis." *Science* 278.5337 (1997): 460-463.

Wang, Yaxi, et al. "Noncanonical regulation of phosphatidylserine metabolism by a Sec14-like protein and a lipid kinase." *Journal of Cell Biology* 219.5 (2020).

Wild, Klemens, et al. "SRP meets the ribosome." *Nature structural & molecular biology* 11.11 (2004): 1049-1053.

Wolf, Dieter H., and Alexandra Stolz. "The Cdc48 machine in endoplasmic reticulum associated protein degradation." *Biochimica et Biophysica Acta (BBA)-Molecular Cell Research* 1823.1 (2012): 117-124.

Wong, Tania A., et al. "Membrane metabolism mediated by Sec14 family members influences Arf GTPase activating protein activity for transport from the trans-Golgi." *Proceedings of the National Academy of Sciences* 102.36 (2005): 12777-12782.

Wu, Wen-I., et al. "A new gene involved in the transport-dependent metabolism of phosphatidylserine, PSTB2/PDR17, shares sequence similarity with the gene encoding the phosphatidylinositol/phosphatidylcholine transfer protein, SEC14." *Journal of Biological Chemistry* 275.19 (2000): 14446-14456.

Xie, Zhigang, et al. "Phospholipase D activity is required for suppression of yeast phosphatidylinositol transfer protein defects." *Proceedings of the National Academy of Sciences* 95.21 (1998): 12346-12351.

Xu, Peng, et al. "COPI mediates recycling of an exocytic SNARE by recognition of a ubiquitin sorting signal." *Elife* 6 (2017): e28342.

Xu, Peng, et al. "Phosphatidylserine flipping enhances membrane curvature and negative charge required for vesicular transport." *Journal of Cell Biology* 202.6 (2013): 875-886.

Yamauchi, Toshimasa, et al. "Adiponectin stimulates glucose utilization and fatty-acid oxidation by activating AMP-activated protein kinase." *Nature medicine* 8.11 (2002): 1288-1295.

Yang, Huiseon, et al. "Structural determinants for phosphatidylinositol recognition by Sfh3 and substrate-induced dimer–monomer transition during lipid transfer cycles." *FEBS letters* 587.11 (2013): 1610-1616.

Zeller, Corinne E., Stephen C. Parnell, and Henrik G. Dohlman. "The RACK1 ortholog Asc1 functions as a G-protein β subunit coupled to glucose responsiveness in yeast." *Journal of Biological Chemistry* 282.34 (2007): 25168-25176.